The Nitrogen Legacy: Understanding Time Lags in Catchment Response as a Function of
Hydrologic and Biogeochemical Controls

by

Kimberly Van Meter

A thesis
presented to the University of Waterloo
in fulfillment of the
thesis requirement for the degree of
Doctor of Philosophy
In
Earth and Environmental Sciences

Waterloo, Ontario, Canada, 2016

Author's Declaration

I hereby declare that I am the sole author of this thesis. This is a true copy of the thesis, including any required final revisions, as accepted by me examiners.

I understand that my thesis may be made electronically available to the public.

Abstract

Global population has seen a more than threefold increase over the last 100 years, accompanied by rapid changes in land use and a dramatic intensification of agriculture.   Such changes have been driven by a great acceleration of the global nitrogen (N) cycle, with N fertilizer use now estimated to be 100 Tg/year globally. Excess N commonly finds its way into both groundwater and surface water, leading to long-term problems of hypoxia, aquatic toxicity and drinking water contamination. Despite ongoing efforts to improve water quality in agroecosystems, results have often been disappointing, with significant **lag times** between adoption of accepted best management practices (BMPs) and measurable improvements in water quality. It has been hypothesized that such time lags are a result of the buildup of legacy N within the landscape over decades of fertilizer application and agricultural intensification.

The central theme of my research has been an exploration of this N legacy, including (1) an investigation of the form, locations and magnitudes of legacy N stores within intensively managed catchments; (2) development of a parsimonious, process-based modeling framework for quantifying catchment-scale time lags based on both soil nutrient accumulations (biogeochemical legacy) and groundwater travel time distributions (hydrologic legacy); and (3) use of a statistical approach to both quantifying N-related time lags at the watershed scale, and identifying the primary physical and management controls on these lags.

As a result of these explorations I am able to provide the first direct, large-scale evidence of N accumulation in the root zones of agricultural soils, accumulation that may account for much of the 'missing N' identified in mass balance studies of heavily impacted watersheds. My analysis of long-term soil data (1957-2010) from 206 sites throughout the Mississippi River Basin (MRB) revealed N accumulation in cropland of 25-70 kg ha^{-1} y^{-1}, a total of 3.8 ± 1.8 Mt y^{-1} at the watershed scale. A simple modeling framework was then used to show that the observed accumulation of soil organic N (SON) in the MRB over a 30-year period (142 Tg N) would lead to a biogeochemical lag time of 35 years for 99% of legacy SON, even with a complete cessation of fertilizer application.

A parsimonious, process-based model, ELEMeNT (Exploration of Long-tErM Nutrient Trajectories), was then developed to quantify catchment-scale time lags based on *both* soil N accumulation (biogeochemical legacy) and groundwater travel time distributions (hydrologic

legacy). The model allowed me to predict the time lags observed in a 10 km^2 Iowa watershed that had undergone a 41% conversion of area from row crop to native prairie. The model results showed that concentration reduction benefits are a function of the spatial pattern of implementation of conservation measures, with preferential conversion of land parcels having the shortest catchment-scale travel times providing greater concentration reductions as well as faster response times. This modeling framework allows for the quantification of tradeoffs between costs associated with implementation of conservation measures and the time needed to see the desired concentration reductions, making it of great value to decision makers regarding optimal implementation of watershed conservation measures.

      To better our understanding of long-term N dynamics, I expanded the ELEMeNT modeling framework described above to accommodate long-term N input trajectories and their impact on N loading at the catchment scale. In this work, I synthesized data from a range of sources to develop a comprehensive, 214-year (1800-2104) trajectory of N inputs to the land surface of the continental United States. The ELEMeNT model was used to reconstruct historic nutrient yields at the outlets of two major U.S. watersheds, the Mississippi River and Susquehanna River Basins, which are the sources of significant nutrient contamination to the Gulf of Mexico and Chesapeake Bay, respectively. My results show significant N loading above baseline levels in both watersheds before the widespread use of commercial N fertilizers, largely due to 19th-century conversion of natural forest and grassland areas to row-crop agriculture. The model results also allowed me to quantify the magnitudes of legacy N in soil and groundwater pools, thus highlighting the dominance of soil N legacies in the MRB and groundwater legacies in the SRB. It was found that approximately 85% of the annual N load in the MRB can be linked to inputs from previous years, while only 47% of SRB N loading is associated with "older" N. In addition, it was found that the dominant sources of current N load in the MRB are fertilizer, atmospheric deposition, and biological N fixation, while manure and atmospheric deposition account for approximately 64% of the current loads in the SRB.

      Finally, long-term N surplus trajectories were paired with long-term flow-averaged nitrate concentration data to as means of quantifying N-related lag times across an intensively managed watershed in Southern Ontario. In this analysis, we found a significant linear relationship between current flow-averaged concentrations and current N surplus values across the study watersheds. Temporal analysis, however, showed significant nonlinearity between N

inputs and outputs, with a strong hysteresis effect indicative of decadal-scale lag times between changes in N surplus values and subsequent changes in flow-averaged nitrate concentrations. Annual lag times across the study watersheds ranged from 15-33 years, with a mean lag of 24.5 years. A seasonal analysis showed a distribution of lag times across the year, with fall lags being the shortest and summer lags the longest, likely due to differences in N delivery pathways. Multiple linear regression analysis of dominant controls showed tile drainage to be a strong determinant of differences in lag times across watersheds in both fall and spring, with a watershed's fractional area under tile drainage being significantly linked to shorter lag times. In summer, tile drainage was found to be an insignificant factor in driving lag times, while a significant relationship was found between the percent soil organic matter and longer N-related lag times.

By moving beyond the traditional focus on nutrient concentrations and fluxes, and instead working towards quantification of the spatio-temporal dynamics of non-point source nutrient legacies and their current and future impacts on water quality, we make a significant contribution to the science of managing human impacted landscapes. Due to the strong impacts of nutrient legacies on the time scales for recovery in at-risk landscapes, my work will enable a more accurate assessment of the outcomes of alternative management approaches in terms of both short- and long-term costs and benefits, and the evaluation of temporal uncertainties associated with different intervention strategies.

Acknowledgements

I would like to thank Nandita Basu, my patient and insightful supervisor, guide, and mentor for her ongoing, invaluable support and intellectual rigor. This thesis would not have been completed without her guidance and unwavering belief in my ability to succeed in the exciting world of research.

I would also like to thank my committee members, Maren Oelbermann, Fereidoun Rezanezhad, Dave Rudolph, Sherry Schiff, and Philippe van Cappellen for their willingness to engage with my research, from its earliest stages, and to provide consistently valuable feedback.

Thanks to members of the Basu group for listening to my endless talks about nitrogen legacies at our group meetings and giving me ongoing feedback and support. Special thanks to Fred Cheng, my excellent office mate, for troubleshooting my codes, fixing my page numbers, talking politics and generally allowing me to procrastinate as needed.

And finally, thanks to my amazing family for the incredible gift of letting me immerse myself in research and complete my degree.

Table of Contents

List of Tables

List of Figures

Chapter 1 - Introduction

1.1   Background

Human modification of the nitrogen (N) cycle has resulted in increased flows of reactive N, with growing evidence that planetary boundaries for maintaining human and ecosystem health have been exceeded (Rockström, Steffen, et al. 2009; Carpenter, Stanley, and Vander Zanden 2011). The creation of large hypoxic zones, and the resulting loss of habitat and species diversity in estuarine and coastal marine ecosystems, has been one of the most significant impacts of such increased flows. In inland ecosystems, excess N, via leaching and surface runoff pathways, can lead to the acidification of pH-sensitive freshwater lakes and streams and pose a threat to drinking water supplies (Vitousek et al. 1997). Both the U.S. and Canada are significantly impacted by N pollution. A study in the Midwestern U.S. showed 27-44% of wells in areas under agricultural production exceeding the 45 mg-NO_3^{-1}/L drinking water standard (Yadav and Wall 1998). In another study of 180 farm wells in southern Ontario, 21 wells were found to have nitrate concentrations exceeding the drinking water standard, with some showing concentrations as high as 244 mg/L ("Monitoring of Trends in Rural Water Quality in Southern Ontario - Eco Issues" 2013). In the state of Iowa, one of the major exporters of high nitrate loads to the Gulf of Mexico, costs associated with a proposed 45% reduction in N export to the Mississippi are estimated at more than 4.5 billion dollars ("AFBF: Balance the Budget - DTN/The Progressive Farmer" 2014).

Although numerous attempts have been made to improve water quality by changing agricultural management practices, the results have generally been disappointing (Meals, Dressing, and Davenport 2010; Jarvie, Sharpley, Withers, et al. 2013). Even in areas where there have been large and abrupt decreases in N fertilizer application, stream N concentrations have not decreased proportionately (Kopáček, Hejzlar, and Posch 2013). In some areas of Eastern Europe, surface water nutrient concentrations actually continued to increase after the dramatic reductions in fertilizer use accompanying the collapse of state-supported agriculture in the late 1980s and early 1990s (Fenton et al. 2011b). More recently, after more than a decade

of attempts by the European Union to reduce N inputs from agriculture, there have been no consistent reductions in nitrate concentrations in streams draining Nitrate Vulnerable Zones in the U.K. (Worrall et al. 2009; Hamilton 2012a).

1.2   Time Lags

One of the major factors causing the apparent lack of response to changes in agricultural management practices is the ***time lag*** that can ensue between the adoption of new practices and improvements in water quality improvement. In a review of studies examining responses of stream nitrate levels to changes in management practices, Meals et al. (Meals, Dressing, and Davenport 2010) have reported response time lags ranging from 4 to more than 50 years. One component of these time lags, the ***hydrologic time lag***, is characterized by the travel times of nutrients and other contaminants from source to receptor via hydrological pathways. Such time lags, which can be a function of soil type, bedrock geology, and climatic factors, are generally well understood (Hamilton 2012a; Sousa et al. 2013) and in Canada are now accounted for in basin-scale risk management plans prepared by the Ministry of Environment (MOE) to protect drinking water sources.

The second component of the time lag, the ***biogeochemical time lag***, is relatively less studied (Jarvie, Sharpley, Spears, et al. 2013) and arises from reactions that a solute undergoes in the landscape, leading to accumulation of the solute in a sorbed form. The existence of a biogeochemical time lag for phosphorus (P) is now well accepted, with accumulation in agricultural soils representing the most pervasive source of legacy P to the environment (MacDonald et al. 2011). In the Saint Lawrence River basin, for example, P mass budget work has been paired with soil data to show a strong linear relationship between watershed P budgets and legacy soil P (MacDonald & Bennett, 2009). Until recently, however, the possibility of such a biogeochemical legacy for N has largely been neglected, as nitrate is non-sorbing in temperate-zone soils and is quickly leached to groundwater (Di and Cameron 2002).

1.3   Nitrogen Mass Balance Studies

Despite the frequent assumption that N levels within watersheds exhibit steady state behavior, mass balance studies of intensively managed catchments throughout the world, consistently indicate the presence of "missing" N stores (Hong,

Swaney, and Howarth 2013; Gilles Billen et al. 2009a; N. Chen et al. 2008) with anthropogenic inputs of N routinely exceeding measured outputs. Goolsby (Goolsby et al. 1999), for example, shows a cumulative residual of more than 50 million Mt of N accumulation within the Mississippi River Basin from the 1950s through 1996, even when taking into account both plant uptake and riverine outputs, as well as estimates of denitrification, immobilization, and volatilization. Similarly, Howden et al. report a post-World War II N accumulation rate of 100 ± 40 kt/yr for the intensively farmed River Thames catchment of the UK (Howden et al. 2011a).

If catchment-level N outputs are not in accordance with current levels of fertilizer and other N input, one is led to ask, where does all the nitrogen go? The fate of this "missing" N, quantified as the difference between net anthropogenic N inputs (NANI) and riverine outputs and also referred to as N retention, is largely unknown. Some speculate that groundwater, or the hydrologic legacy, is the major N sink, while others have simply assumed that net N inputs are offset by soil and in-stream denitrification processes (Howden et al. 2011a; Hamilton 2012a), such that there is no N retention (van Egmond, Bresser, and Bouwman 2002a). The existence of such a balance, however, is based on an assumption of steady-state N dynamics, an assumption that has been validated for pristine systems over long timescales (Ayres, Schlesinger, and Socolow 1996) but that likely no longer holds with the current high inputs of reactive N in intensively managed landscapes (Galloway et al. 2004; Galloway et al. 2008; Gruber and Galloway 2008). Recent work in a heavily impacted watershed in Italy, for example, suggests that denitrification accounts for, at most, only 20% of unaccounted for N (Bartoli et al. 2012). Globally, it is estimated that, even after accounting for groundwater storage and reasonable estimates of denitrification, approximately 46 Tg N/yr of net anthropogenic N inputs remain unaccounted for (Schlesinger 2008).

1.4   A Soil Nitrogen Legacy?

Although some have suggested that fertilized agricultural soils could be a long-term receptacle for N (Grimvall, Stålnacke, and Tonderski 2000) no direct estimate of this potential increase in soil N has been obtained (Haag and Kaupenjohann 2001). The results of one recent study exploring temporal variations in soil organic carbon

(SOC) and total N (TN) down to the 100-cm level in fields at 19 Illinois fields under row crop (Mark B. David et al. 2009), however, suggest that a more comprehensive analysis of agricultural soils could provide us with such estimates. In the Illinois study, David et al. obtained soil samples from sites that had been previously sampled in 1957 and that had remained under continuous cultivation between 1957 and 2002. Analysis of the 2002 samples showed that, almost no change in C and N concentrations had occurred in the surface layers (0-20 cm) over this time period (**Figure 1.1**). However, a significant *increase* was found in both C and N in the lower 20-100 cm of cultivated soil.

Figure 1.1. Nitrogen accumulation with depth in agricultural soil under intensive cultivation, 1957-2002. Adapted from David et al. (2010).
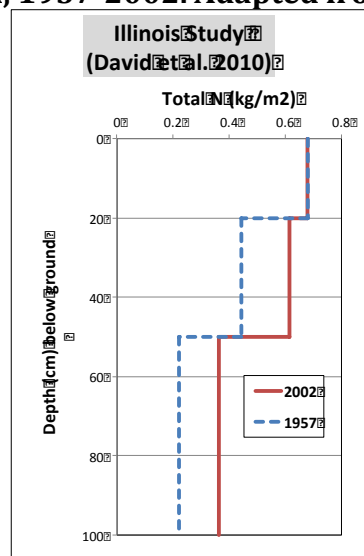
How do we reconcile a potential accumulation of SOC and total N over decades of intensive agriculture with the generally accepted knowledge that agriculture results in a loss of soil organic matter (SOM) (Baker et al. 2007; Gál et al. 2007): Losses of soil organic carbon (SOC) following conversion of natural to agricultural lands are estimated to be as much as 60% in temperate regions and 75% in tropical areas (Gál et al. 2007). The reasons for this initial decrease in SOM continue to be a source of debate, with some attributing it to the increased aeration of the soil in response to plowing and the draining of wetland areas (Reicosky 2003; John M. Baker et al. 2007), and others relating it to a conversion from primarily perennial grasses and forests, providing year-round groundcover, to agricultural systems dominated by

annual crops that leave the land bare for extended periods (J.M. Baker and Griffis 2005). Regardless of the reason, it is clear that these losses of SOM (which include both SOC and N) do occur, and that they occur throughout the soil profile (Mark B. David et al. 2009; Mikhailova et al. 2000). Acknowledgment of these initial losses, however, does not eliminate the possibility that there may be subsequent gains in SOM in land under intensive cultivation that may offset these earlier losses.

1.5   Modeling Nutrient Legacies and Time Lags

While it is well accepted that there are time lags between implementation of landscape-scale best management practices and improvements in water quality (Meals et al., 2010; Nature Geosciences paper), there is a lack of an integrated modeling framework that can predict the timing and magnitude of water quality improvements as a function of changes in land use and land management. Most studies to date have focused on predicting the percentage concentration reduction given a certain fraction of land-use change, but have provided no information on the time required for achieving that concentration reduction (Jha, Gassman, and Arnold 2007; S. Rabotyagov et al. 2010). For example, Jha et al. (2007) used SWAT to model the water quality benefits of converting from 6-100% of row-crop area to grassland within an intensively farmed watershed in central Iowa, USA; based on their simulations, they have reported that nutrient loadings at the watershed outlet can be decreased proportionally by increasing the amount of land enrolled in the Conservation Reserve Program, such that a 40% increase in CRP lands results in a full 40% decrease in NO_3^- loadings. In another study, tradeoffs between costs and nutrient concentrations were modeled to identify least-cost intervention scenarios to reduce the size of the Gulf of Mexico's hypoxic zone (Rabotyagov et al. 2010). The simulations in such studies, however, provide only snapshot information on the concentration reduction benefit that will be achieved at infinite time, with no consideration of the time that will be required to achieve that goal. Such consideration, however, is critical for watershed managers who must make decisions regarding allotment of limited resources, and mange expectations about achievable water quality improvement goals.

1.6   Objectives

My overall objective in the present work was to explore N dynamics in agricultural landscapes subjected to intensive farming practices, specifically those including the heavy use of chemical and manure-based fertilizers.   My central hypothesis is that intensively managed catchments have *legacy* stores of N that have built up over decades of fertilizer application and that contribute to catchment time lags after land-use change or implementation of best management practices. I have specifically attempted to answer the following research questions:

1) Do N legacies exist in agricultural landscapes?

2) What are the magnitudes of these legacy N stores, and in what forms do they exist?

3) What are the accumulation and depletion trajectories of such legacies?

4) How does the existence of such legacies impact N concentration dynamics at the catchment outlet after land-use change or changes in management practices?

5) Can legacy-related time lags be quantified in intensively managed watersheds, and what are the dominant controls on these lags?

I have approached these questions from both a data-analysis and a modeling perspective according to the following four sub-objectives. Objective 1 primarily focuses on data synthesis to quantify legacies (Chapter 2), Objectives 2 and 3 focus on the development of a process based modeling framework that explicitly take into account spatial patterns of land use change (Chapter 3), and long term N input trajectories (Chapter 4). Finally, Objective 4 focuses on developing a statistical approach that quantifies watershed scale time lags based on N input and output trajectories.

Objective 1:   Carry out a synthesis of current research and analysis of publicly available data sources regarding N sources and sinks in anthropogenically impacted catchments so as to quantify potential N accumulation and reduce the uncertainty associated with watershed-scale N-budgets.

Objective 2:   Develop a process-based biogeochemical model to quantify time lags and concentration reductions as a function of both natural (e.g. soil type, landscape characteristics, climate) and anthropogenic (management practices) controls, with specific focus on quantifying the effect of spatial placement of management practices.

Objective 3:   Expand the modeling framework developed in Objective 2 to incorporate long term N input and output trajectories, and effectively capture the accumulation and depletion dynamics of N pools in the Mississippi and Susquehanna River Basins over a 200-year time frame

Objective 4:   Develop a statistical framework to quantify N-related time lags in an agricultural watershed in Southern Ontario, and to identify dominant controls on these lags

1.7   Thesis Outline

The thesis includes an introductory chapter (Chapter 1), four research chapters (2 through 5) and a conclusion chapter (6). A brief description of and specific objectives for each of the research chapters are discussed below.

Chapter 2, which was published in *Environmental Research Letters* (Van Meter et al. 2016) provides an analysis of long-term soil data across the Mississippi River Basin. The working hypothesis in this work was that decades of high-input agriculture have led to significant accumulations of soil organic N across the landscape and that this accumulation may contribute to time lags in catchment response after changes in management practices. My objective was to (1) use historical and current soil sampling data to provide direct evidence of potential changes in soil N content over time; (2) to place such evidence in the context of watershed-scale mass balance studies; and (3) to develop a parsimonious modeling framework to explain decadal-scale changes in soil organic N. The study area for this work was the Mississippi River Basin, an area covering approximately 41% of the contiguous United States and including more than 800,000 km^2 cropland.

Chapter 3, which was published in PLOS ONE (Van Meter and Basu 2015) describes the development of a parsimonious analytical model to quantify the

7

concentration reduction benefits associated with watershed restoration efforts as a function of both hydrologic and biogeochemical controls, with particular attention being paid to the ways in which spatial patterns of landscape conversion impact concentration-reduction scenarios. My objective in this work was (1) to explore scenarios of land-use conversion and compare these results with concentration trajectories observed in a small Midwestern watershed undergoing an extensive prairie habitat restoration project; and (2) to use these relationship to establish an optimization framework for meeting concentration reduction goals; and (3) to evaluate the performance of conservation measures under spatially varying patterns of intervention as a function of legacy N accumulation, N removal dynamics in the subsurface, and watershed travel time distributions.

Chapter 4, which is in preparation to be submitted to the journal *Global Biogeochemical Cycles* (Van Meter, Van Cappellen, and Basu)*, focuses on a more than two-century analysis of N dynamics across the Mississippi and Susquehanna River Basins, with specific attention being paid to the development of legacy sources and sinks of anthropogenic N in these watersheds. My goal in the present work was to develop a process-based modeling approach to place current observed stream N dynamics in the context of long-term trajectories of N use. My specific objectives involved (1) quantifying N inputs and outputs over a period of more than 200 years for the Mississippi and Susquehanna River Basins; using these N input trajectories to drive a parsimonious, process-based model capable of accounting for N dynamics in subsurface reservoirs; and (3) to chart decadal-scale changes in N magnitudes within the vadose zone and in groundwater, and to predict the timescales of change in surface water N loading in response to changes in land use and N management.

Finally, in Chapter 5, which is in preparation to be submitted to *Environmental Science and Technology* (Van Meter and Basu), my goal was to quantify N-related time lags and to identify the primary physical and management controls on these lags. Specifically, my objectives were to (1) determine the strength of the relationship between current annual N surplus values and current flow-averaged nitrate concentrations; (2) explore whether long-term N surplus data can be used to quantify

time lags in catchment-scale N response; (3) explore seasonal variations in N-related time lags; and (4) identify dominant natural and anthropogenic controls on time lags.

Chapter 2 - The Nitrogen Legacy: Emerging Evidence of Nitrogen Accumulation in Anthropogenic Landscapes

2.1   Introduction

Human modification of the nitrogen (N) cycle has resulted in increased flows of reactive N (N_R), with growing evidence that planetary boundaries for maintaining human and ecosystem health have been exceeded (Rockström, Steffen, et al. 2009; Carpenter, Stanley, and Vander Zanden 2011).   The creation of large hypoxic zones, and the resulting loss of habitat and species diversity in estuarine and coastal marine ecosystems, has been one of the most significant impacts of such increased flows (R. Howarth, Chan, et al. 2011). While the need to manage N flows and their associated ecological impacts is increasingly recognized, implementation of conservation measures to reduce stream N concentrations has had only limited success (Meals, Dressing, and Davenport 2010; Kopáček, Hejzlar, and Posch 2013).

Growing evidence suggests that this lack of success can be attributed to diffuse legacy sources that continue to impair water quality even after agricultural inputs have ceased (Grimvall, Stålnacke, and Tonderski 2000; Baily et al. 2011). These sources can lead to time lags between management changes and measurable improvements in water quality, lags that can make it difficult to evaluate the effectiveness of the management practices employed or to maintain public support of costly, ongoing interventions (Meals, Dressing, and Davenport 2010; Larry J. Puckett, Tesoriero, and Dubrovsky 2011a; Hamilton 2012b). Such time lags, which have been defined as the time between the initiation of a restoration practice and the point at which a change is an observed in the target water body (Meals, Dressing, and Davenport 2010; Hamilton 2012b), have been observed in Europe and the United States, where nitrate concentrations in streams and aquifers have remained high despite reductions in N loadings to watersheds (Worrall et al. 2009; Sprague, Hirsch, and Aulenbach 2011; Howden et al. 2011b).

The presence of legacy sources is also suggested by the frequent references to "missing" N, also referred to as N retention (Leip, Britz, et al. 2011), in mass-balance

studies of intensively managed catchments (van Breemen et al. 2002; Boyer et al. 2002). In such catchments, anthropogenic inputs of N routinely exceed measured outputs, creating watershed-scale N budgets that appear significantly out of balance. Indeed, both regional and continental scale studies suggest that an inefficient use of N is common in heavily agricultural watersheds, leading to a large N surplus (defined as N inputs - usable outputs) (Erisman et al. 2005; Parris 1998; Leip, Britz, et al. 2011). A portion of this N surplus exits the watershed as riverine output, while the fate of the residual N, although not wholly unknown, remains largely unquantified at watershed scales. In particular, denitrification and subsurface storage constitute well-known pathways by which N may either exit a catchment or be retained over a long period, and these N sinks are frequently grouped under the heading of "N retention" (**Figure 2.1**). Our synthesis of N mass balance studies for watersheds across the world shows a mean N retention of approximately 50 kg ha^{-1} y^{-1} (Supplementary Table A1), but, as discussed below, precise quantification of N fluxes via specific retention pathways has remained elusive (Hofstra and Bouwman 2005; Galloway et al. 2008).

Figure 2.1. Schematic showing the stores and fluxes of reactive N in a human-impacted watershed, explicitly including both point and non-point sources. The box on the left represents terrestrial system N dynamics, which are driven by N inputs at the soil surface, while that on the right represents urban and industrial point sources. Fluxes are labeled with letters that are carried over to Figure 2.4, which provides the magnitudes of these fluxes in a watershed-scale mass balance for the Mississippi River Basin.
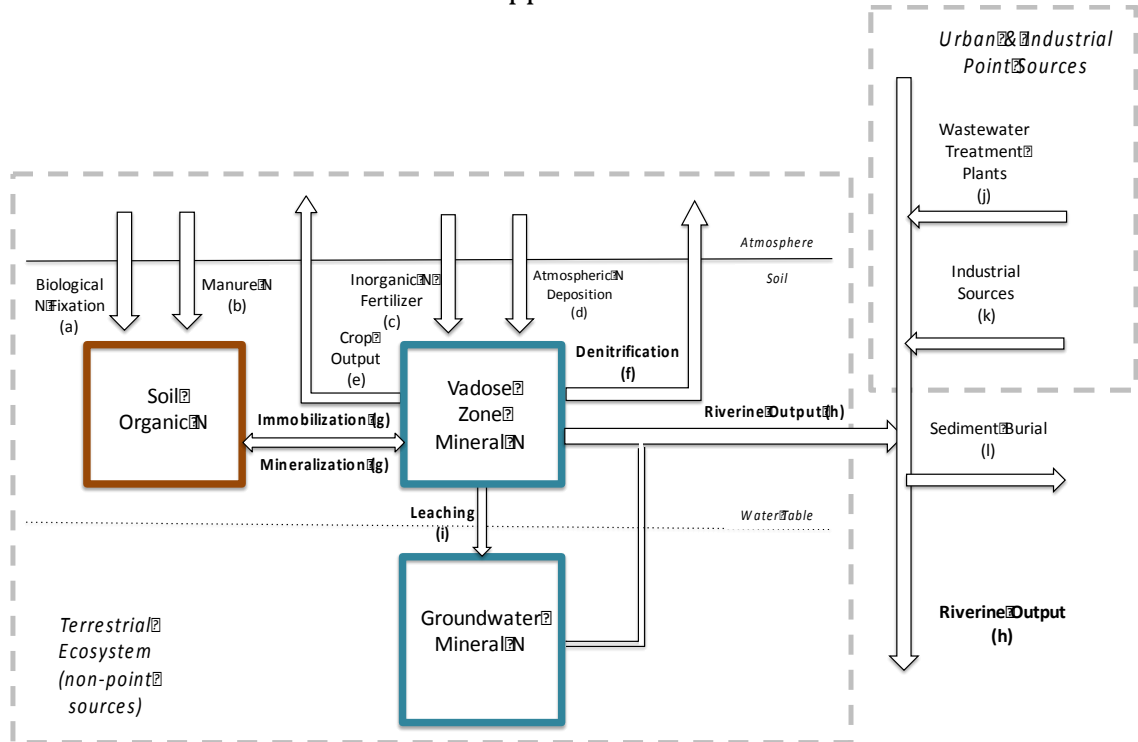
Denitrification, which occurs in both soils and stream sediments (Barton et al. 1999; Mulholland et al. 2004), is the process by which N_R is removed from a system via reduction to nitrous oxide (N_2O) and nitrogen gas (N_2) (Seitzinger et al. 2006; Canfield, Glazer, and Falkowski 2010; Larry J. Puckett, Tesoriero, and Dubrovsky 2011a; Tesoriero and Puckett 2011). Due to inherent difficulties in direct measurement of denitrification products, considerable uncertainty exists regarding denitrification rates in terrestrial systems (Hofstra and Bouwman 2005; Seitzinger et al. 2006). As a result, denitrification is often used simply as a balancing term in mass balance studies, with denitrification rates being estimated based on differences between N inputs and all other N storage and loss terms for the watershed (R. W. Howarth et al. 2002; van Egmond, Bresser, and Bouwman 2002b; van Breemen et al. 2002). The existence of such a balance, however, is based on an assumption of steady-

state dynamics for terrestrial N reservoirs, with all anthropogenically and naturally fixed N_R being denitrified and returned to the atmosphere on an annual timescale (Seitzinger et al. 2006). Although such an assumption has been hypothesized to be valid for pristine systems over long timescales (Ayres, Schlesinger, and Socolow 1996), it has been shown to be no longer applicable with the current high inputs of N_R in intensively managed landscapes (J N Galloway et al. 2004; Gruber and Galloway 2008; J.N. Galloway et al. 2008; Canfield, Glazer, and Falkowski 2010). Indeed, modeled estimates of denitrification are often significantly lower than those suggested by national-scale mass balance-based estimates (Clair et al. 2014).

The other possible fate of the "missing N" is storage within the subsurface. We can conceptualize the subsurface environment to be composed of three major N pools: (1) dissolved NO_3^- in the vadose zone or (2) in groundwater aquifers, and (3) organic N within the soil profile (**Figure 2.1**). Large vadose zone stores of inorganic N have been demonstrated in desert and semi-arid regions, with accumulation magnitudes in deep vadose zones (30 - 50 m) varying as a function of rainfall, tillage and irrigation history (Walvoord et al. 2003; McMahon et al. 2006b; Scanlon, Reedy, and Bronson 2008). The existence of a significant groundwater reservoir has been proposed based on observations of increasing groundwater N concentrations over time in both the U.S. and Europe (Larry J. Puckett, Tesoriero, and Dubrovsky 2011a; Worrall, Howden, and Burt 2015). Although the existence of such subsurface reservoirs for N is well accepted, determination of the magnitude of N accumulation is subject to significant uncertainty due to the presence of complex aquifer systems and difficulties in measuring spatially varying patterns in NO_3^- concentrations and groundwater storage (L. A. Baker et al. 2001). In one of the few studies attempting to quantify stores of groundwater N over time, Worrall et al. (2015) estimate that N accumulation in groundwater beneath the River Thames Drainage Basin in the UK reached a peak between 2000 and 2004 of 1571 ± 608 Mg N.

The third potential subsurface storage reservoir is organic N held within the soil profile (**Figure 2.1**). Indeed, the largest pool of N in most terrestrial ecosystems is soil organic N (SON) (Jaffe 1992; J. N. Galloway 2003), and at current levels of N input, it is suggested that terrestrial N sequestration may be occurring at a global

scale on the order of 20-100 Tg N y^{-1} (Fowler, Coyle, et al. 2013; Zaehle 2013; J. Galloway et al. 2004). The potential for increased N storage in forested soils has long been accepted for landscapes subjected to elevated levels of atmospheric N deposition (Fenn et al. 1998). For example, a study of N retention and C sequestration in European forests estimated N sequestration in forested soils to have occurred at a rate of 4.7 kg-N ha^{-1} y^{-1} from 1960-2000 (De Vries et al. 2006). It has similarly been suggested that N may be accumulating in agricultural soils (V. Smil 1999a; Fenn et al. 1998). Yan et al. (Yan et al. 2014) found the average soil N content of Chinese croplands to increase by 5.1% between 1979-82 and 2007-08, while mass balance and modeling studies in Canada (Clair et al. 2014), Europe (Leip, Achermann, et al. 2011), and the U.S. (Science Advisory Board 2011) suggest an annual accumulation of N within agricultural soils on the order of 15-20% of total N inputs. Fenn et al. (1998) have shown that soils in which C and N pools have been reduced by disturbance, such as those under agricultural cropping, may exhibit the highest levels of N retention. Smil (1999a) has estimated that in agricultural soils receiving regular fertilizer inputs, N accumulation is likely occurring at a rate of 25-35 kg ha^{-1} y^{-1}, and Worrall et al. (2015), in their recent study of the Thames basin, suggest that SON has accumulated at a rate of 55 kg ha^{-1} y^{-1} since 1973.

In general, however, little attention has been given to the possibility of soil N storage in the context of watershed-scale N balance studies, primarily due to assumptions of either ongoing N depletion (Gilles Billen et al. 2009b) or steady-state dynamics under conventional agriculture (R. W. Howarth et al. 2002; Bouwman 2005). For example, although Billen et al. (Gilles Billen et al. 2009a) note that storage in the soil organic matter reservoir could potentially account for missing N in the soil N budget for the Seine and Somme watersheds, this possibility is discarded because "soil organic matter content is generally considered as decreasing due to continuous cropping." Howarth et al. (R. W. Howarth et al. 2002) explicitly assume no potential for soil N accumulation, noting that after a large net release of N following conversion of land to agricultural use, the N status of soils reaches a steady state, with N immobilization, on average, equaling N mineralization on an annual basis.

Indeed, it is well-documented that dramatic losses of SON and C can occur after cultivation, particularly in nutrient-rich soils like those found in the North American prairie region (Beniston et al. 2014; Mark B. David et al. 2009; Davidson and Ackerman 1993a; Lal, Follett, and Kimble 2003; Solomon et al. 2002; Whitmore, Bradbury, and Johnson 1992). As early as 1905, for example, it was reported that Canadian prairie soils had lost more than 20-30% of the organic matter originally present in the plow layer (Janzen 2001). This fast depletion trajectory is due in part to a loss of physical protection provided by soil aggregates (Six et al. 2002a), with cultivation breaking up aggregate structures and leading to increases in oxidation and mineralization rates (Lal, Follett, and Kimble 2003). After these initial losses, however, SOM has been found to stabilize (Arrouays and Pelissier 1994; Murty et al. 2002), and it has been proposed that such losses could be reversed in response to the ongoing addition of root matter and other crop residues to soil (Lal, Follett, and Kimble 2003). It is this period, after stabilization, when it has been proposed that accumulations can occur, that is the focus of our study.

Our central hypothesis is that decades of high-input agriculture have led to a significant accumulation of SON within the landscape and that this accumulation may contribute to time lags in catchment response after changes in management practices. Our objective is (1) to use historical and current (mid-20th century to present) soil sampling data to provide direct evidence of potential changes in soil N content over time, (2) to place such evidence in the context of watershed-scale mass balance studies, and (3) to develop a parsimonious modeling framework to explain decadal-scale changes in SON. Our specific focus is on agricultural soils of the Mississippi River Basin (MRB), an area that covers approximately 41% of the contiguous United States and includes more than 800,000 km^2 cropland, much of which has been under intensive cultivation since the mid-19th century (R. E. Turner and Rabalais 2004). Thus, our paper focuses on answering the following two questions:

- Is N accumulating in agricultural soils, and if so, in what form, and in what magnitude?

- What are the implications of such accumulation with respect to time lags between changes in management practices and water quality benefits?

2.2   Materials and Methods

2.2.1 Soil Resampling Studies

We synthesize data from two studies, the first (carried out by the authors) in Iowa and the second a smaller study in Illinois (Mark B. David et al. 2009), both of which were designed to assess anthropogenic changes in agricultural soils of the United States Midwest over multiple decades. Details on sample collection and analysis methodologies for the two studies are provided in supplement 2. In both studies, soil cores were obtained from plots under row crop agriculture that had been previously sampled in the mid-1900s and analyzed for total N (TN) content. Accumulation or depletion was estimated as the difference between the current and the mid-1900s N content. Such a resampling approach has commonly been employed to assess changes in soil C stocks over time (Murty et al. 2002; West and Post 2002), but has not been broadly utilized to evaluate potential changes in soil N.

In the Iowa study, soil samples from 61 representative pedons belonging to 46 different soil series in 21 counties across Iowa were obtained in 2007 (**Figure 2.2**). These sites were previously sampled as part of the National Cooperative Soil Survey (NCSS) (between 1943 and 1963, median sampling year 1959), and all but three of these sites remained under intensive cultivation during this time frame (see Veenstra (Veenstra 2010; Veenstra and Burras 2015)).   Data from the Illinois study is based on samples obtained from six sites in central Illinois (**Figure 2.2**) located on poorly drained Mollisols that were under corn-soybean rotations, were tile-drained, and had no history of manure application (Mark B. David et al. 2009).   All six sites were originally sampled in 1957 and resampled in 2002.

Figure 2.2. Accumulation of TN in the subsurface based on historical resampling studies of agricultural sites in the Mississippi River Basin (MRB).
The top left panel shows the MRB with the location of the sites in Iowa and Illinois, while the top right panel shows the 61 sampling locations for Iowa. The bottom left panel shows the mean TN accumulation (g N/Mg soil) between 1957 and 2002 for the six sites in Illinois.[19] The bottom right panel shows the mean TN accumulation (g N/Mg soil) for the 61 Iowa sites.[20] Error bars in both plots correspond to the standard error of the mean. Both studies show net N accumulation across the soil profile, with the majority of accumulation occurring from 25–100 cm.
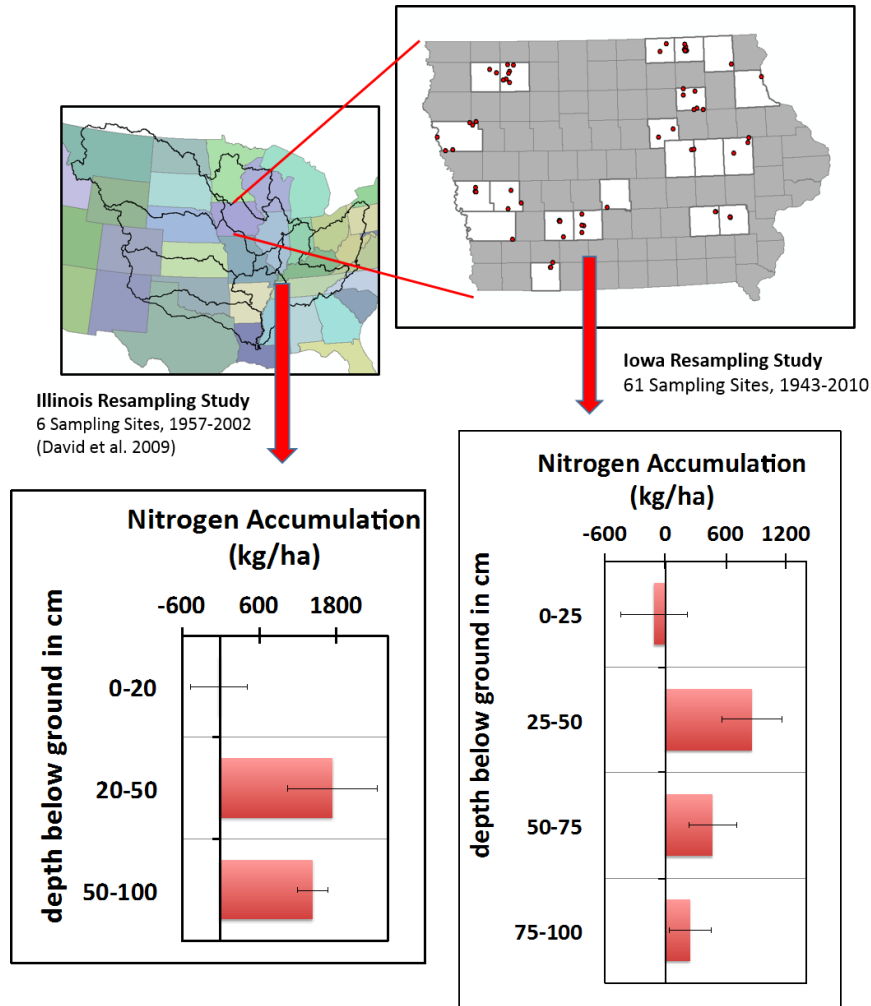
2.2.2   Trend Analysis of Soil Data across the MRB

The resampling study described in the previous section was used to quantify N accumulation at specific locations based on two points in time, an approach commonly used for the assessment of C sequestration in plots under long-term tillage (John M. Baker et al. 2007). We complemented this historical resampling approach with analysis of NCSS soil samples (NCSS 2014) obtained across the MRB from 1980 to 2010 (**Figure 2.3**) to test for negative or positive trends over time in TN. Reported values for bulk density and TN were standardized to depth layers of 25 cm (0-25 cm, 25-50 cm, 50-75 cm, 75-100 cm). TN concentrations (g Mg^{-1}) were obtained directly from NCSS chemical analysis data (NCSS 2014), reported in the database as percent N. Area-based estimates of TN content were calculated from the thicknesses of the soil layers and bulk density values.

Samples were selected for analysis based on the following criteria: availability of (1) TN data to a depth of *at least* 25 cm; (2) soil texture data, including percentages of clay, sand and silt; and (3) latitude and longitude data. Only sample sites falling on land classified as cropland were included in the analysis, as confirmed using United States Geological Society land-use data sets (Price et al. 2007). Based on this criteria, a total of 2069 samples were available at the $0 - 25$ cm depth, 1759 samples for the $25 - 50$ cm depth, 1505 samples for $50 - 75$ cm, and 1320 samples with complete data from 0 - 100 cm. Trend analysis was carried out at each depth range with all the available samples for that range, and also over the entire 100-cm depth using the subset of 1320 samples. Multiple linear regression (MLR) was performed to account for the impact of multiple explanatory variables (e.g. climate and soil texture) on the observed trends in TN (Helsel and Hirsch 1992). See supplement 3 for further description of the MLR analysis.

Figure 2.3. Accumulation of TN in agricultural soils across the MRB, 1980-2010, based on 2069 soil samples from the NCSS database.
The number of soil samples for the different depths and in the different years are presented in Supplementary table 4. (a) The number of samples used for the TN analysis, by sub-basin. (b) TN accumulation rates for the four depth intervals (0-25 cm, 25-50 cm, 50-75 cm, 75-100 cm). Data points correspond to yearly means, and error bars to standard errors for the yearly means. Trend lines are obtained from multiple linear regression analysis of TN data (c) Depth patterns of soil TN content in 1980 and 2010 reveal the greatest accumulation in the top 25 cm.
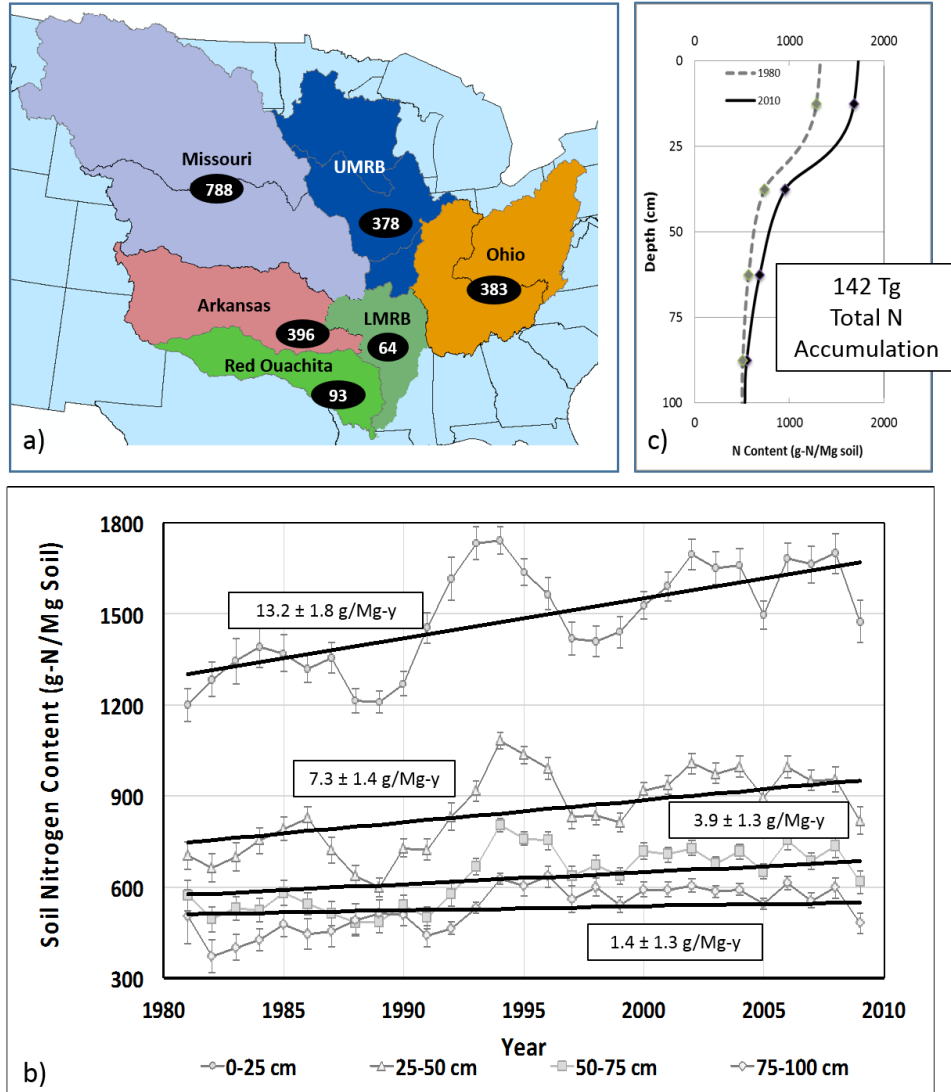
2.3   Modeling Framework and Illustrative Case Study

We developed a parsimonious model to describe decadal-scale changes in SON following the initial conversion of grassland or forested land to agriculture, and then its trajectory under intensive agriculture.

We considered the mass of SON in the landscape M(t) (kg ha^{-1}) to be made up of two pools, an active pool M_{act} (kg ha^{-1}) subject to mineralization or immobilization, and a protected pool M_{prot} (kg ha^{-1}) which, when conditions controlling physical and chemical protection mechanisms remain stationary (Six et al. 2002a), persists in a steady state, with no net mineralization or immobilization. Using this framework, the time (t) evolution of the SON pool is expressed as:

$$M(t) = M_{prot} + \left[\frac{\lambda}{k}(t-1) + \frac{a_0}{k}\right] + \left(M_{act\_0} + \frac{\lambda}{k} - \frac{a_0}{k}\right)e^{-kt} \qquad (2.1),$$

where M_{act_0} is the initial mass of the active SON pool, a_0 the initial net N input, λ (kg ha^{-1}) is the rate of increase in the net N inputs, and k is the mineralization rate constant (y^{-1}) (details of the derivation provided in supplement 4). Net N inputs are the difference between total N inputs (fertilizer N, atmospheric N deposition, biological N fixation) and N outputs via crop uptake. As described below, different phases of the landscape's evolution are characterized by different values of a_0, M_{act_0} and λ.

Using the above framework, we used Rooks County, Kansas as a case study to explore dynamics in SON depletion and accumulation before and after cultivation and under different management regimes. Rooks County was selected due to its location within the MRB, its long history of cultivation (1870-present), the high proportion of county land maintained under high-input agriculture (50% cropland, wheat/sorghum rotation), and the availability of both pre- and post-cultivation estimates of SON as well as detailed N mass balance data over time (1910-1978) (Burke et al. 2002). We modeled five different phases to represent the anthropogenically induced evolution of the landscape: (1) native grassland, pre-cultivation (1840-1890); (2) post-cultivation, low-input agriculture (1890-1910); (3) post-cultivation, low-input agriculture, reduced productivity (1910-1950); (4) post-cultivation, high-input agriculture (increasing inputs) (1950-2000); and (5) post-cultivation, high-input agriculture

(stabilized input levels) (2000-2010). Rationales for the parameters in the different periods are provided in supplement 4. Our objective in developing the model was to provide an illustrative tool for exploring the potential for legacy N accumulation under intensive agriculture. Rigorous calibration and validation of the model requires additional site-specific input data that is beyond the scope of this paper.

2.4   Results

2.4.1   Changes in Soil N Stocks

2.4.1.1 Resampling Studies in Iowa and Illinois. For the Iowa resampling study, our results show a net increase in TN of 1478 ± 547 kg ha^{-1} over the 0 – 100 cm study depth. The TN content in the surface layer (0-25 cm) was found to decrease slightly, from 2140 ± 60 g-N Mg^{-1} soil to 2110 ± 70 g-N Mg^{-1} soil, although the difference was not significant (Wilcoxon signed rank test, $p=0.162$) (Figure 2.2, Table 2.1). At greater depths, however, significant increases were observed. As shown in Table 2.1, the TN content increased by 22% from 25-50 cm, by 20% from 50-75 cm and by 14% from 75-100 cm ($p<0.001$, $p=0.013$, $p=0.040$). Assuming a constant rate of increase over the study period (1959 to 2007), the above result suggests a yearly accumulation rate of 30.8 ± 11.4 kg ha^{-1} y^{-1}.

Table 2.1. Historical and current magnitudes of soil TN content based on resampling sites originally sampled in the mid 1900s.

Sixty-one Iowa sites were first sampled at a median date of 1959 and then resampled in 2007. A significant change in the TN content of the soils is evident for the Iowa study, particularly from 25-50 cm. Positive values indicate accumulation. The six Illinois sites were sampled first in 1957 and then again in 2002. Increases in the soil TN content were also observed in the Illinois study; the increases were not significant, however, due to the smaller sample size.

Location	0-150 cm	Historical	Current	Number of Samples	Accumulation/Depletion		
		g-N/Mg soil	g-N/Mg soil	n	g-N/Mg soil (kg-N/ha)	p-value	Percent Change
Iowa Study (1959-2007)	0-25 cm	2,140 ± 60	2,110 ± 70	61	-30 ± 90 (-110 ± 331)	0.162	-1%
	25-50 cm	1,060 ± 40	1,290 ± 70	61	230 ± 80 (864 ± 300)	<0.001	22%
	50-75 cm	610 ± 40	740 ± 50	25	120 ± 60 (474 ± 237)	0.013	20%
	75-100 cm	440 ± 40	500 ± 30	12	60 ± 50 (250 ± 209)	0.040	14%
	0-100 cm	1,063 ± 23	1,160 ± 29	-	95 ± 36 (1478 ± 547)	–	9%
Illinois Study (1957-2002)	0-20	2,733 ± 176	2,583 ± 119	6	-150 ± 213 (-17 ± 443)	0.516	-5%
	20-50 cm	1,088 ± 127	1,387 ± 164	6	298 ± 77 (1746 ± 689)	0.140	27%
	50 -100 cm	297 ± 29	492 ± 38	6	195 ± 12 (1436 ± 235)	0.016	66%
	0 - 100 cm	1022 ± 54	1179 ± 58	-	157 ± 49 **(3,164 ± 1033)**		15%

The Illinois resampling results demonstrate a 16% net increase in TN, or 3,164 ± 450 kg ha^{-1} averaged over the 0 – 100 cm depth, between 1957 and 2002. Similar to the Iowa study, an insignificant (5%) decrease in TN was observed in the surface layer (0-20 cm) (p=0.516) (**Figure 2.2**, **Table 2.1**), while TN increased from 20-50 cm (27%) (p=0.140) and from 50-100 cm (66%) (p=0.016). Again assuming a constant increase in TN content over this time period, the total increase corresponds to a yearly rate of 70.3 ± 10.0 kg ha^{-1} y^{-1}. Despite the small sample size for the Illinois study (n=6), these findings are significant (p=0.016) from 50-100 cm and are suggestive of potential increases in TN at a decadal scale in soils under high-input agriculture.

2.4.1.2 Trend Analysis of Soil TN Data across the MRB. Data from 2,069 NCSS soil samples (NCSS 2014) obtained from all six sub-basins of the MRB (**Figure 2.3a**) between 1980 and 2010 was utilized to identify possible trends in the TN content of MRB agricultural soils. Results of the multiple linear regression (MLR) analysis indicate significant increases in soil TN concentrations (g-N Mg^{-1}) between 1980-2010 in the 0-25, 25-50 and 50-75 cm layers (13.2 g-N Mg^{-1}, p<0.001; 7.3 g-N Mg^{-1}, p<0.001; 3.9 g-N Mg^{-1}, p=0.003) (**Table 2.2**, **Figure 2.3b)**. An increase (1.4 g-N Mg^{-1} y^{-1}) was also seen from 75-100 cm, although the difference was not significant (p=0.294). Over the entire depth range, using data only from pedons sampled to a depth of 100 cm, the accumulation rate is 3.4 $\pm$ 1.6 g-N Mg^{-1} y^{-1} (p=0.003). Based on reported bulk density values, these results correspond to total increases (0-100 cm) of 54.8 ± 25.8 kg ha^{-1} y^{-1}.

Table 2.2. Accumulation rates for TN in soil samples across the Mississippi Basin (1980-2010) based on MLR analysis of the NCSS dataset.
All available samples at each depth range were used to calculate the depth-specific accumulation rates. Overall accumulation rates (0-100 cm) are calculated not simply as the mean of the four smaller depth increments, but as part of a separate analysis in which only pedons with complete sampling data to 100 cm were considered. As the thickness of the soil profile can vary significantly, and because organic matter may accumulate preferentially in the upper layers of shallower soils (69), we use the more conservative estimate of accumulation suggested by the integrated analysis for the 0-100 cm depth range in subsequent discussions of estimated accumulation rates across the MRB.. See supplementary table 7 for results by sublayer for the 1320-sample subset, and a discussion of the differences in the two estimation methodologies.

Soil Parameter	Depth (cm)	Number (n)	Bulk Density (g cm^{-3})	Rate of Change (g Mg^{-1} y^{-1})	Rate of Change (kg ha^{-1} y^{-1})	p-value
	0-25	2069	1.55	13 ± 1.8	51 ± 7.0	<0.001
	25-50	1759	1.61	7.3 ± 1.4	29 ± 12.9	<0.001
Total Nitrogen	50-75	1505	1.64	3.8 ± 1.3	16 ± 5.3	0.003
	75-100	1320	1.65	1.6 ± 1.4	6.6 ± 5.8	0.250
	0-100	1320	1.61	3.4 ± 1.6[a]	55 ± 25.80	0.003

[a] Mass-per-area accumulation rates (0-100 cm, kg ha^{-1} y^{-1}) are calculated using the mass-per-mass accumulation rates (0-100 cm, g Mg^{-1} y^{-1}) and the corresponding bulk density.

2.5   Discussion

2.5.1 Quantifying Legacy: Synthesis of Mass Balance and Soil Sampling Results

The first question posed in the introduction was whether N is accumulating in agricultural soils, and if so, in what magnitude. The results from the Iowa resampling study, based on data obtained from 61 sites across Iowa, show a 9% increase in TN and suggest an accumulation rate of 30.8 ± 11.4 kg ha^{-1} y^{-1} from 0 – 100 cm. A somewhat larger percent increase (15%) was seen from 0-100 cm at the Illinois resampling sites by David et al.(Mark B. David et al. 2009), corresponding to an accumulation rate of 70.3 ± 18.4 kg ha^{-1} y^{-1}. Furthermore, our analysis of 2069 soil samples in the MRB demonstrates a 10% increase in soil TN from 0-100 cm between 1980 and 2010, corresponding to an accumulation rate of 54.8 ± 25.8 kg ha^{-1} y^{-1} in cropland soil and an overall accumulation magnitude of 142 Tg N over the MRB over the 30-year period (**Figure 2.3c**). While other studies have alluded to the possibility of N_R accumulating within the soil profile based on mass balance or modeling-based estimates (V. Smil 1999b; Clair et al. 2014; Leip, Achermann, et al. 2011), our study for the first time, provides direct, large-scale evidence of such accumulation.

We next explored the relationship between these accumulation magnitudes and estimates of N fluxes in MRB to assess the significance of these magnitudes at the basin scale. We have calculated watershed-scale net N inputs for the years 1980-1996 in the MRB to be 7.1 Mt y^{-1} based on data reported by Goolsby et al. (Goolsby et al. 1999). During this period, the riverine flux of nitrate from the MRB to the Gulf of Mexico is estimated to have been 1.6 ± 0.1 Mt y^{-1} (Goolsby et al. 1999), which constitutes approximately 23% of net N inputs. In this context, our estimate of soil N accumulation across the MRB (3.8 ± 1.8 Mt y^{-1}) suggests that soil N accumulation could account for another 53 ± 25% of net N inputs (**Figure 2.4**). While significant uncertainty remains regarding the actual magnitude of this estimate of N accumulation, the present results strongly suggest that changes in soil N stocks constitute a *significant* fraction of total N inputs under intensive agriculture and thus should be explicitly considered in watershed as well as regional and global-scale N mass balance studies.

Figure 2.4. The fate of anthropogenic N inputs across the MRB.
The figure shows a watershed-scale mass balance for the MRB calculated based on data from Goolsby et al. (Goolsby et al. 1999). The letters correspond to fluxes represented schematically in **Figure 2.1**. Riverine N output (*h*) from the Mississippi accounts for approximately 23% of net N inputs. The present study indicates that legacy N accumulation (*g*) within agricultural soils may account for as much as 3.8±1.8 Mt/y (approximately 53±25% of net N inputs). Although direct measurements of other fluxes are scarce, recent measurement data from the U.S. corn belt suggest an annual nitrous oxide (N_2O) flux (*f*) for the MRB river network of 0.1 $\pm$0.01 Mt/y (~1 % of net inputs) (P. A. Turner et al. 2015). Denitrification to N_2 (*f*) likely represents a much larger portion of the budget, but the magnitudes remain largely unconstrained (Fowler, Coyle, et al. 2013). Modeled estimates of sediment burial (l) in reservoirs across the MRB suggest an additional N sink on the order of 0.6 Mt y^{-1} (8% of net inputs) (Stallard 1998; Stephen V. Smith et al. 2005).
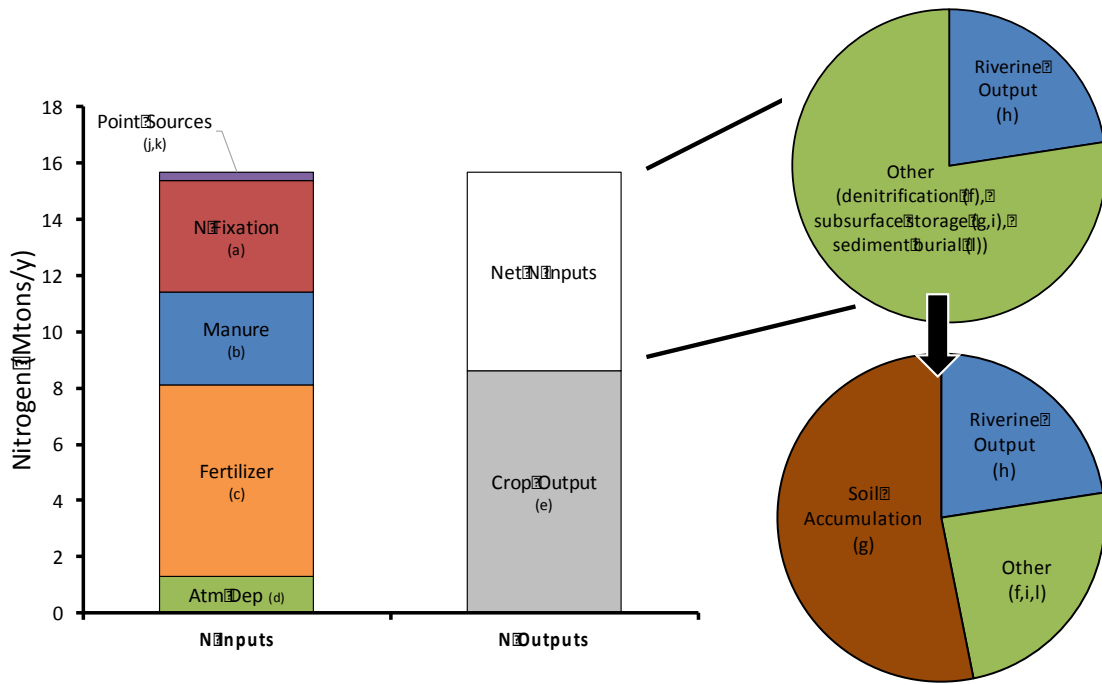
2.5.2 Understanding Legacy: A Conceptual Model to Explain N Depletion and Accumulation Dynamics

The importance of agricultural soil as an N-sink, as described above, leads us next to question the mechanism behind such subsurface N accumulation. We hypothesize that such accumulation is a direct result of increased N fertilizer use (inorganic and manure N), increases in N fixation due to dramatic increases in soybean cultivation between 1940 and the present, and the adoption of conservation tillage practices (Y.-K. Zhang and Schilling 2006; Davidson and Ackerman 1993b). Accordingly, we can utilize the parsimonious modeling framework introduced in section 2.3 to describe not only the depletion of SON following the initial conversion of grassland or forested land to agriculture, but also the accumulation of N suggested by our analysis of soil data from the MRB (**Figure 2.4**).

In the pre-cultivation period (Phase I: 1840 - 1890), SON is assumed to be at steady state, with most of the organic nitrogen in the protected pool (**Figure 2.5**). The start of cultivation (Phase II: 1890 - 1910) leads to conversion of a portion of the protected SON to active SON, which can then be mineralized and leached from the soil profile. Net N inputs are negative in this period due to intensive cropping practices, but little input of fertilizer (Burke et al. 2002). With these changes, there is an exponential decrease in the total mass of SON, with the system eventually evolving to a new steady state (**Figure 2.5**). After the first 20 years of cultivation (Phase III: 1910 — 1950), we assume crop productivity to be diminished which leads to an increase in the net N inputs, and a stabilization of soil N levels (**Figure 2.5**). Finally in Phase IV (1950 – 2000), the system transitions to a high-input state and soil N levels begin to rise. Then, at the start of Phase V, with the stabilization of net N inputs, soil N levels also stabilize.

Figure 2.5. Modeling framework describing N depletion following conversion of native prairie/grassland to conventional agriculture, and N accumulation following agricultural intensification.

On the top left is a model schematic representing the flow of N through the active pool of soil organic N. The figure on the bottom shows the evolution of the protected and active N pools following land-use change according to the five phases described in the text. The inputs corresponding to the five phases are shown in the inset, while the values of the model parameters corresponding to the phases are provided in the table.
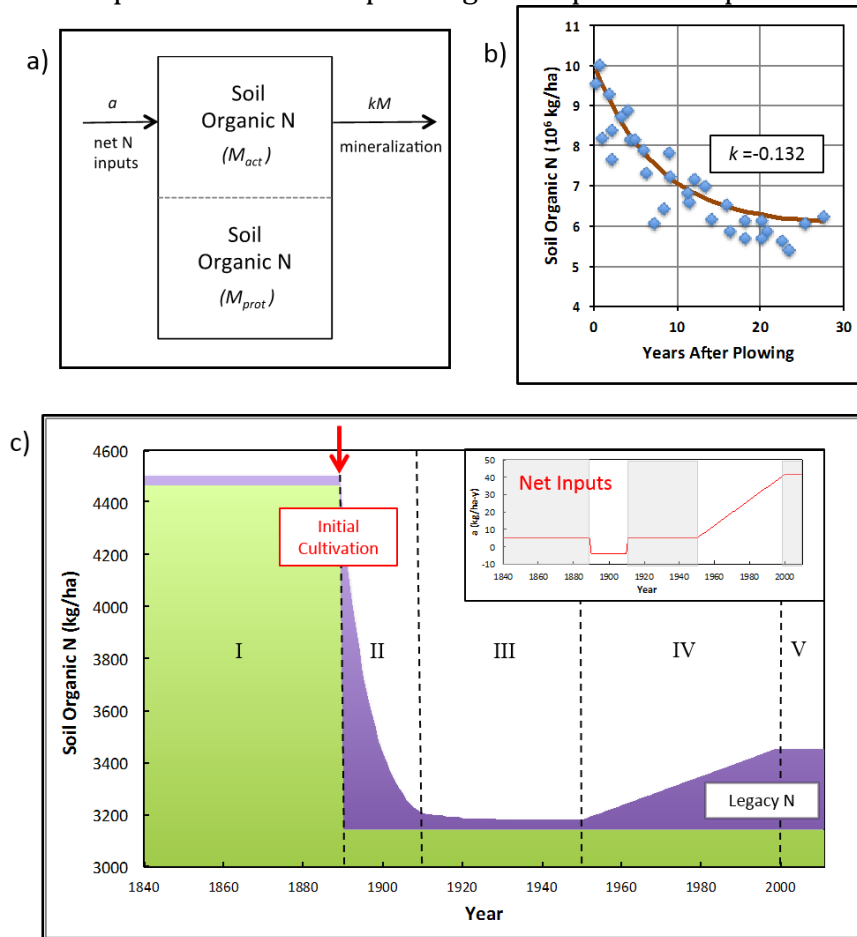
The accumulated or legacy N, conceptualized as the difference between the Phase III and Phase V steady states, corresponds to an approximately 9% increase over SON levels in the depleted steady state. This value is similar to the 10% increase observed over time in our MRB soil sampling data and the 9% increase observed in the Iowa resampling study. The modeling results suggest not only that soil N accumulation is possible in land under continuous cultivation, but that the trajectory

of change can be described using the same approach as that used to describe the more well-known depletion of soil organic matter after initial cultivation.

Of course, the above simulation is based on a simplification of the trajectories of change in management practices and land use. We have assumed step changes between phases, but in reality changes occur more gradually. In its current state, the model described herein is primarily conceptual in nature, used to demonstrate the possibility of N accumulation in agricultural landscapes, and will require further modifications in terms of model parameterization as well as descriptions of inputs and outputs to more fully simulate landscape-scale changes in SON.

2.5.3 Implications of Legacy: Time Lags in Landscape Response

The most significant implication of such a buildup of soil N relates to time lags observed between land-use changes and alterations in stream N concentrations (Meals, Dressing, and Davenport, n.d.). Based on the current results, we contend that there are two components of this time lag attributable to two different types of legacy: a hydrologic legacy and a biogeochemical legacy. The hydrologic legacy corresponds to dissolved N in groundwater reservoirs and unsaturated zones, and its existence contributes to the *hydrologic time lag* – defined as the average time required for dissolved N species to move from the point of application to the point of concern. The existence of the hydrologic time lag is well accepted, with a variety of hydrogeologic controls having been found to result in travel times ranging from days to decades (Hamilton 2012b; L. J. Puckett 2004; Molenat and Gascuel-Odoux 2002). The second type of legacy, the biogeochemical N legacy, arises from retention of N within the root zone, likely in organic form, and constitutes a long-term source for mineralization and NO_3^- leaching. The existence of such a biogeochemical legacy for phosphorus (P) is well known due to its reactive properties, and legacy sorbed P accumulation has been reported in both soil and sediments (Jarvie, Sharpley, Spears, et al. 2013; Hamilton 2012b). The possibility of such a biogeochemical legacy for N, however, has been mostly neglected, as N in the form of NO_3^- is non-sorbing and is easily leached from soils (Hamilton 2012b).

The magnitude of the associated biogeochemical time lag is a function of not only the mass of TN accumulation, which has been the focus of this paper, but also the rates of organic N mineralization and the loss of dissolved N through the different biogeochemical and hydrologic pathways. Further research is needed to clarify these mechanisms and pathways. However, as a first estimate, we can utilize the modeling framework developed in Section 4.2 to determine the time lag associated with depletion of the 142 Tg of legacy N suggested by our analysis of MRB soil data. Assuming a complete cessation of agricultural production in the region and a return of net annual inputs (a) to the pre-cultivation levels of 5 kg ha^{-1} y^{-1}, our model results indicate a biogeochemical time lag of 35 years for 99% depletion of the legacy N. The total lag time would then be a function of both the biogeochemical and the hydrologic lag time, and the latter in itself can be on the order of decades depending on the sizes of saturated and unsaturated zone reservoirs. With such long time frames for recovery, it is thus critical to understand both the accumulation and the ultimate fates of these significant stores of subsurface N for sustainable management practices in large-scale agroecosystems such as the MRB.

2.5.4 Intersecting Lines of Evidence

Understanding the long-term dynamics of N in agricultural soils is complex due to the poorly constrained fluxes of denitrification, mineralization and immobilization over varying spatio-temporal scales (Hofstra and Bouwman 2005; J.N. Galloway et al. 2008). However, recent research, as described below, provides intersecting lines of evidence that point towards the accumulation of legacy N in the soil profile in much larger magnitudes than previously conceptualized. For example, using a combination of mass balance and process based modeling, the United States Environmental Protection Agency estimates cropland N accumulation in US to be equal to 17% of fertilizer N inputs (Science Advisory Board 2011), while accumulation in Canada has been estimated to be equal to 19% of total N inputs (Clair et al. 2014). Accumulation is also suggested by isotope tracer studies that show a 15% retention of ^{15}N-labeled NO_3^- fertilizer within the soil profile nearly 30 years after application, implying that N fertilizer has a significant residence time in the SON pool (Sebilo et al. 2013).   The existence of legacy N is further corroborated by observations of biogeochemical

stationarity for N in landscapes under intensive agriculture (Nandita B. Basu, Destouni, et al. 2010; Sally E. Thompson et al. 2011). In such landscapes, the supply of N to surface waters appears to be transport-limited rather than source-limited, suggesting that the existence of legacy N within the landscape provides an ongoing N source and therefore a positive, linear correlation between riverine N flux and discharge, with N concentrations remaining relatively invariant. This behavior is in contrast to that observed in more pristine landscapes, where N concentrations vary in time in response to source limitations (Godsey, Kirchner, and Clow 2009).

Our work makes a unique contribution to this literature by providing the first *measured* estimate of large-scale N accumulation in soils across the MRB. The intersection of such varying lines of evidence, both direct and circumstantial, leading to estimates of soil N accumulation, suggests (a) that we must acknowledge the existence of a growing pool of SON in agricultural landscapes and (b) that we must more explicitly explore the impacts of such a pool on future water quality.

2.6 Conclusion

Our study has three fundamental contributions. First, our finding of significant N accumulation in agricultural soils across the MRB (3.8±1.8 Mt/y) makes a critical contribution towards clarifying the fate of the "missing" N that is consistently referred to in reports of watershed-scale mass balance studies (21,78–80). Although caution must be exercised in relying upon the precise magnitude of accumulation due to large uncertainties in the data, by identifying a clear possibility of significant N accumulation within agricultural soils we make considerable progress towards the closing of N budgets, from the watershed to the global scale. Second, we have developed a simple model that describes both the accumulation and depletion dynamics of SON arising from anthropogenic perturbations on the landscape, thus confirming our hypothesis that the same underlying mechanism can be used to describe both N depletion following plowing and N accumulation as a result of high-input agriculture. The third contribution of this study is with respect to time lags between best management practices and water quality benefits. The significant mass of organic N accumulating in agricultural soils implies that stream N concentrations will persist for decades after fertilizer inputs have ceased. Indeed, the time lag would

in most cases be significantly greater than that estimated based on the hydrologic legacy alone. Our study for the first time links multiple lines of evidence to show convincingly that N, like P, has a biogeochemical legacy, a legacy that complicates our previous understanding of the fate of this nutrient in anthropogenic landscapes and that must be accounted for in intervention efforts to improve water quality.

2.6   Acknowledgements

Chapter 3 - Catchment Legacies and Time Lags: A Parsimonious Watershed Model to Predict Effects of Legacy Storage on Nitrogen Export

3.1   Introduction

High levels of nonpoint source pollution associated with current agricultural practices have contributed to water quality impairment and destruction of aquatic ecosystem habitats at both local and global scales (R. W. Howarth et al. 2002; Tilman et al. 2002). In particular, increased nutrient loads delivered from watersheds due to agricultural intensification, industrialization, and urbanization have led to the persistence of large hypoxic zones in both inland and coastal waters (Kling et al. 2014; Diaz and Rosenberg 2008; W. M. Kemp et al. 2009; N. N. Rabalais et al. 2010; Osterman et al. 2009). Watershed management practices to target these non-point source pollutants have in many cases resulted in little or no improvement in water quality, even after extensive implementation of conservation measures (Meals, Dressing, and Davenport 2010; Hamilton 2012a; Jarvie, Sharpley, Withers, et al. 2013). The *lag time* between implementation of conservation measures and resultant water quality benefits has recently been recognized as an important factor in their "apparent" failure (Meals, Dressing, and Davenport 2010; Y.-K. Zhang and Schilling 2006). Conservation measures are often implemented, however, without explicit consideration of such lag times, and with the expectation that they will lead to immediate benefits. Failure to meet such expectations then discourages vital restoration efforts (Meals, Dressing, and Davenport 2010). In order to address this problem, it is important to quantify the lag times associated with watershed management efforts a priori and to implement restoration strategies that are targeted specifically at minimizing lag times as well as maximizing restoration benefits.

The focus of the present research is to develop a framework for understanding the time lags between land-use change or implementation of conservation measures and stream water quality benefits. We hypothesize that such time lags arise from legacies that have accumulated in the landscape over decades of human impact (Nandita B. Basu, Destouni, et al. 2010; MacDonald and Bennett 2009; S. E. Thompson

et al. 2011). Legacies can be conceptualized as hydrologic legacy, in the form of dissolved solute that is delayed in its transport to the stream due to slow groundwater transport pathways, and biogeochemical legacy, arising from solute that has undergone biogeochemical transformation and that is retained within the soil matrix. Both solute and watershed attributes define whether such legacy sources will be created, and, if created, their spatial location within the watershed.

In the present study, we focus specifically on the fate of anthropogenic nitrogen (N) in predominantly agricultural watersheds. Significant time lags between land-use change and the expected decreases in stream nitrate concentrations have consistently been noted (Meals, Dressing, and Davenport 2010). Such time lags have chiefly been attributed to what we have defined as the *hydrologic* N legacy, a legacy existing primarily in groundwater reservoirs or thick unsaturated zones in the form of dissolved nitrate (Hamilton 2012a; McMahon et al. 2006a; L. A. Baker et al. 2001). Recent work, however, suggests that consideration of this hydrologic legacy alone does not adequately account for the magnitude of legacy N existing within intensively managed landscapes. Watershed-scale mass balance studies, for example, consistently indicate the presence of "missing" N stores(Hong, Swaney, and Howarth 2013; Mark B. David, Drinkwater, and McIsaac 2010a; Boyer et al. 2002; Gilles Billen et al. 2009a; Kroeze et al. 2003; N. Chen et al. 2008; Liu, Watanabe, and Wang 2008; Janzen et al. 2003), and recent modeling of the global N cycle has led to estimates of terrestrial N sequestration ranging from 27-100 Tg N/yr (Schlesinger 2008; Fowler, Pyle, et al. 2013; Zaehle 2013). At the plot scale, a recent isotopic tracer study designed to investigate the long-term fate of nitrate fertilizer has shown that approximately 15% of fertilizer N applied to agricultural land is present within the soil profile in organic form 30 years after its initial application (Sebilo et al. 2013). In another study (Haag and Kaupenjohann 2000), isotopic data were used to demonstrate that the nitrate measured in streams is generated from organic nitrogen created from fertilizer applied to the landscape decades previously. These results are indicative of high levels of N retention within agricultural soil over a multi-year period, and thus the existence of a biogeochemical N legacy, which is corroborated by

our recent research showing a basin-wide accumulation of organic N in the Mississippi River Basin (Van Meter et al., n.d.).

Despite such studies demonstrating the existence of both hydrologic and biogeochemical N legacies, most mechanistic watershed models lack an explicit mechanism to describe the effects of these legacies on stream nitrate concentrations (Meals, Dressing, and Davenport 2010; Sanford and Pope 2013; Bouraoui and Grizzetti 2014). Most lumped watershed models such as SPARROW and GlobalNEWS as well as the Net Anthropogenic Nitrogen Inputs (NANI) mass balance approach assume the N cycle to be at a steady state, either on a yearly basis or over a multi-year period, such that stream export is a fixed percentage of net annual inputs (R. W. Howarth et al. 2006; Alam and Goodall 2012; Swaney et al. 2012a; Wellen et al. 2012; D. Chen, Hu, and Dahlgren 2014). Even attempts at quantifying the benefits of different pollution-reduction scenarios (e.g. land-use change, reductions in fertilizer application, etc.) using mechanistic models such as SWAT have focused only on the concentration reduction benefit that will be achieved at infinite time, with no consideration of the time that will be required to achieve concentration-reduction goals (Jha, Gassman, and Arnold 2007; Rabotyagov et al. 2010). Such consideration, however, is critical for watershed managers who must make decisions regarding the allocation of limited resources for conservation (Meals, Dressing, and Davenport 2010).

In this paper, we develop a parsimonious analytical model to quantify the concentration reduction benefits associated with watershed restoration efforts as a function of both hydrologic and biogeochemical legacies, with particular attention being paid to the ways in which spatial patterns of landscape conversion impact concentration reduction scenarios. Concentration reductions are considered to occur as a function of both the groundwater travel time distribution and biogeochemical controls, including the existence of a biogeochemical N legacy within the soil profile and denitrification dynamics along groundwater pathways. The paper presents analytical relationships between: (a) percent reductions in mean concentrations at the watershed outlet as a function of the fractional watershed area over which the management practice is implemented, and (b) the temporal trajectory of watershed

response that defines the time required to achieve required reductions in contaminant concentrations. Using these analytical relationships, we explore idealized scenarios of land-use conversion and compare these results with concentration trajectories observed in a small Midwestern watershed undergoing an extensive prairie habitat restoration project. We further use these relationships to establish an optimization framework for meeting concentration reduction goals by exploring tradeoffs between costs associated with the conversion of land out of row-crop production and the time required to achieve the desired concentrations. Such explorations enable analysis of the performance of conservation measures under spatially varying patterns of intervention as a function of legacy N accumulation, N removal dynamics in the subsurface, and watershed travel time distributions.

3.2   Model Development

Our conceptual framework is based on the assumption that legacy nutrient stores are present within anthropogenic landscapes and lead to time lags between land-use change and improvements in water quality. Such nutrient legacies have developed in agricultural watersheds as a function of long-term application of N and phosphorus (P) fertilizers, with a strong linear correlation having been found between N and P levels in soils and multi-decadal cumulative nutrient surpluses (MacDonald and Bennett 2009; Van Meter et al., n.d.; Lewis et al. 2006a). Our focus herein is specifically on the N legacy in agricultural watersheds, but this approach could be readily adapted to other solutes.

As shown in **Figure 3.1**, nutrient legacies produce an internal landscape memory, thus contributing to elevated stream nutrient concentrations for years after external nutrient loading is reduced or stopped altogether. In order to develop an expression for the concentration trajectory at the catchment outlet following land-use change, we conceptualize the landscape to be composed of a bundle of stream tubes, with each point on the landscape being associated with an individual stream tube characterized by a specific groundwater travel time to the catchment outlet (Jury et al. 1990). The full amalgamation of points for the catchment leads to a specific groundwater travel time distribution for the catchment outlet, $f(t)$ This distribution,

in turn, controls the concentration trajectory at the outlet, $C(t)$ (Maloszewski and Zuber 1982; Haitjema 1995; McGuire and McDonnell 2006a), as described by the following equation:

$$C(t) = \int_0^\infty C_s(t - t)f(t)e^{-kt}\,dt \qquad (3.1),$$

where, $C_s(t - t)$ is the contaminant input function or "source function" from the unsaturated zone, and k [T^{-1}] is the first-order rate constant that describes removal processes in the aquifer.

Figure 3.1. Conceptual framework for predicting catchment scale time lags as a function of hydrologic and biogeochemical legacies in the landscape.
The left frame represents depletion of biogeochemical legacy in the source zone. The source zone depletion function is then convoluted with the groundwater travel time distribution (middle frame) to ultimately describe concentrations at the catchment outlet (right frame).
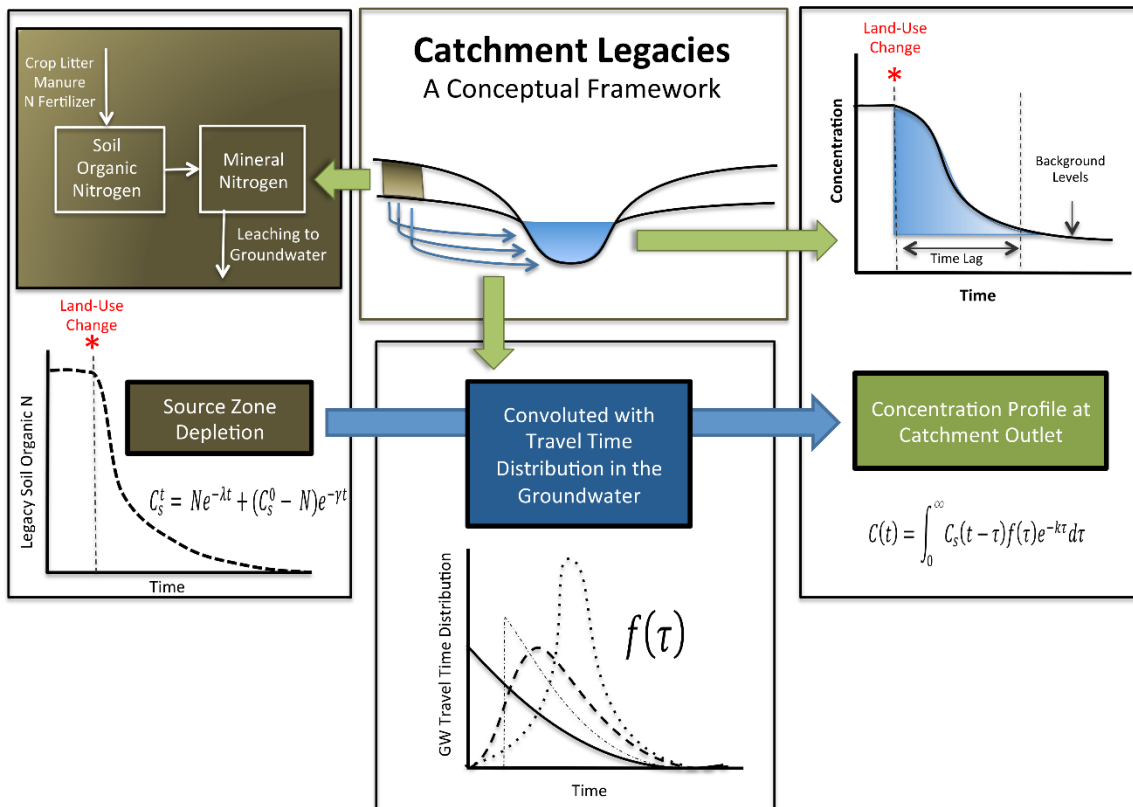
The source function (**Figure 3.1**), developed in Section 3.2.1, is controlled by the biogeochemical legacy in the unsaturated zone, which for N is a function of both

historic anthropogenic N inputs to the landscape and the rate of N depletion from such stores. Each point in the watershed is characterized by its particular source function, which changes form as a function of the timing of human interventions such as land-use change or implementation of conservation measures. While biogeochemical legacy is conceptualized using the "source function," the hydrologic legacy is captured in the travel time distribution, which describes how the source concentrations are being modified as they travel through the watershed (Section 3.2.2). The resulting outlet concentration is a function of both the hydrologic and biogeochemical legacy, and the patterns of land-use change, as described in the following sections.

3.2.1   Biogeochemical Legacy and the Source Function

The left frame of **Figure 3.1** provides a simple schematic for our model of biogeochemical legacy depletion within the source zone after conversion from row-crop agriculture to grassland. Within this framework, excess soil organic N, which has accumulated in response to long-term application of fertilizer N and which constitutes the biogeochemical N legacy, is mineralized to inorganic N, entering the soil mineral N pool. This inorganic N then leaches to groundwater, primarily in the form of nitrate. Although plant uptake and litter inputs will continue to occur after conversion to grassland, we consider these processes to be part of a baseline scenario and therefore only take into account dissipation of excess N through the leaching pathway. In our current simulations, we consider only scenarios in which landscape conversion results in a complete cessation of fertilizer application to the soil system, although this formulation can be easily modified to include cases with ongoing but reduced levels of fertilizer application.

Decomposition of soil organic matter is typically modeled as having first-order reaction kinetics, proportional to the amount of substrate to be decomposed (Porporato et al. 2003; Manzoni and Porporato 2009). Accordingly, within our modeling framework the excess (legacy) soil organic N (SON) is considered to decay over time as a first-order process with a rate constant $/$ (T^{-1}), such that the mass of legacy N (M_{son}) at any time t is given by:

$$\frac{dM_{son}}{dt} = -\, /\, M_{son} \tag{3.2},$$

The N leaving the SON pool enters the mineral N pool that leaches into the groundwater, such that at any point in time the concentration of dissolved N (C_s; M/L^3) can be described by the following equation:

$$\frac{d(V_w C_s)}{dt} = /\, M_{son} - QC_s \tag{3.3},$$

where, Q is the mean annual recharge and V_w (= nsV) is the water volume in the source zone, with n being the porosity, s the saturation and V the volume of the soil column per unit area within the source zone. Here, the first term on the RHS is the input from the organic pool and the second term is the loss from the source zone via leaching. Solving **Equations 3.2** and **3.3** leads to:

$$M_{son} = M_{son}^0 e^{-\, /\, t} \tag{3.4},$$

$$C_s^t = N e^{-\, /\, t} + (C_s^0 - N) e^{-gt} \tag{3.5},$$

where $N = \dfrac{/\, M_{son}^0}{(Q - /\, snV)}$; $g = \dfrac{Q}{snV}$; M_{son}^0 is the initial mass of SON; C_s^0 is the initial concentration of nitrate within the source zone; and C_s^t is the nitrate concentration at time t within the source zone, and acts as the source function described in **Equation 3.1**. The source function can thus be described as a Heaviside function, with C_s^0 being the initial steady-state concentration prior to initiation of land-use change, and C_s^t describing the concentration trajectory after land-use change has been initiated.

3.2.2 Hydrologic Legacy and Patterns of Land-Use Change

We define the hydrologic nutrient legacy as nutrients present in a dissolved form in both the saturated and unsaturated zones. Time lags associated with hydrologic legacy can range from days to weeks to hundreds of years as a function of the distance groundwater must travel to the catchment outlet, the physical properties of the underlying aquifer, and the gradient driving flow through the subsurface (Pijanowski et al. 2007; Hamilton 2012a).

Land-use change in a watershed leads to switching of the source function between C_s^0 and C_s^t. Theoretically, individual points in the landscape may be switched at different points in time, or not switched at all, leading to an infinite number of scenarios that are convoluted as in Equation 1, creating unique concentration trajectories at the outlet. Here, we conceptualize three end-member scenarios based on the distribution of travel times for the watershed. As shown in **Figure 3.2**, spatial patterns of land-use change can be described as truncations of the groundwater travel time distribution, with the three scenarios of change being: (a) frontal, (b) distal and (c) random. The frontal approach corresponds to scenarios where land parcels with the shortest travels times to the catchment outlet are preferentially converted and involves a left-to-right truncation of the exponential travel time distribution (**Figure 3.2a**), as indicated by the grey shaded area of the figure. Conversely, a distal approach corresponds to a preferential conversion of parcels with the longest travel times to the outlet and involves a right-to-left truncation (**Figure 3.2b)**. The third approach, a random conversion, corresponds to a scenario where land-use change has occurred randomly throughout the catchment, with no correlation between land-use change and the groundwater travel time distribution (**Figure 3.2c**).

Figure 3.2. Conceptual framework showing spatial patterns of land-use change as truncations of the groundwater travel time distribution.
The grey shaded areas correspond to the fractional areas (p) of the watershed over which land-use change has occurred for the (a) frontal, (b) distal and (c) random conversion scenarios. The red line in the frontal and distal scenarios is equal to the abscissa of the cumulative frequency distribution of travel times, corresponding to an ordinate of p (or 1-p for the distal scenario), and is the demarcation line between areas that have and that have not undergone land-use change.
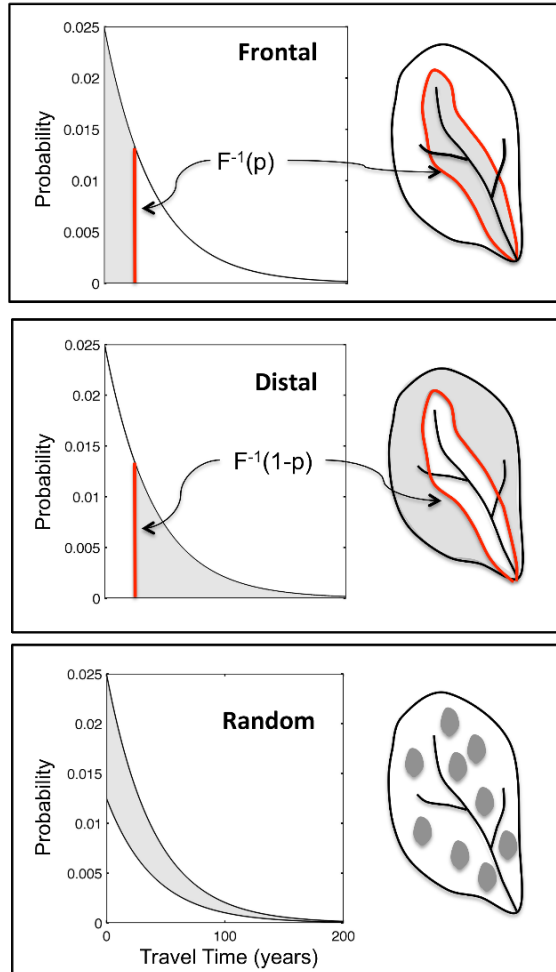
Equations for the flow-averaged concentrations at the outlet at any time t after initiation of land-use change, $C_{ac}(t;p)$ normalized by the concentration before the change $C_{bc}(t;p)$ for the three different spatial conversion scenarios, and a fractional land-use change p can be developed as follows:

40

Frontal

$$\frac{c_{ac}}{c_{bc}}(t;p) = \begin{cases} \dfrac{\displaystyle\int_0^t C_s^{t-t}f(t)e^{-kt}\,dt + \int_t^\infty C_s^0 f(t)e^{-kt}\,dt}{\displaystyle\int_0^\infty C_s^0 f(t)e^{-kt}\,dt}, & 0 \le t < F^{-1}(p) \\[4ex] \dfrac{\displaystyle\int_0^{F^{-1}(p)} C_s^{t-t}f(t)e^{-kt}\,dt + \int_{F^{-1}(p)}^\infty C_s^0 f(t)e^{-kt}\,dt}{\displaystyle\int_0^\infty C_s^0 f(t)e^{-kt}\,dt}, & t \ge F^{-1}(p) \end{cases}$$ (3.6),

Distal

$$\frac{c_{ac}}{c_{bc}}(t;p) = \begin{cases} 1, & 0 \le t < F^{-1}(1-p) \\[4ex] \dfrac{\displaystyle\int_0^{F^{-1}(1-p)} C_s^0 f(t)e^{-kt}\,dt + \int_{F^{-1}(1-p)}^t C_s^{t-t}f(t)e^{-kt}\,dt + \int_t^\infty C_s^0 f(t)e^{-kt}\,dt}{\displaystyle\int_0^\infty C_s^0 f(t)e^{-kt}\,dt}, & t \ge F^{-1}(1-p) \end{cases}$$ (3.7),

Random

$$\frac{c_{ac}}{c_{bc}}(t;p) = \frac{\displaystyle\int_0^t pC_s^{t-t}f(t)e^{-kt}\,dt + \int_0^t (1-p)C_s^0 f(t)e^{-kt}\,dt + \int_t^\infty C_s^0 f(t)e^{-kt}\,dt}{\displaystyle\int_0^\infty C_s^0 f(t)e^{-kt}\,dt}$$ (3.8),

Here $F^{-1}()$ is the inverse cumulative distribution function of the groundwater travel time distribution. It represents the travel time associated with a specific fractional area of landscape conversion and acts as a dividing line (red line in **Figures 3.2a** and **3.2b**) between areas of the watershed bringing in "converted" groundwater and areas bringing in "unconverted" groundwater. The above equations have been developed with the assumption that the groundwater travel time distribution is a complete distribution from 0 to infinity. In actuality, however, these distributions would be truncated, with the maximum travel time being defined by the size as well as the geomorphic characteristics of the watershed, and the equations can be easily modified for truncated distributions following Jawitz et al. (Jawitz et al. 2005).

Groundwater travel time distributions have been assumed to have multiple functional forms based on a range of model types, from the simplest piston-flow model, which assumes that all flow paths have the same velocity and path length, to a dispersion model based on a 1-D solution of the advection dispersion equation

(McGuire and McDonnell 2006a). One of the simplest and most widely used forms is the exponential:

$$f(t) = \frac{1}{m}e^{-\frac{t}{m}} \tag{3.9},$$

where t is the travel time and m is the mean travel time for the watershed. Here, we have used the exponential distribution to develop algebraic expressions for the flow-averaged concentration after land-use change following the three different patterns of intervention described in **Equations 3.6, 3.7,** and **3.8**.

Frontal

$$\frac{c_{ac}}{c_{bc}}(t;p) = \begin{cases} c_1\frac{N}{C_0}(e^{-/t}-e^{-st})+c_2\frac{(C_s^0-N)}{C_s^0}(e^{-gt}-e^{-st})+e^{-st} & 0\le t < F^{-1}(p) \\ c_1\frac{N}{C_0}(e^{-/t}-e^{-F_f(k-/+\frac{1}{m})-/t})+c_2\frac{(C_s^0-N)}{C_s^0}(e^{-gt}-e^{-F_f(k-g+\frac{1}{m})-gt})+e^{-F_fS} & t\ge F^{-1}(p) \end{cases} \tag{3.10},$$

Distal

$$\frac{c_{ac}}{c_{bc}}(t;p) = \begin{cases} 1 & 0\le t < F^{-1}(1-p) \\ 1+c_1\frac{N}{C_0}(e^{-F_d(S-/)-/t}-e^{-t(S-/)})+c_2\frac{(C_s^0-N)}{C_s^0}(e^{-F_d(S-g)-/t}-e^{-t(S-g)})-e^{-F_dS}+e^{-st} & t\ge F^{-1}(1-p) \end{cases} \tag{3.11},$$

Random

$$\frac{c_{ac}}{c_{bc}}(t;p) = 1-p(1-c_1\frac{N}{C_0}(e^{-/t}-e^{-st})-c_2\frac{(C_s^0-N)}{C_s^0}(e^{-/t}-e^{-st})-e^{-st}) \qquad t\ge 0 \tag{3.12},$$

where

$$S = 1+mk; \quad c_1 = \frac{1+mk}{1+mk-/m}; \quad c_2 = \frac{1+mk}{1+mk-gm};$$

$$F_f = F^{-1}(p); \qquad\qquad F_d = F^{-1}(1-p)$$

Here, F_f and F_d represent the longest and shortest groundwater travel times, respectively, for land parcels that have undergone land-use conversion. Note that in the above formulations we have implicitly assumed that the watershed is homogeneous in terms of land use. This assumption is not, however, a limitation of the approach. For heterogeneous land use, the groundwater travel time distribution of interest is that of the areas contributing solute to the watershed outlet. For example, when only a fraction of the watershed area is under row crops and the

management practice involves conversion of row crops to prairies, the travel time distribution used in **Equation 3.9** would be that of the cells originally under row crop.

3.3 Materials and Methods

3.3.1 The Walnut Creek Case Study

3.3.1.1 Site Description. A watershed habitat restoration and agricultural management project was implemented by the United States Fish and Wildlife Service (USFWS) at the Neal Smith National Wildlife Refuge (NSNWR) within the Walnut Creek Watershed (WCW) (52 km^2) of Jasper County, Iowa (**Figure 3.3a**). The project involved conversion of a large portion of the WCW from row-crop agriculture to native prairie and savanna (Keith E. Schilling and Wolter 2007; Drobney 1994). The NSNWR represents one of the first attempts at agricultural land-use conversion towards ecosystem restoration at the watershed scale, and is one of the few sites where water quality has been monitored both in the groundwater directly below the reconstruction and in surface water at multiple scales within the watershed. The site is thus an ideal choice for testing the applicability of the modeling framework introduced in this paper.

The WCW is located in the Southern Iowa Drift Plain landscape region of Iowa, which is characterized by steeply rolling hills and well-developed drainage (Prior 1991). The climate of the area is humid and continental. Temperatures in the region vary widely, ranging from average maximum values over 20°C between June and September to less than 0°C in December and January. Annual precipitation averages around 850 mm, with maximum rainfall typically occurring in the months of May and June.

In 1990, the land cover in the watershed was predominantly agricultural, with 70% of the area being covered by row crops. From 1990 to 2005, row-crop cover throughout the watershed was decreased from 70% to 55% as a part of prairie conversion efforts. In subwatershed WNT5 (7.9 km^2), which is our focus herein, the row crop cover was decreased from 77 % to 46%, and surface water quality was monitored subsequently over a period of 13 years (Keith E. Schilling and Wolter 2007). Trajectories for groundwater nitrate concentrations throughout the conversion area were established based on water sampling from 19 monitoring wells

across a chronosequence of sites, as indicated by the data points in **Figure 3.3b** (Keith E. Schilling and Jacobson 2010). For the chronosequence work, sites were selected to represent a conversion time series, with three of the sites still under row crop and the rest having been converted 2-13 years prior to the sampling date. Nitrate concentrations were measured at the outlet of subwatershed 5 and were used to calculate mean annual concentrations (**Figure 3.3c**). This site thus provided us with an opportunity to test the ability of the model to capture the dynamics in biogeochemical legacy depletion based on groundwater data, and combined hydrologic and biogeochemical legacy depletion based on surface water data.

Figure 3.3. Site Information and Results for the Walnut Creek Case Study.
(a) Subwatershed 5 (7.9 km^2) of the Walnut Creek watershed, Jasper County, Iowa; (b) Data points correspond to groundwater nitrate concentrations in 19 monitoring wells across a chronosequence of restorations sites. Biogeochemical Legacy Depletion: Source Zone Nitrate-N Concentration as a function of time since land-use change; (c) Hydrologic and Biogeochemical Legacy Depletion: Data points correspond to mean annual nitrate concentrations measured at the outlet of subwatershed 5 as a function of time since land-use change. The grey shaded area in the figure corresponds to a range of values for the denitrification rate constant (k = 0.24 ± 0.08 y^{-1}).
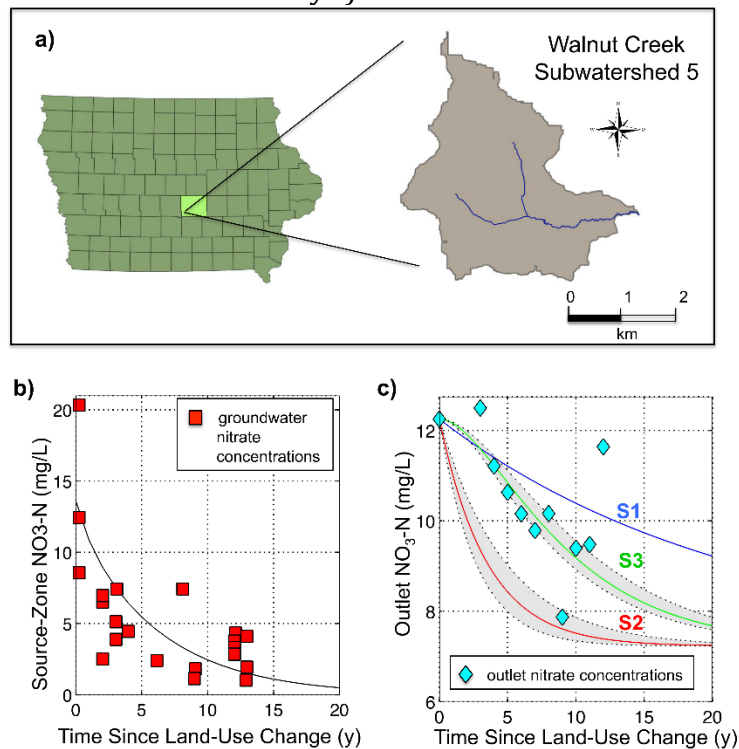
3.3.1.2 Model Parameters. As described in Section 3.2.1, our model assumes changes in source zone concentrations over time after conversion from row crop to grassland as a function of both the depletion of legacy soil organic nitrogen (SON) and annual recharge rates to groundwater. To model the biogeochemical legacy dynamics within the source zone, legacy SON is considered to exist within the soil profile to a depth of 1 m at a quantity of 100 kg/ha over baseline (pre-agricultural intensification) levels. This value is a conservative estimate based on N accumulation rates of 6 kg/ha-y for a soil depth of 0-100 cm observed across Iowa under intensive agricultural practices over a period of 70 years (1940-2010) (Veenstra 2010), with an assumption that approximately 75% of this accumulation would remain protected via both physical and chemical stabilization mechanisms (Six et al. 2002a) and that the remaining 25% would be in a readily mineralizable form. Initial NO_3-N concentrations in the source zone are assumed to be 15 mg/L based on a reported range of 10-20 mg NO_3-N/L in tile drainage and groundwater under corn-soybean rotations (Li et al. 2006; Strock, Porter, and Russelle 2004).

The groundwater travel time distribution for the WCW was determined using a MODFLOW model that was calibrated against measured groundwater elevations at 84 monitoring wells within the site (Keith E. Schilling et al. 2012; Nandita B. Basu et al. 2012; Jindal 2010). A particle-tracking simulation revealed an exponential travel time distributions for the row-cropped area of the WCW ($\sim$ 70% of the watershed is row-cropped) (Nandita B. Basu et al. 2012). Reported data on prairie plantings (Keith E. Schilling and Wolter 2007) and spatial maps of watershed travel times created using the MODFLOW model (Jindal 2010) demonstrated that the pattern of land-use conversion for WNT5 was predominantly random, which is consistent with our general understanding of land-use shifts for restoration being driven more strongly by the availability of land parcels than design of an optimal land-use change scheme for maximization of water quality benefits. We use a denitrification rate constant (k) varying over a range of 0.24 ± 0.08 y^{-1}, which corresponds to a reported range of denitrification rate constants for shallow aquifers with upland surficial geology characterized by glacial outwash and till (Tesoriero and Puckett 2011), as is found at the Walnut Creek site. Other parameters used in the model are included in **Table 3.1**.

Table 3.1 Model Parameters for the Walnut Creek Watershed

Model parameters	Walnut Creek Values
Initial Source Zone Nitrate Concentration	15 mg NO_3-N/L
Initial Mass of Legacy SON	100 kg/m^2
Legacy N depletion rate constant (λ)	0.16 y^{-1}
Denitrification Rate (k)	0.24 ± 0.08 y^{-1}
Mean Travel Time (μ)	21.6 y
Mean Annual Recharge (Q)	129.5 mm/y
Soil Saturation (s)	0.5
Soil Porosity (n)	0.3
Fractional Land Area Converted	0.41

3.3.2 Metrics for Evaluating Concentration Reduction Benefits

To quantify the concentration reduction benefits achievable at a specified time interval (t) based on a given percent land-use change, we have developed the CR_t metric, defined as:

$$CR_t = 1 - \frac{c_{ac}}{c_{bc}} \tag{3.13},$$

For the special case of concentration reductions at very long times $t \rightarrow \infty$, thus representing the maximum benefit that can be achieved by land-use conversion, the CR_{inf} metric is used, defined as:

$$CR_{inf} = 1 - \lim_{t \rightarrow \infty} \frac{c_{ac}}{c_{bc}} \tag{3.14},$$

3.4 Results and Discussion

The objective of the present study was to develop a framework to quantify catchment-scale time lags based on both biogeochemical and hydrologic nutrient legacies in intensively managed catchments. Our first intent was to develop a set of analytical equations to quantify water-quality benefits, taking into account both soil legacy accumulation and denitrification dynamics along the groundwater pathway.

Our results, based on idealized scenarios of land-use conversion, are compared with results related to actual patterns of land-use conversion in the Walnut Creek watershed. Additionally, our intent was to utilize the analytical equations to explore concentration-reduction benefits associated with different spatial patterns of land-use conversion, and thus to further our understanding of both natural and anthropogenic controls on such benefits and any associated time lags. Benefits are gauged in terms of (1) the relative magnitude of the watershed chemical response to the cropland conversion and (2) the arrival time of the response at the outlet. These results are used to establish an optimization framework that clarifies tradeoffs between the land area taken out of row-crop production and the time required to achieve desired concentration-reduction benefits.

3.4.1 Model Validation: The Walnut Creek Case Study

We first applied our model, which takes into account both biogeochemical legacy and the groundwater denitrification dynamics, to the Walnut Creek watershed. The temporal trajectory of source-zone nitrate concentrations $C_s(t)$ in land parcels that had undergone conversion from row-crop to grassland was modeled using **Equations 3.4** and **3.5**. A legacy depletion rate constant, λ, of 0.16 per year was able to capture the observed trends in the groundwater chronosequence data described in Section 3.3.1.1 and as shown in **Figure 3.3b**. The time required to achieve a 50% concentration reduction in the source zone was found to be approximately 5 years, while a 95% concentration reduction in the source zone corresponded to a lag of approximately 19 years.

The concentration trajectory at the catchment outlet was then derived as a function of $C_s(t)$, the groundwater travel time distribution, the denitrification rate constant, and the pattern of land-use change, following **Equations 3.10**, **3.11** and **3.12**. The exponential travel time distribution derived from the MODFLOW model (mean travel time μ = 21.6 years) was used long with an assumption of a random pattern of land-use conversion (see Methods 3.2), to model three different scenarios for trajectories of water-quality change after land conversion for the WNT5 subwatershed (**Figure 3.3c**).

The first scenario (S1) parallels the approach used by Schilling et al. (Keith E. Schilling and Wolter 2007), assuming the presence of hydrologic legacy but no biogeochemical legacy, with no denitrification occurring along the groundwater pathway. Accordingly, there is nitrate dissolved in groundwater that continues to arrive at the outlet over a defined time period (as a function of the groundwater travel time distribution) after land-use conversion, thus shaping the outlet concentration trajectory. The second scenario (S2) maintains the same assumptions as those utilized in S1, but adds denitrification in the saturated groundwater. Under this scenario, nitrate concentrations decrease as they travel from the source zone to the outlet, as nitrate is reduced to N_2 or N_2O and leaves the system in a gaseous form. Both S1 and S2 assume that groundwater concentrations in the source zone, beneath the land parcels for which the land-use shift has occurred, drop immediately from C_s to 0, and that the observed concentration trajectory at the outlet is only a function of dynamics along the groundwater flow pathways.

In contrast, the third scenario (S3) takes into account both denitrification and the presence of biogeochemical legacy in the source zone. The $C_s(t)$ function in the model, as shown in **Figure 3.3b**, is convoluted with the groundwater travel time distribution following **Equation 3.1** to estimate the concentrations at the catchment outlet. As can be seen in **Figure 3.3c**, the base case scenario S1, after year 3, generally overestimates the concentration at the outlet. Conversely, the S2 scenario, which takes into account denitrification dynamics, consistently underestimates the achieved concentrations, even when considering the full range of possible values for the denitrification rate constant (k). However, with S3's combined consideration of both denitrification and biogeochemical legacy, there is a close match between predicted concentration reductions and the observed data for WNT5. In particular, S3 captures the time lag between the initial land conversion and the first observed drop in concentrations at year 4.

The model thus provides a parsimonious way of describing the concentration trajectory, both at the parcel in which land use change has occurred, and at the catchment outlet. Although in the present study we used the more computationally intensive MODFLOW/MODPATH approach to estimate the groundwater travel time

distribution, previous work (Nandita B. Basu et al. 2012) suggests that a simple GIS-based approach, which uses the land surface as a surrogate for the water table, can be used to construct the travel-time distribution. The latter method is based on readily available DEM data and hydraulic conductivity values, which can be obtained at the local scale from soil databases and at larger, regional scales from recently constructed global maps of near-surface permeability (Gleeson et al. 2011).

3.4.2   Concentration Reduction as a Function of Spatial Patterns of Land-Use Change

We next utilized our analytical equations to explore concentration-reduction benefits associated with different spatial patterns of land-use conversion. The temporal trajectories for the outlet concentration after conversion (50% land-use conversion, k=0.18 ± 0.12 y^{-1}) normalized to the mean concentration before conversion are presented in **Figure 3.4a.** The frontal conversion leads to the fastest response and the distal the slowest, with the random somewhere in the middle. For both frontal and random truncation of the groundwater travel time distribution, partial benefits are immediately realized at the watershed outlet, but for a distal truncation there is a time lag between the implementation of change and the start of benefit realization. This time lag corresponds to the minimum travel time of the altered land-use parcels, $F^{-1}(1-p)$, and is a function of both the groundwater travel time distribution characteristics and the fractional land-use change. In the modeled scenario, this time lag is approximately 16 years, whereas in the frontal and random scenarios concentration reductions of approximately 85% and 43%, respectively, have already been achieved at 16 years after conversion (**Figure 3.4a**).

Importantly, not only the time required to achieve a desired concentration reduction, but also the maximum achievable concentration reduction at infinite time (CR_{inf}), differs according to the spatial pattern of conversion. This spatial dynamic is captured in **Figure 3.4b**, in which CR_{inf} values are plotted as a function of the fractional land-use conversion, p, for frontal, distal, and random conversion scenarios. As can be seen in the figure, the frontal pattern of intervention provides the greatest maximum concentration reduction benefit at all percentages of landscape conversion, with the greatest difference between the frontal and distal scenarios occurring under

the 50% conversion scenario. The relatively low CR_{inf} values for the distal scenarios demonstrate that even at very moderate denitrification rates (k=0.18 $\pm$ 0.12 y^{-1}), land parcels with relatively greater travel times make very little contribution to stream nitrate concentrations. Accordingly, conversion of those parcels will have virtually no impact on nitrate concentrations at the watershed outlet.

Figure 3.4. Normalized concentration reduction trajectories under different patterns of land-use change.
(a) Normalized concentration trajectories at the catchment outlet plotted as a function of time (years) after land-use change for the frontal, random and distal patterns of conversion; fractional land-use conversion p = 0.5; (b) Concentration reduction fraction at infinite time as a function of land use conversion fraction p. In both figures, k=0.18 ± 0.12, which corresponds to a range of "moderate" denitrification rates (Tesoriero et al. 2011). Other parameters used are lambda = 0.23 y^{-1} and μ = 21.6 y. A 1:1 relationship between CR$_{inf}$ and p, with no dependence on the k values is apparent for the random truncation.
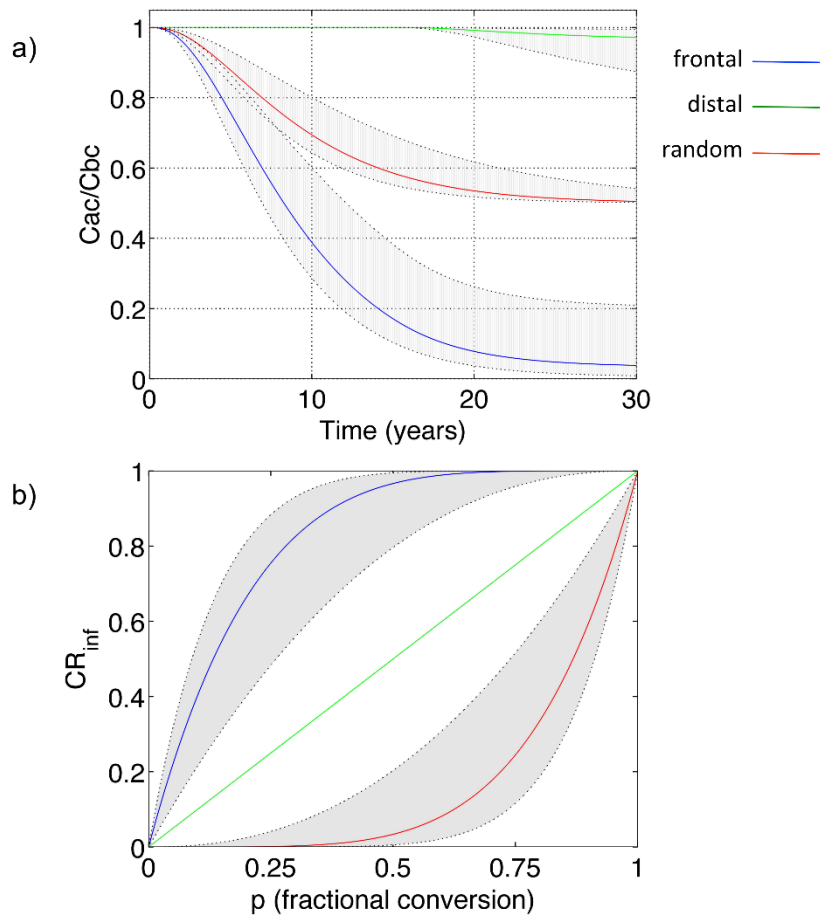
In contrast, it should be noted that a random pattern of intervention provides a 1:1 concentration reduction benefit. In other words, when interventions are applied randomly throughout a watershed, a 20% conversion of watershed area will result in a 20% reduction in concentration. Mathematically, this 1:1 relationship between land-use conversion and water quality benefits arises due to the property by which a probability distribution created by taking a large enough random sample from any frequency distribution will have the same attributes as the original distribution. It should also be noted that though a range of CR_{inf} values is obtained for the frontal and distal conversion scenarios, based on the range of denitrification rate constants, the values for the random scenario are not a function of this rate constant and therefore do not deviate from the 1:1 relationship between land-use conversion and concentration reductions.

3.4.3 Concentration Reduction as a Function of Natural and Anthropogenic Controls

3.4.3.1 Concentration Reductions at Infinite Time. In the above sections, we have focused on concentration-reduction benefits corresponding to one, unique travel time distribution (exponential with $m = 26$ years). In order to understand how such benefits vary as a function of the travel time distribution, we have plotted contours of maximum concentration reductions (CR_{inf}) along a continuum of values for both the mean travel time (m) and the fractional area within a watershed being removed from row-crop production (p) **(Figure 3.5)**. Three different plots are presented (**3.5a, 3.5b, 3.5c**), corresponding to the frontal, random and distal, patterns of intervention, respectively. For a particular watershed (characterized by its m value), the CR_{inf} benefit achieved for a specified fractional land-use change (p) is equal to p for the random truncation scenario (**Figure 3.5b**), greater than p for the frontal scenarios (**Figure 3.5a**) and less than p for the distal scenarios (**Figure 3.5c**). For a particular conversion fraction p, the concentration reduction benefits increase with increasing mean travel times for the frontal truncation scenario, while they decrease for the distal truncation and remain invariant with m for the random truncation.

Figure 3.5. Maximum normalized concentration reduction (CRinf) contours plotted as a function of the fractional land-use conversion p and mean watershed travel time μ.

Contours are plotted for the (a) frontal, (b) random and (c) distal truncation scenarios ($k=0.06$ y^{-1}, $\lambda=0.16$ y^{-1}).
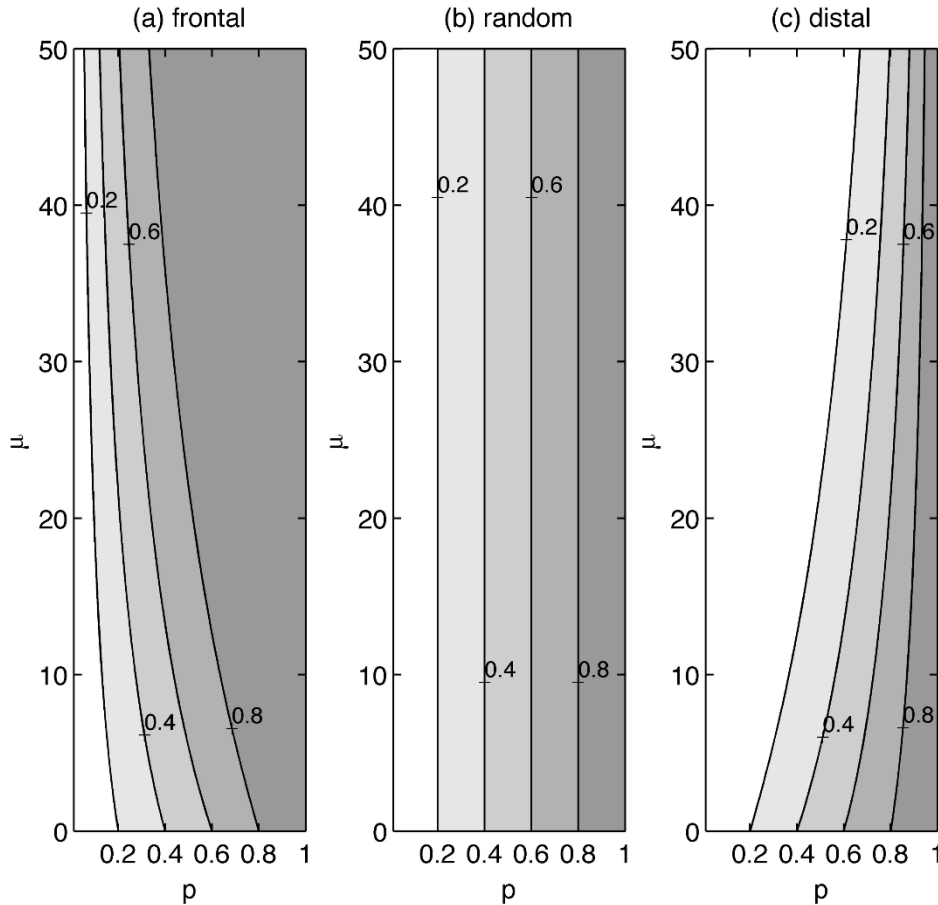
3.4.3.2 Concentration Reductions at Specified Times. The above analysis describes concentration reduction benefits occurring at infinite time. Decisions regarding land management, however, are not made based on hypothetical benefits achieved at infinite times, but on realistic concentration reductions achievable within specific time frames. In **Figure 3.6**, we show the concentration reduction profiles achievable 5 years after landscape conversion (CR_5 values) as a function of p and m.

With a frontal conversion (**Figure 3.6a**), it can be seen that 5 years after conversion ($t_d=5$), the concentration reductions for a particular watershed (characterized by a m value) increase with increases in p up to a point, and then become invariant with p. Beyond this point, further land-use conversion in this

watershed results in no additional stream water quality benefits within the 5-year period, as land being converted beyond this threshold point has an associated travel time greater than 5 years, and thus has no impact. As m increases, this threshold point shifts to the left, implying that the threshold is crossed at lower and lower p values. This trend occurs because for larger watersheds, a 5-year threshold is only a small percentage of its overall area, and thus benefits cease beyond a relatively small value of p. The thicker line connecting the threshold points thus divides the plot are into two zones, one where benefits are still being realized and another for which benefits have ceased, with the line being mathematically denoted by $F^{-1}(p) = t_d$.

Figure 3.6. Normalized concentration reduction contours at t = 5 years (CR5) plotted as a function of the fractional land-use conversion p and mean watershed travel time.

Contours are plotted for the (a) frontal, (b) random and (c) distal truncation scenarios (k=0.06 y^{-1}, $/$ =0.16 y^{-1}).
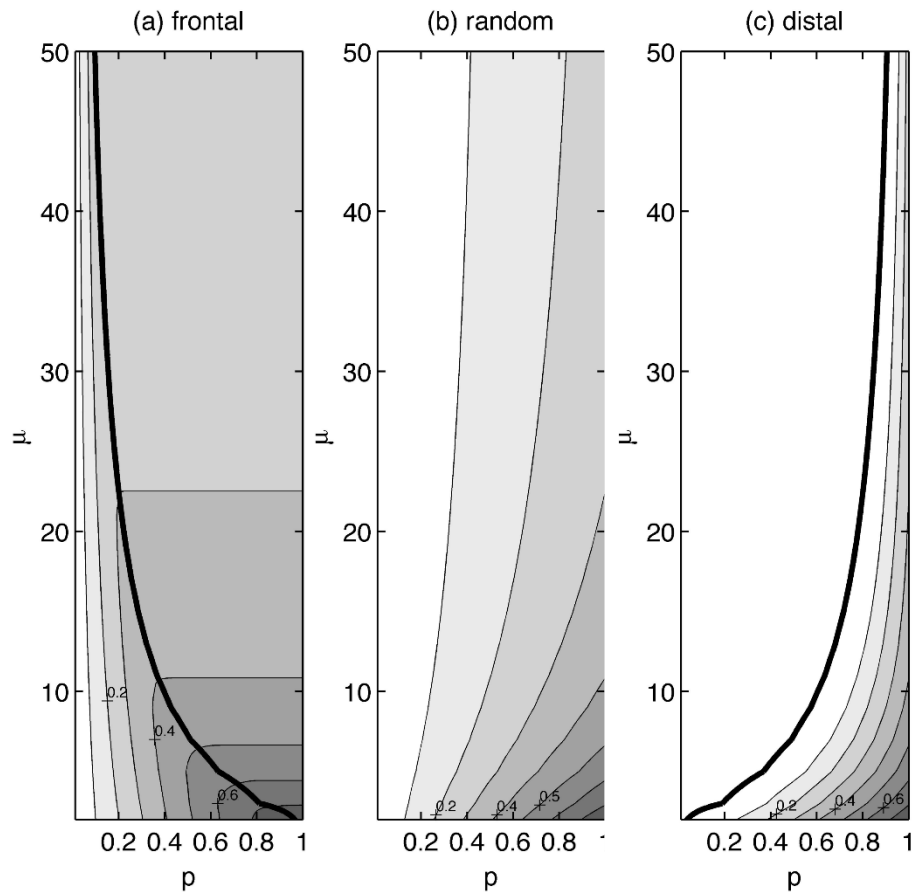
It is important to understand the existence of this threshold when designing restoration schemes. For example, land managers working in a watershed with a mean groundwater travel time of 15 years may be under pressure to reduce stream NO_3^- concentrations by 50% over a period of 5 years. Knowing that proportionally greater benefits will be achieved with a frontal approach to restoration, they begin converting land with the smallest travel times. **Figure 3.6a**, however, shows that under these conditions, a concentration reduction of approximately 35% is the greatest benefit that can be achieved within the 5-year period, even if 100% of the land is converted from row-crop production to native prairie.

The results are quite different, however, for the distal and random conversion scenarios. With a distal conversion, the threshold line is the zero-benefit contour (the heavy dark line in **Figure 3.6c**), such that to the left of this line, no concentration reduction benefit can be achieved. Compared with the frontal scenario, it can be seen that a distal approach provides much poorer outcomes, requiring a much greater conversion area and/or a much longer time periods to see results. Assuming the same scenario as above, with a mean groundwater travel time of 15 years, land managers would be forced to convert approximately 90% of the watershed from row-crop to prairie to achieve the same 30% concentration reduction that could be achieved with an approximately 20% conversion area under the frontal approach. Finally, with a random approach, as shown in **Figure 3.6b**, concentration benefits scale continuously with p and μ. Additionally, as was seen in the CR_{inf} plots in **Figure 3.5**, a random conversion approach provides poorer concentration reduction outcomes than the frontal approach, but better outcomes than the distal approach.

3.4.3.3 Time Lags and Tradeoffs. With an understanding of catchment-scale time lags, an optimization approach can be developed to clarify the tradeoffs involved with achieving a specified concentration reduction benefit. In our case, conversion of land in row-crop agriculture to native prairie can be understood within the framework of two competing objectives. Objective 1 (O1) is to achieve specified nitrate concentration reduction goals within a desired time frame. Objective 2 (O2) is to minimize both societal and individual farmer costs associated with implementation of environmental interventions while still meeting concentration reduction goals.

Figure 3.7 provides a visualization of Pareto-optimal fronts for these conflicting objectives, with the contour lines representing progressively greater concentration reduction goals, from 25 to 75% reduction. In the figure, the x-axes correspond to the time in years after land conversion from row-crop to native prairie necessary for the concentration reductions to be realized (O1), while the y-axes correspond to the economic costs of land converted (O2), with the fractional land are converted (*p*) serving as a proxy for costs incurred. The three columns correspond to the frontal, random and distal approaches to intervention, with each resulting in its own family of optimized values for land conversion and time required to see the specified concentration reduction benefit. Watersheds with different travel time distributions are also represented here, with rows 1, 2 and 3 corresponding to mean travel times of 10, 20 and 50 years, respectively.

Figure 3.7. Normalized concentration reduction contours at infinite time as a function of the allowable lag time and the fractional land-use conversion.
The three rows represent different watershed mean travel times, while the three columns represent frontal, random and distal patterns of land-use change (k=0.06 y^{-1}, / =0.16 y^{-1}).

55
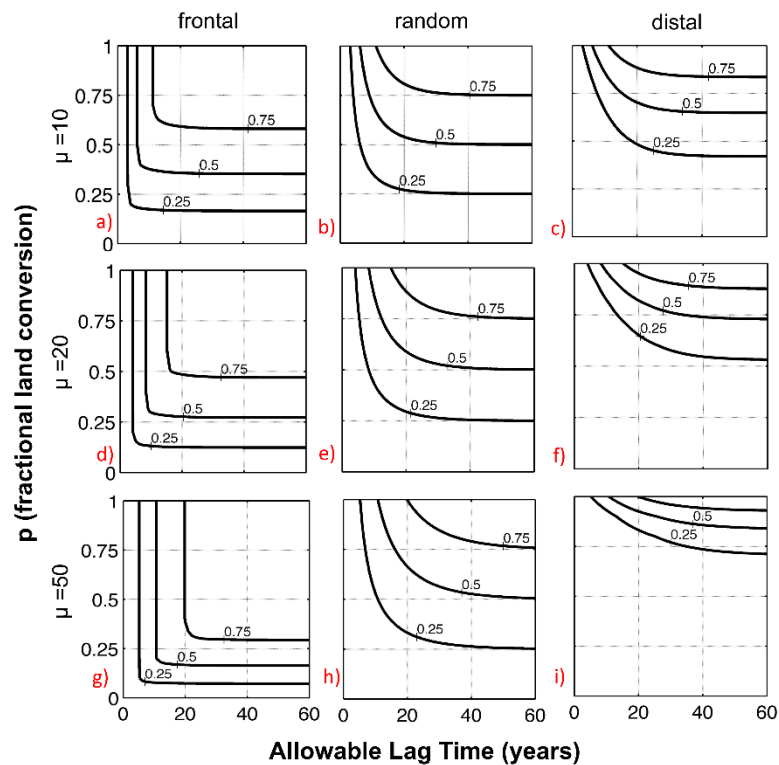
As can be seen in the figure, to achieve progressively greater concentration reduction goals, tradeoffs are necessary between the percent land converted and the time to concentration reduction. For example, if a random approach is taken to carrying out land conversion, as is typical in most watersheds, and a 50% concentration reduction is desired, the time required to achieve the desired concentration benefit ranges from approximately 8 to 30 years (m =10 years) (**Figure 3.7c**). If Objective 1 is prioritized, to give the fastest possible response time, a more than 90% conversion away from row-crop must be carried out. Conversely, if Objective 2 (cost) is prioritized, to maintain the maximum land in production, a 50% conversion is required, with the understanding that there will be a multi-decade time lag between conversion and fully meeting CR goals. An optimal compromise position, within the constraints of the random approach, would likely occur somewhere near the midpoint of the contour line, with approximately 70% of area being converted and an 11-year lag time. To further reduce the necessary percent land conversion, and thus to further minimize the economic impact, a frontal approach could be utilized. Although the fastest that a 50% concentration reduction can be achieved with the frontal approach remains at approximately 8 years (**Figure 3.7a**), the percent conversion necessary to achieve this reduction within this time period is reduced from 90% to 40%.

Such tradeoffs are also a function of the mean travel time for the watershed. In watersheds of the same size but with different mean travel times, the greater benefits of the frontal approach correlate positively with the travel time, allowing concentration reduction objectives to be achieved with significantly less commitment of resources. For example, in the m =10 year watershed, a 50% CR requires, at minimum, a close to 40% conversion of land area out of row crop. In contrast, in the m =50 year watershed the same reduction can be achieved with a 30% conversion over a similar time frame.

In general, it can be seen that the concentration reduction response scales according to both watershed characteristics (mean travel time) and the employed management approach (spatial patterns of intervention), and with such changes the

optimal level of intervention can be either more widely or more narrowly defined. If considering only tradeoffs between fractional land-use change (cost) and the time required to achieve target concentrations, the frontal approach provides a more clearly defined optimal intervention, with conversion of additional land area providing little or no additional time advantage beyond a threshold value. In contrast, with a random or more distal approach, the tradeoffs between time and the fractional converted area scale over a wider range of values, thus leading to more room for debate regarding the best path towards achieving concentration reduction goals.

3.5   Summary and Implications

In recent years, there has been great interest and investment of both private and public funds in the implementation of conservation-oriented management practices and other measures to minimize the negative environmental impacts of modern agricultural practices. Such interventions range from the retirement of agricultural land through programs such as the U.S. Conservation Reserve Program, to reductions in fertilizer application and the creation of riparian buffer zones. Interest is also growing in the potential mitigating impacts of large-scale conversion from grain-based cropping systems to the cultivation of perennial biofuel crops such as switchgrass and miscanthus, which have been found to result in reduced nitrate leaching at the plot scale (C. M. Smith et al. 2012). Although numerous studies have attempted to demonstrate the potential water-quality benefits garnered by implementing such changes (Jha, Gassman, and Arnold 2007; Ng et al. 2010), there has been little acknowledgement of the often long time periods required to achieve such benefits (Meals, Dressing, and Davenport 2010). In addition, most existing models such as SWAT and AGNPS (Grizzetti et al. 2003; Young et al. 1989), which are commonly utilized for agricultural landscapes, do not have an explicit mechanism to either account for such legacies or to predict time lags (D. Chen et al. 2014).

In the present work, we have developed a framework that allows for the parsimonious modeling of concentration-reduction benefits over time as a function of spatial patterns of land-use conversion or implementation of conservation measures across the landscape, and the existence of hydrologic and biogeochemical nutrient legacies. Specifically, we have focused on nitrogen, such that biogeochemical legacy

refers to sorbed organic nitrogen within the root zone, while hydrologic legacy refers to nitrate dissolved in groundwater. The model was able to capture the concentration dynamics in both shallow groundwater beneath sites undergoing landscape conversion as well in-stream concentrations at the catchment outlet. Our findings indicate that the existence of biogeochemical legacy can more than double the time needed to see meaningful concentration reductions at the catchment scale. In addition, we show that while a random approach to landscape conversion will lead to a 1:1 relationship between land-use conversion and maximum concentration reduction benefits at infinite time, a preferential conversion of land parcels with shorter travel times will lead to both faster recovery times and greater maximum achievable concentration reductions.

Our modeling framework provides a first attempt at fully describing and quantifying the often-ignored time lag in catchment management questions. In its present form, it allows for the quantification of tradeoffs between costs associated with implementation of conservation measures and the time needed to see the desired concentration reductions, thus making it a potentially powerful tool for land management as agricultural pressures on the environment continue to intensify. The analytical framework is also conducive towards assessing uncertainty in predicted concentration reductions and lag time metrics. In the future, the approach can be further refined by consideration of spatially varying denitrification rate constants, coupled dynamics of denitrification and dissolved organic carbon availability, and by the introduction of hydrologic variability in relation to both rainfall and evapotranspiration dynamics, as they affect the travel-time distribution for the catchment. Such refinements will lead to even further benefits with regard to decision-making support for implementation of conservation measures in intensively managed watersheds.

3.6   Acknowledgements

Chapter 4 - Two Centuries of Nitrogen Dynamics: Legacy Sources and Sinks in the Mississippi and Susquehanna River Basins

4.1   Introduction

Over the last century, intensive agricultural practices and increasing fossil fuel consumption have led to high levels of non-point source nutrient pollution, threatening drinking water quality and contributing to the destruction of aquatic ecosystems from the local to the global scale (Beusen et al. 2016; Rockström, Falkenmark, et al. 2009; R. Howarth, Swaney, et al. 2011; Carpenter et al. 2012). At the local level, high nutrient concentrations in agricultural runoff have increased the costs of drinking water treatment (USEPA 2014) and, recently, have led to litigation calling for greater regulation of agricultural nutrient sources(Stowe 2016). At larger scales, nutrient loading to near-shore coastal waters has fed the growth of large hypoxic zones, decreasing marine biodiversity and altering ecosystem structures. Before 1970, there were only scattered reports of coastal hypoxia in the literature (Rabotyagov et al. 2014); recent reviews, however, suggest that there may well be over 500 coastal "dead zones" worldwide, with the numbers doubling each decade (Diaz and Rosenberg 2008; Conley et al. 2009).While information gaps remain regarding the factors contributing to hypoxia, overwhelming evidence suggests that anthropogenic fertilization of marine systems by excess nitrogen (N) drives the onset and duration of hypoxic events in affected coastal waters (Diaz and Rosenberg 2008; Nancy N. Rabalais, Turner, and Scavia 2002).

Over the last two decades, there has been increasing interest in linking riverine N export to current human-induced N inputs at the watershed scale (Hong, Swaney, and Howarth 2011; Swaney et al. 2012a). Howarth et al. (1996) and others have repeatedly demonstrated that net anthropogenic N inputs (NANI) to a watershed are good predictors of riverine N export across a range of watersheds (Hong, Swaney, and Howarth 2013; Boyer et al. 2002; Gilles Billen et al. 2009a). The majority of the NANI-based studies, however, have been carried out based only on snapshots in time or on multi-year averaging of N inputs and outputs, thus limiting their ability to effectively

capture long-term responses to changes in inputs. Indeed, it is increasingly recognized that there may be decadal-scale time lags between changes in N inputs and measurable changes in water quality (Meals, Dressing, and Davenport 2010; Sanford and Pope 2013; Van Meter and Basu 2015; Hamilton 2012a; Fenton et al. 2011a). Such time lags have been attributed to the presence of both hydrologic and biogeochemical nutrient legacies within watersheds (Van Meter et al. 2016; Worrall, Howden, and Burt 2015).For nitrogen, the hydrologic legacy corresponds to dissolved N, primarily in the form of nitrate, in the unsaturated zone and groundwater reservoirs, while the biogeochemical N legacy corresponds to the buildup of organic N in the root zones of soils, as has recently been shown in soils across the Mississippi River Basin (Van Meter et al. 2016). Legacy N in intensively managed watersheds can serve as a long-term source to surface and groundwater. Accordingly, a steady-state approach to linking N inputs with outputs is inadequate for capturing time-lag effects on watershed-scale N dynamics and thus limits the predictive value of the established input-output relationship.

To overcome this limitation, some attempts have been made to interject a time component into the NANI-based approach. McIsaac et al. (2001), for example, developed a regression model for the Mississippi River Basin showing current-year N loading to be impacted by N surplus values for the previous 9 years. More recently, Chen et al. (2014) have employed cross-correlation analysis over a period of 30 years to determine the lag time between changes in N inputs and changes in riverine N export. Their analysis, in a study of the Yongan River watershed in eastern China, showed on average a 7-year lag between changes in net N inputs and changes in N export between 1980 and 2009. Although these results represent progress in linking long-term N input trajectories to N export, the modeling approach utilized by Chen et al. is regression-based rather than process-based and therefore does not explicitly account for or distinguish between biogeochemical and hydrologic time lags within the watershed and cannot explicitly predict how outputs will change in response to significant changes in inputs.

The purpose of the present study is to use a process-based modeling approach to place current observed stream N dynamics in the context of long-term trajectories

of N use. Such an approach is important in the context of watershed management, allowing us to more accurately quantify future changes in water quality based on current or future changes in input. The first step in meeting the above goal was to quantify N inputs and outputs over a period of more than 200 years for two major U.S. watersheds, the Mississippi River Basin (MRB) and Susquehanna River Basin (SRB), which are the sources of significant nutrient contamination to the Gulf of Mexico and Chesapeake Bay, respectively. The second was to use these N input trajectories to drive a parsimonious, process-based model capable of accounting for N dynamics in subsurface reservoirs. In particular, our modeling approach allows us to chart decadal-scale changes in N magnitudes within the vadose zone and in groundwater, and to predict the timescales of change in surface water N loading in response to changes in land use and N management.

Through this work, we are attempting to answer the following questions:

1) How has N loading changed since pre-industrial times, and what is the impact of N legacies on the loading trajectories for these two watersheds?

2) What have been the magnitudes of N depletion and/or accumulation in soil and groundwater reservoirs across the study period (1800-2014)?

3) What are the estimated times of delivery of N within a watershed, from application at the land surface to exit at the catchment outlet, and how have these times changed over time?

4) How have the sources of N at the catchment outlet changed over time?

4.2   Model Development

The ELEMeNT modeling approach (Exploration of Long-tErM Nutrient Trajectories) utilizes a coupled framework (**Figure 4.1**) that pairs source-zone dynamics, which include the accumulation and depletion of soil organic N (SON) within the root zone, with a travel time-based approach that accounts for transport and transformations in the groundwater to determine N loading trajectories at the catchment outlet.

ELEMeNT is based on the fundamental principle that the behavior of the landscape at any point in time is a function not only of current conditions, but also of

past land use and nutrient dynamics contributing to the buildup or depletion of legacy stores in soils (biogeochemical legacy) and groundwater (hydrologic legacy). ELEMENT's consideration of both current-year inputs as well as the role of legacy N stores in driving current nutrient fluxes distinguishes it from other watershed models and allows us to more effectively explore how fluxes may change over time as a function of land use and land management. To allow such consideration, each landscape unit in the ELEMeNT framework maintains a memory of past land use and management. Thus, although current land use for two landscape units may be the same, one may have undergone conversion from cropland back to non-agricultural land in 1950 and the other in 1980. Accordingly, these two areas would represent two different land-use trajectories with different N legacies and thus different current N fluxes. To account for this diversity of past use, ELEMeNT treats the landscape not as a patchwork of spatial units based not on current land use (the most common approach), but as a distribution of unique land-use trajectories, such that the model is able to maintain landscape memory and thus more adequately simulate legacy-related nutrient dynamics.

Figure 4.1. Conceptual framework for predicting catchment scale time lags as a function of hydrologic and biogeochemical legacies in the landscape.
The source-zone box (left) represents the flow of N through soil organic matter and the accompanying accumulation/depletion of biogeochemical legacy within the source zone. In this schematic, N_s represents the annual N surplus, and h is a "protection" coefficient, determining which portion of annual inputs enter the active, more metabolically active N pool, and which the more stable, protected pool of organic matter. Mass depletion from the source zone is convoluted with the groundwater travel time distribution (middle) to ultimately describe N loading trajectories at the catchment outlet (right).
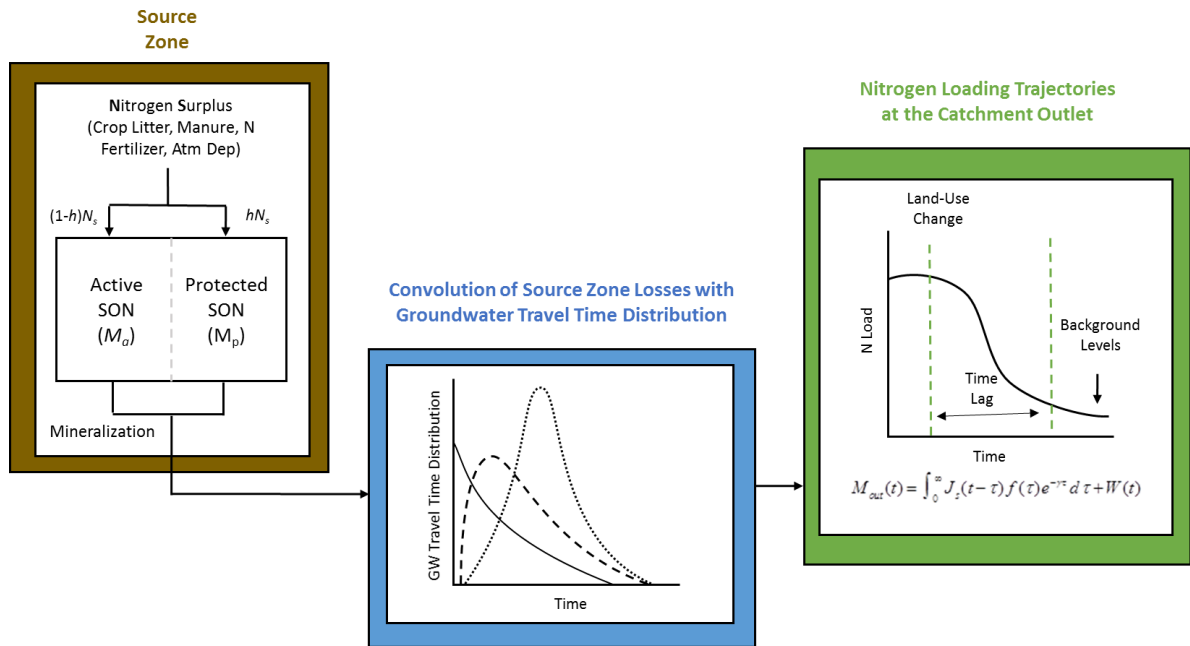
4.2.1 Outlet N Loading Trajectories: A Travel Time-Based Approach

To quantify nitrate-N load trajectories at the catchment outlet following land-use change, ELEMeNT conceptualizes each point on the landscape as corresponding to an individual stream tube characterized by a unique groundwater travel time to the stream network (Jury et al. 1990). Within this framework, the landscape as a whole functions as a bundle of stream tubes having a unique distribution of travel times to the nearest stream, $f(\tau)$, with travel times through the stream to the catchment outlet being considered negligible. The travel time distribution, in turn, controls nitrate-N mass flux trajectories at the outlet, $M_{out}(t)$ (Maloszewski and Zuber 1982; Haitjema 1995; McGuire and McDonnell 2006a), as described by the following expression:

$$M_{out}(t) = \int_0^\infty J_s(t - \tau) f(t) e^{-gt}\, dt + W(t) \qquad (4.1),$$

where, $J_s(t - \tau)$ is the contaminant input function or "source function" that describes the mass flux of nitrate from the unsaturated zone to the groundwater, developed in Section 4.2.2, k [T⁻¹] is the first-order rate constant that describes N removal via denitrification in the aquifer, and *W(t)* is the N mass input from wastewater (**Figure 4.1**). Here, we focus on N travel times through the groundwater pathway, as it is the dominant pathway responsible for time lags in catchment response. In contrast, wastewater N inputs, *W(t)*, are considered to directly enter surface waters, also with negligible travel times to the catchment outlet.

Figure 4.2. The ELEMeNT Modeling framework
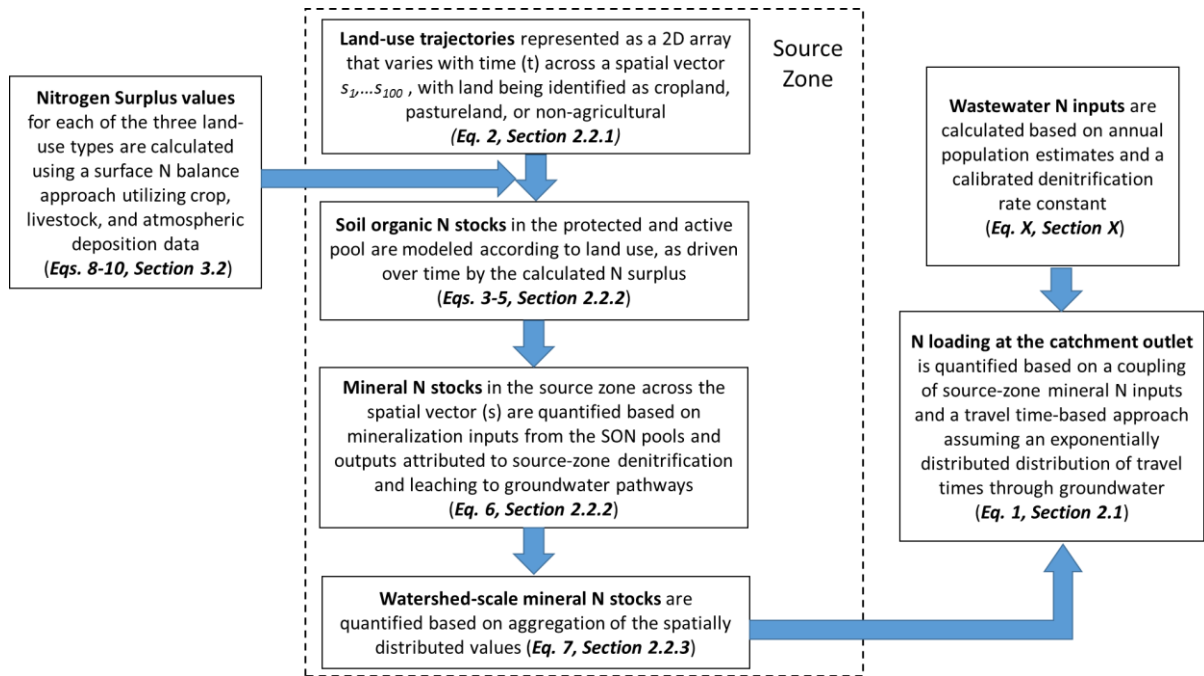
4.2.2 Source-Zone Dynamics

4.2.2.1 Watershed Land-Use Trajectories. The watershed is segmented into *s* distinct units corresponding to distinct land use trajectories, and the temporal evolution of each unit is stored within a 2D land-use array, *LU(s,t)* representing a distribution of

land use (cropland, pastureland, non-agricultural) over time (t) via the following equation:

$$LU(s,t) = \begin{cases} 2 & s \leq A_{crop}(t) & cropland \\ 1 & A_{crop}(t) < s \leq [A_{crop}(t) + A_{past}(t)] & pastureland \\ 0 & s > [A_{crop}(t) + A_{past}(t)] & other \end{cases} \qquad (4.2),$$

where A_{crop} and A_{past} correspond to watershed-scale percent cropland and percent pastureland, respectively. Land-use data to create these trajectories is based on state-level cropland and pastureland data from U.S. Agricultural Census and Survey data (USDA-NASS), supplemented by historical modeled cropland data from Ramankutty and Foley (1999), aggregated to the watershed scale.

4.2.2.2 Estimation of the Source Function. Each of the *s* distinct LU trajectories have a corresponding Js (s,t) that describe the mass leaching from the unsaturated zone at any time t, such that the source function, which is the watershed scale mass leaching from the source zone to the groundwater J_{s_wshd} (kg/ha), can be estimated as the sum of the source-zone values across the distribution of land-use trajectories *(s):*

$$J_{s_{wshd}}(t) = \sum_{s=1}^{1000} J_s(s,t) \qquad (4.3),$$

ELEMeNT utilizes a parsimonious modeling framework (**Figure 4.2**) to estimate the biogeochemical legacy mass residing in the source zone and the mass leaching from the source zone at any time *t*, $J_s(s,t)$. The mass residing in the source zone is the sum of the mass in the soil organic matter, $M_{SON}(s,t)$ and the mass in the mineral pool, $M_s(s,t)$. The soil organic matter pool can further be conceptualized as the sum of an active pool $M_a(s,t)$ (kg ha^{-1}) with faster reaction kinetics, and a more protected passive pool $M_p(s,t)$ (kg ha^{-1}) with slower kinetics. In the following sections, we develop the equations for M_a, M_p, M_s and J_s.

Within this framework, we consider that all of the annual N surplus (N_s (i,t), kg ha^{-1} y^{-1}; I = 0, 1, 2 for the three LU types considered) cycles through either the active

or protected SON pools, with the outputs being inorganic N $M_s(s,t)$ produced by the mineralization of SON. This pathway is consistent with the results of isotope studies indicating that the majority of NO_3^- leachate has undergone biogeochemical transformation within the soil organic pool before being mineralized and lost from the system (Haag and Kaupenjohann 2001; Spoelstra et al. 2001). Mineralization is conceptualized as a first-order process with the rate constants k_a (y^{-1}) and k_p (y^{-1}). Partitioning of the annual N surplus between the active and protected pools is considered to occur as a function of land use and tillage practices (Six et al. 2002b; Janssen 1984) and is represented within the model via a protection coefficient, h, the value of which is determined based on model calibration, as described in Section 4.3.3.

Using this framework, N dynamics for the active and protected pools of SON across the distribution of land-use trajectories, s, can be represented via the following differential equations:

$$\frac{dM_p(s,t)}{dt} = \begin{cases} h N_s(LU(s,t),t) - k_p M_p(s,t), & LU(s,t-1)=2 \\ hN_s(LU(s,t),t) - (M_p(s,t) - 0.7M_{p\_prist}), & LU(s,t)=2 \ and \ LU(s,t-1)=0,1 \end{cases} \quad (4.4),$$

$$\frac{dM_a(s,t)}{dt} = \begin{cases} (1-h)NS(s,t) - k_a M_a(s,t), & LU(s,t) \leq 1, LU(s,t)=2 \ and \ LU(s,t-1)=2 \\ (1-h)NS(s,t) + (M_p(s,t) - 0.7M_{p\_prist}), & LU(s,t)=2 \ and \ LU(s,t-1) \leq 1 \end{cases} \quad (4.5),$$

where M_{p_prist} (kg/ha) corresponds to the protected soil N stocks under pristine land-use conditions, and h is the protection coefficient. The annual N surplus array, $N_s(LU(s,t),t)$, is developed based on land use-specific N surplus values, calculated as described in Section 4.3.2.

Within this conceptual framework, which focuses on changing dynamics between cultivated and non-cultivated landscapes, ELEMeNT considers physical protection mechanisms such as soil aggregation to be the primary determinant of whether SON remains within the protected pool (Six et al. 2002b). When land is transitioned from pastureland (LU=1) or non-agricultural land use (LU=0) to cropland (LU=2), we assume physical protection mechanisms to be disrupted, leading M_p to be reduced, in a step function, to 70% of the protected SON stock under the pristine

condition (M_{p_prist}). Such an assumption is based on empirical evidence across multiple landscapes of fast decreases in SON on this order of magnitude after initial cultivation (Davidson and Ackerman 1993b; Beniston et al. 2014; Whitmore, Bradbury, and Johnson 1992). Within the modeling framework, this mass of N from the protected pool is transferred to the active pool upon cultivation, making it subject to fast mineralization. Accordingly, just as the net N inputs are partitioned between the active and protected pools as a function of land use, the partitioning of SON stocks between the pools also changes as a function of changes in land use. These dynamics are expressed in **Equations 4.4** and **4.5** above.

Nitrogen leaving the SON pool enters the source zone mineral N pool (M_s), from which it will either leach into groundwater or leave the soil system via denitrification. Source zone N trajectories can be described using the following equation:

$$\frac{dM_s(s,t)}{dt} = k_a M_a(s,t) + k_p M_p(s,t) - \lambda_s M_s(s,t) - J_s(s,t) \qquad (4.6),$$

$$J_s(s,t) = \begin{cases} M_s(s,t)\dfrac{Q(t)}{V_w}, & Q(t) < V_w \\[2mm] M_s(s,t), & Q(t) > V_w \end{cases} \qquad (4.7),$$

where $\lambda(t)$ (y^{-1}) is the denitrification rate constant in the source zone, $Q(t)$ is the annual discharge and V_W (= nsV) is the water volume in the source zone, with n being the porosity, s the saturation and V the volume of the soil column per unit area within the source zone. Here, the first two terms on the right-hand side of the top equation represent the input from the active and protected organic pools, protected pools, the third term is the loss from the source zone via denitrification, and the last term is losses from leaching to groundwater. Note that when annual flow is greater than the water volume in the source zone, the mass of mineral N in the source zone goes to zero.

4.3   Methods and Data Sources

4.3.1   N Mass Balance

Annual N surplus values (*NS*) were calculated using a surface N balance approach (Bouwman, Van Drecht, and Van der Hoek 2005), which considers N inputs

and outputs to the landscape, with the N surplus being defined as N inputs – usable outputs (Erisman et al. 2005; Parris 1998; Leip, Britz, et al. 2011). Using this approach, inputs are calculated separately for cropland, pastureland, and non-agricultural land:

$$N_s(crop,t) = BNF_{crop} + FERT_{crop} + MAN_{crop} + DEP - CROP \qquad (4.8),$$

$$N_s(past,t) = BNF_{past} + FERT_{past} + MAN_{past} + DEP - GRASS \qquad (4.9),$$

$$N_s(other,t) = BNF_{nat} + DEP \qquad (4.10),$$

where $N_s(crop,t)$, $N_s(past,t)$, and $N_s(other,t)$ represent surplus N applied to cropland, pastureland, and non-agricultural land respectively, at the soil surface, BNF_{crop}, $BNF_{past,}$ and BNF_{nat} refer to biological nitrogen fixation, $FERT_{crop}$ and $FERT_{past}$ to applied inorganic N fertilizer, MAN_{crop} to manure applied to cropland, MAN_{past} to manure applied to cropland as well as animal N excreted during grazing, DEP to atmospheric N deposition, $CROP$ to crop N output, and $GRASS$ (kg/ha) to grass N consumption by grazing livestock, all in units of kg ha^{-1}.

Biological N fixation (*BNF*), the process by which non-reactive atmospheric N is converted to reactive N via microbial activity (James N. Galloway et al. 1995) was calculated based on state-level cropped area and crop production data obtained through the U.S. Agricultural Census (http://www.agcensus.usda.gov/) and U.S. Agricultural Survey (USDA-NASS) using area and yield-based methods (Han and Allan 2008; Hong, Swaney, and Howarth 2013; Bouwman, Van Drecht, and Van der Hoek 2005). Fertilizer N inputs (*FERT*) are based on county-level estimates of N fertilizer application for the conterminous U.S. (Ruddy, Lorenz, and Mueller 2006) as well as FAO estimates of mean N fertilizer application to pastureland (Francis 2000). Manure N inputs (*MAN*) were calculated based on livestock data from the U.S. Agricultural Census (http://www.agcensus.usda.gov/) and U.S. Agricultural Survey (USDA-NASS), animal N intake and excrement parameters (Hong, Swaney, and Howarth 2011;

Vaclav Smil 1999; Bouwman, Van Drecht, and Van der Hoek 2005) and estimates regarding the distribution of livestock between unconfined and confined feeding operations (R. L. Kellogg et al. 2000). Removal of N via crop production (*CROP*) and grazing (*GRASS*) was calculated using census data for harvest yields and livestock production (USDA-NASS) and relevant parameter values for crop N content and livestock grass consumption obtained from the literature (Hong, Swaney, and Howarth 2011; Bouwman, Van Drecht, and Van der Hoek 2005). For further details regarding calculations for the N mass balance, see Appendix 2.

4.3.2 Uncertainty Analysis for the N Mass Balance

Uncertainty analysis, utilizing Monte Carlo simulations, was carried out to characterize the uncertainty associated with the calculation of N surplus values (Mishra 2009; Chen et al. 2014). For each parameter used in the mass balance calculations, we assumed a normal probability distribution with a CV value of 0.3. A total of 1000 simulations were carried out to obtain median and interquartile range values for the N surplus trajectory across the study period.

4.3.3 Sensitivity Analysis & Model Calibration

4.3.3.1 Sensitivity Analysis. Global parameter sensitivity analysis (PSA) was carried out to identify model parameters contributing most significantly to soil organic N (SON) levels and stream N loading (Mishra 2009; Muleta and Nicklow 2005). As given in **Supplementary Tables A2.1 & A2.2** in Appendix 2, 10 potentially calibratable parameters were chosen from the model and were assumed to follow a uniform distribution across a designated range (Haan et al. 1998). Ranges for each parameter were assigned based on a combination of literature review and knowledge of the two study watersheds. The Latin hypercube sampling (LHS) technique, a form of stratified Monte Carlo sampling, was used to generate 1000 parameter sets from these ranges, assuming a uniform distribution across each range. The model simulations were then run, and the output variables of interest (residual sum of squares values for (1) median SON values, 1950-2015, (2) SON accumulation, 1980-2010, and (2) annual N loading at the catchment outlet) were extracted. Output data was rank-transformed to account for non-linearities in model behavior (Iman & Conover 1979). Stepwise regression analysis was carried out with the 1000 input-output pairs for both SON

values and annual N loading. A threshold value of p<=0.05 was used as criteria for inclusion of individual parameters in the model. Results of the regression analysis are given in **Supplementary Tables A2. 3 & A2.4**, Appendix 2.

4.3.3.1 Model Calibration. Model parameters were selected for optimization based on the results of the sensitivity analysis. The model was calibrated to optimize simulation of (1) current levels of SON and (2) N loading at the catchment outlet. Median SON levels for the watersheds were calculated based on USDA gridded soil survey data (Soil Survey Staff 2015). For the MRB, catchment N loading values are based on USGS water quality data (Mississippi River near St. Francisville, Louisiana and Atchafalaya River at Melville, Louisiana) and discharge data (Mississippi River at Tarbert Landing, Old River Outflow Channel near Knox Landing, Atchafalaya River at Simmesport, Ohio River at Metropolis, Missisippi River at Thebes) via the regression-based rating-curve method (Aulenbach 2006; USEPA 2014). For the SRB, N loading was calculated at Conowingo by the WRTDS weighted regression method (R. Hirsch, Moyer, and Archfield 2010) via the EGRET software package (R. M. Hirsch and De Cicco 2014). The mean absolute error (MAE) was used as the objective function to assess goodness of fit to the observed data from a series of Monte Carlo simulations. Optimization was carried out in an iterative fashion, with the top-performing 10% of parameter sets from each set of simulations being selected based on goodness of fit to the specified objective function. Median values were extracted for all relevant parameters, as provided in **Supplementary Tables A2.5,** Appendix 2.

4.3.4   Site Descriptions

4.3.4.1 Mississippi River Basin. The Mississippi River basin (MRB), which covers approximately 40% of the land area of the contiguous U.S. (2,981,076 km^2) is an intensively managed system that over the last 200 years has undergone radical transformation, both terrestrially and hydrologically. In 1866, cropped area in the MRB made up only 6% of watershed area (**Figure 4.4**). By 1940, however, the area in cropland had nearly quadrupled. Between 1866 and 1890, the rate of increase was at its greatest, resulting in close to 15,000 km^2 of land—the equivalent of the state of

Connecticut—being brought under new cultivation each year. The MRB now accounts for approximately 70% of U.S. cropland and contains approximately 60% of all cattle of 90% of all hogs raised within the U.S. (Smith et al. 2005). Soil in the MRB is highly fertile, with soil organic carbon (SOC) content ranging from median values of 7.1 kg m^{-2} ($\sim$0.7 kg m^{-2} SON) in the Tennessee River subbasin to 12.5 kg m^{-2} ($\sim$1.0 kg m^{-2} SON) in the Missouri River subbasin (Buell and Markewich 2003). Widespread agricultural land use in the basin has led to high levels of fertilizer application and intensive livestock production, resulting in high levels of nutrient loading to offshore waters (Rabalais, Turner, and Scavia 2002).   Currently, the Mississippi delivers more than 900 Mtons of N to the Gulf of Mexico each year, with a long-term mean discharge volume of 17,000 m^3/sec ($\sim$180 mm y^{-1}) (Goolsby et al. 1999; Murphy, Hirsch, and Sprague 2013; Turner and Rabalais 2003).

4.3.4.2 Susquehanna River Basin. The Susquehanna River Basin (SRB) (70,160 km^2), extends through portions of Maryland, Pennsylvania and New York and empties into the northern region of the Chesapeake Bay, immediately downstream from the Conowingo dam (Foster, Lippa, and Miller 2000). With a daily mean discharge of 1,030 m^3/s ($\sim$460 mm y^{-1}), the Susquehanna is the largest river draining into the Chesapeake Bay and accounts for more than half of the annual nutrient load to the bay (Foster, Lippa, and Miller 2000; W. M. Kemp et al. 2005). Soil fertility in the SRB is significantly lower than that in the MRB, with median SOC and SON levels of approximately 2.6 kg m^{-2} and 0.2 kg m^{-2}, respectively, less than one-fourth levels in the MRB. Agricultural land use in the SRB peaked early in the 20th century (Houghton and Hackler 2000) (**Figure 4.3**). Since then, the basin has experienced both increasing urbanization and widespread reforestation of previously cleared land (D'elia, Boynton, and Sanders 2003; Kemp et al. 2005; Drummond and Loveland 2010; Thompson et al. 2013). Despite the declining proportion of the watershed devoted to agriculture, increased use of commercial fertilizers and importation of animal feed paired with high levels of atmospheric N deposition have led to anthropogenically induced increases in primary productivity and associated problems of hypoxia in the Chesapeake Bay (Kemp et al. 2005).

Figure 4.3. Land use and population trajectories for the Mississippi and Susquehanna river basins.
Cropland and pastureland Land-use trajectories are based on state-level cropland and pastureland data (USDA-NASS), supplemented by historical modeled cropland data from Ramankutty and Foley (1999), aggregated to the watershed scale.
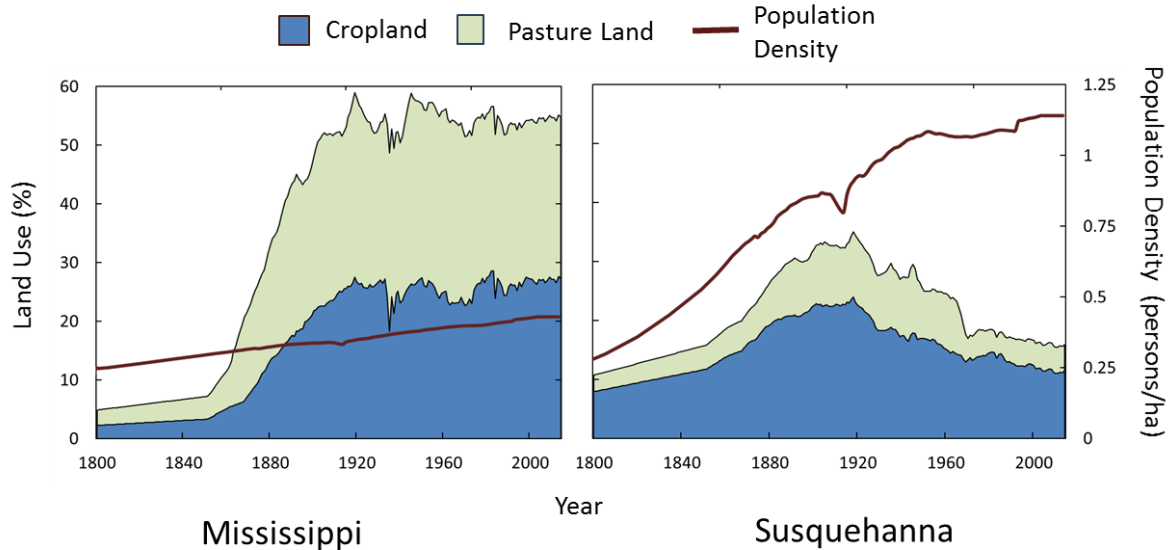
4.4   Results & Discussion

The objective of the present study was to develop a modeling framework, ELEMeNT, to quantify long-term, watershed-scale N fluxes, and to use this new framework to quantify N legacies and to assess their impacts on water quality. To carry out this objective, we synthesized land-use, population and agricultural production data to create soil-surface N surplus trajectories for the years 1800-2015 across the Mississippi and Susquehanna river basins. These input trajectories were then used to model N dynamics across the study period. As described below, the model results allow us to quantify depletion and accumulation trajectories of subsurface N stores. In addition, model results allow us to explore questions regarding the travel times of N from its entry into the terrestrial system to its exit at the catchment outlet, as well as the sources of annual N outputs.

4.4.1   N Surplus Trajectories, Cropland

Cropland N surplus trajectories in both the MRB and SRB are characterized by large increases in N inputs between 1945 and 1980, primarily driven by increases in fertilizer application during this period (**Figure 4.4**). Interestingly, it can be seen that

despite differences in climate, land use, and soil fertility between the two watersheds, N surplus values for cropland are quite similar. For example, for the period 1990-2014, the mean N surplus for cropland was 63.7 ± 15.4 kg ha^{-1} y^{-1} for the MRB and 78.2 ± 18.5 kg ha^{-1} y^{-1} for the SRB. The relative importance of specific sources of N, however, does vary between watersheds. For example, the mean rates of fertilizer application to cropland in the MRB during this period were approximately 25 kg ha^{-1} higher in the MRB than the SRB (**Figure 4.5**). Other N inputs (BNF, Manure N, atmospheric N deposition), however, were all greater in the SRB, making up this difference and ultimately leading to a somewhat higher N surplus for SRB cropland. Atmospheric N deposition was found to be a particularly important portion of the N budget in the SRB, accounting for approximately 13% of N inputs to cropland from 1990-2014 (23.0 ± 5.6 kg ha^{-1} y^{-1}) compared to the 6% of inputs (10.6 ± 1.1 kg ha^{-1} y^{-1}) in the MRB, primarily due to high nitrogen oxide emissions from fossil fuel combustion in the Northeastern United States (Jaworksi et al. 1997). Both manure (14.6 ± 0.6 kg ha^{-1} y^{-1}, SRB; 5.1 ± 0.2 kg ha^{-1} y^{-1}, MRB) and biological N fixation (88.9 ± 1.9 kg ha^{-1} y^{-1}, SRB; 79.2 ± 7.0 kg ha^{-1} y^{-1}, MRB) from the growth of N-fixing crops such as alfalfa and soybean account for a larger proportion of N inputs to cropland in the SRB than the MRB due to higher densities of livestock production in the SRB and the smaller area of land in agricultural production available for manure application.

Figure 4.4. Nitrogen inputs to agricultural land, 1866-2014.
The figure shows net N input trajectories for both the Mississippi and Susquehanna
river basins (a). In the lower panels (b), individual components for the N balance are
shown, with inputs (fertilizer, atmospheric deposition, manure, biological N fixation)
represented by the stacked lines and crop N outputs represented by white bars.
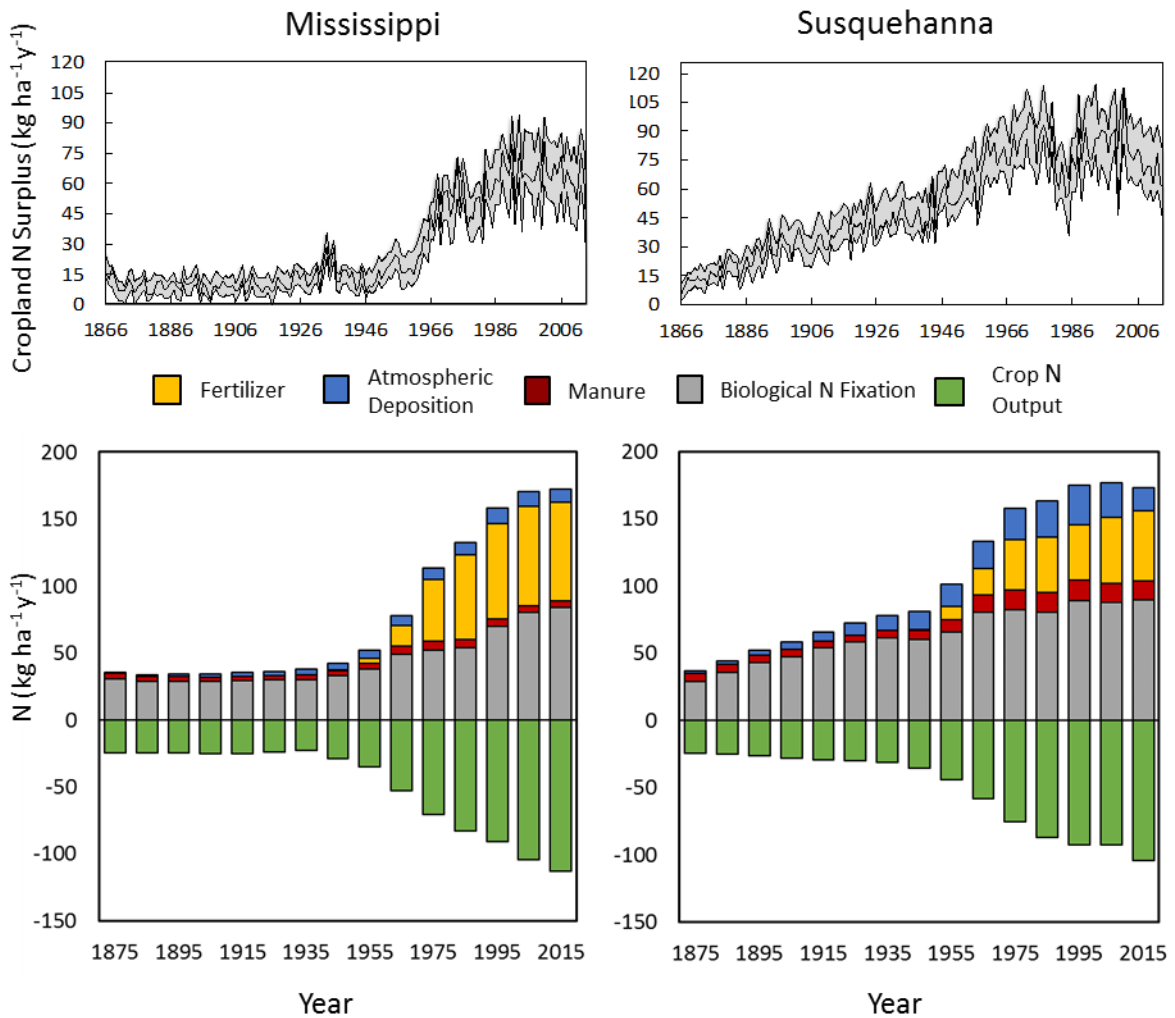
4.4.2 Sensitivity Analysis and Model Calibration

Sensitivity analysis showed that the primary parameters impacting 1950-2010
median SON levels were the mineralization rate constants (k_a, k_p) for active and
protected SON and the humification coefficients for non-cultivated and cultivated land
(h_{nc}, h_c) (**Supplementary Tables A2.3 & A2.4, Appendix 2**). N loading at the

catchment outlet was found to be chiefly impacted by denitrification rate constants in soil and groundwater (λ_s,) as well as the mean travel time (μ) through groundwater pathways.

Calibration results for the model are given in **Supplementary Table A2.5,** Appendix 2. Calibrated parameter values are of the same order of magnitude between the two basins. The most significant difference in parameterization for the two basins is in the soil mineralization rate constant, kp, for protected soil, which is more than six times greater for the SRB than for the MRB (1.4×10^{-4} y^{-1}, MRB; 9.2×10^{-4} y^{-1}, SRB). This difference accounts for the much higher levels of soil organic matter and thus higher fertility in soils of the MRB.

Modeled and measured N loads at the outlets of the Mississippi and Susquehanna river basins are shown in **Figure 4.5**. Modeled loads are shown for the entire study period (1800-2014), and annual estimates based on measured concentration values are provided where available. For the MRB (**Figure 4.6a**), measured data for the period 1979-2013 indicate median nitrate-N loading to the Gulf of Mexico of 3.3 kg ha^{-1} y^{-1} (980 ktons y^{-1}). These results are well-matched by the model results, which predict loading of 3.2 kg ha^{-1} y^{-1} (968 ktons y^{-1}), a difference of only 1.3%. For the SRB, measured data indicate N loading of 6.0 kg ha^{-1} y^{-1} (42.9 ktons y^{-1} for the period 1979-2013 (**Figure 4.6b**), compared with the model-predicted loading of 6.2 kg ha^{-1} y^{-1} (43.0 ktons y^{-1}), a difference of only 2.5%.

It should be noted here that model calibration was carried out for both basins for the years 1979-2013. Although for the SRB, no measured data is available before that period, we do have estimates of annual N loading for the MRB back to 1955, which allows us the opportunity to validate the model during a period with a significantly different N input regime. More specifically, the annual catchment-scale N surplus in the MRB was only 16.5±2.3 kg ha^{-1} for the period 1955-1970, approximately half that calculated for the later calibration period (29.6±3.3 kg ha^{-1}). Modeled values for 1955-1970, however, show an excellent match with measured values (1.2±0.2 kg ha^{-1}, modeled; 1.1±0.3 kg ha^{-1}, measured), a statistically insignificant difference, depite the much lower N fertilization rates for the 1955-1970

period and the rapidly changes changes in management practices during this period, including a major shift from the growth of small grains such as barley and wheat to the more widespread cultivation of N-fixing soybeans (Foufoula-Georgiou et al. 2015). The good model fit for this period suggests that our pre-1955 trajectories are also also defensible and provide a good estimate of long-term N loading trajectories for the MRB.

Figure 4.5. Catchment-Scale N Loading to the Mississippi and Susquehanna River Basins, 1800-2014.
Load values are area-normalized to the total catchment area for the Mississippi (a) and Susquehanna (b). Red diamonds represent measured N loads for the two basins, while the black line represents the modeled values. The grey area indicates the 95% confidence interval based on the calibrated parameter values.
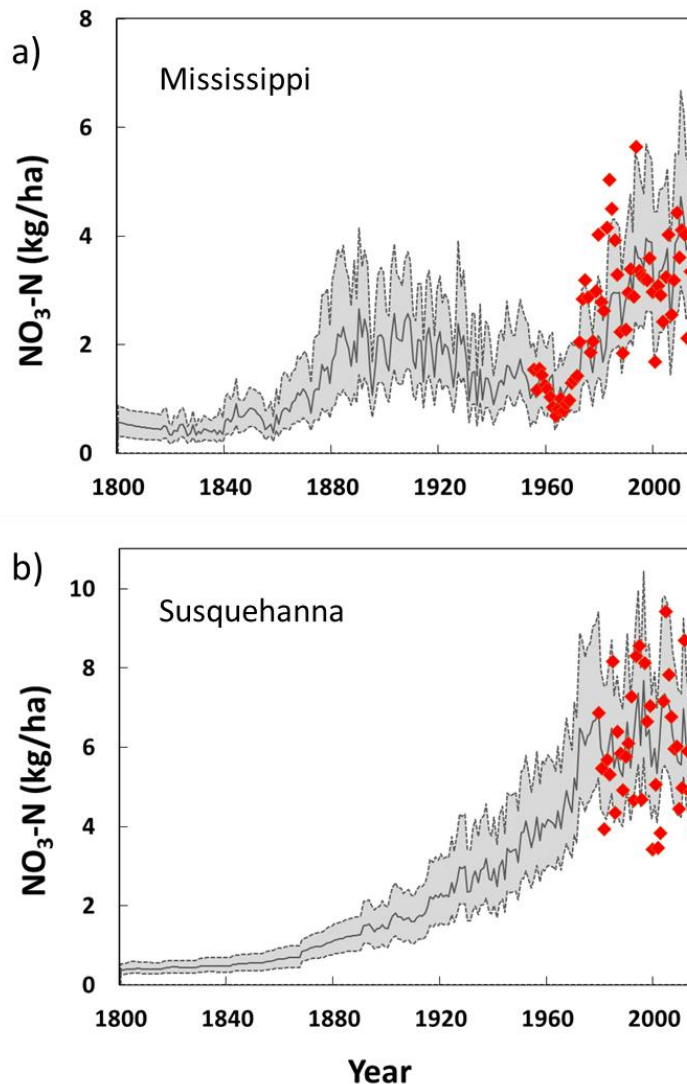
4.4.3 Nitrogen Fluxes and Stores

4.4.3.1 Stream N Loading. The long history of N input data developed herein for the Susquehanna and Mississippi River Basins together with the ELEMeNT modeling framework allows us to provide a historical reconstruction of nitrate-N loading over the past two centuries. Using this approach we are able not only to estimate pre-industrial N loading levels and to better understand trajectories of change for the rivers themselves and for receiving water bodies.

In the present study, our model results suggest that pre-industrial (1800-1840) riverine nitrate fluxes were on the order of 0.5 kg ha^{-1} y^{-1} for both of the study basins, corresponding to concentrations of approximately ~0.4 mg L^{-1} and MRB and ~0.1 mg L^{-1} in the SRB). These results indicate that nitrate-N loads have increased approximately 7-fold in the MRB since 1840, and more than 14-fold in the SRB since the pre-industrial period. Our modeled estimates are in line with previous estimates by Howarth et al. (1996), who have reported 2- to 20-fold increases in N fluxes in North Atlantic watersheds, and those by Kemp & Dodds (2001), whose data show 6 to 40-fold increases in nitrate-N in North American prairie streams. Both of these earlier estimates are based on space-for-time substitutions, which assume that current N fluxes from pristine or near-pristine catchments can accurately represent historical conditions.

While such large increases in N loading between the current and the pre-industrial periods are expected, the trajectories of change for the two basins may be considered surprising. First, although the fastest 20th-century rates of change in loading for both watersheds occurred between approximately 1960 and 1980 (~3-5% increases in nitrate-N loading each year), corresponding to large increases in commercial fertilizer application during this period (**Figure 4.2**), our results suggest that N-loading prior to this period was already elevated approximately 3-4 times above baseline levels (1.4±140 kg ha^{-1} y^{-1}, MRB; 2.8±0.3 kg ha^{-1} y^{-1}, SRB). For the SRB, increases in N-loading were relatively linear from 1850-1950, reflecting a steady intensification of agriculture as well as N deposition from industrial sources. For the MRB, however, the loading trajectory appears to have been more threshold-based,

coinciding with the plowing of North American prairie lands, and a sharper land use change trajectory. As seen in **Figure 4.6**, nitrate-N loads more than tripled between 1850 and 1890, and then decreased again to near-pristine levels until the widespread adoption of commercial N fertilizer use in the mid-20th century.

This early increase in N loading for the MRB corresponds to a period of fast and far-reaching land-use change, as pristine or minimally impacted lands were converted to row-crop agriculture across the basin, and is comparable to the increases observed following the widespread plowing of permanent grasslands in the UK after World War II (Howden 2011). Such large, landscape-scale losses of N are also similar to those currently being seen in the Amazon Basin, which has begun to show elevated N loading due to the effects of deforestation and new cultivation, despite the overall N surplus for the region remaining relatively low (Howarth et al. 1996; Biggs, Dunne, and Martinelli 2004; Fonseca et al. 2014). Our finding of a mid-19th century increase in N loading for the MRB is also supported by increases in the levels of biologically bound silica (BSi) that have been found in marine sediments in the Gulf of Mexico from this period (Turner and Rabalais 2003). As N is the nutrient that most frequently limits primary productivity in near-coastal waters (Mitsch et al. 2001; Howarth et al. 2006), Bsi levels, which are directly linked to levels phytoplankton production, can be used as a proxy measure of N loading to these waters.

A decoupling of N surplus values from nitrate-N loads due to N legacy or N storage-related effects can be seen for both the MRB and SRB in **Figure 4.6.** In the figure, nitrate-N loading at the catchment outlet is plotted against the annual N surplus, with the slopes of the regression lines corresponding to the percent of the N surplus being lost as riverine output. For the period 1965-2014, the MRB N load shows a strong relationship with N surplus values (slope 0.16, R^2=0.63, p<0.001) (**Figure 4.6a**). Prior to this period, however, N loading is largely decoupled from N inputs. From 1850-1890, for example, the fast rate at which land was brought under cultivation and the high levels of SON in prairie soils led to an additional 9000 ktons of N reaching the mouth of the Mississippi compared with N loading for the previous 40 years, despite only minimal increases in the overall N surplus. Accordingly, the

regression line for the load vs surplus relationship is nearly vertical for this period (slope 0.92), reflecting the large-scale release of landscape N legacies. In the subsequent period, during which this newly released N began leaving the system, N loading actually shows an inverse relationship with surplus values, with legacy N dynamics completely masking the more direct input-out relationship.

For the SRB, new cultivation during the pre-industrial period occurred over longer time scales and soil N stores in pristine land were less than a third those in the MRB, leading to a much lower impact of cultivation on early N dynamics. Accordingly, N loading is strongly correlated with annual N surplus values before approximately 1970 (slope 0.12, R^2=0.96, p<0.001) (**Figure 4.6b**). After 1970, however, N surplus values began to level off (1971-1989) and then to decrease (1990-2014), primarily due to decreases in atmospheric N deposition rates. During these periods, catchment-scale N loading began to be more strongly driven by N legacies than by current-year N inputs. In the figure, this shift is reflected by the nonlinear relationship between surplus values and N loading after 1970. The pattern of response between surplus values and N loading plotted in the figure is hysteretic, with the counter-clockwise path of the response loop suggesting a time delay in the recovery trajectory for the basin, despite clear reductions in N surplus values.

Figure 4.6. Relationship between N loading at catchment outlet and N surplus values.
For the MRB (**a**), N loading shows a strong linear relationship (p<0.001, R^2=0.63) between 1965 and 2014. Similarly, a direct linear relationship can be seen for the SRB (**b**) from 1860-1970 (p<0.001, R^2=0.96). Outside of these periods, however, N loading is decoupled from annual N surplus values due to the impacts of large landscape-scale release of SON (MRB) and, more recently in the SRB, anthropogenic N legacies. In particular, a pattern of hysteresis can be seen for the SRB since 1971 (blue diamonds), as N loading remains elevated despite decreases in the N surplus.
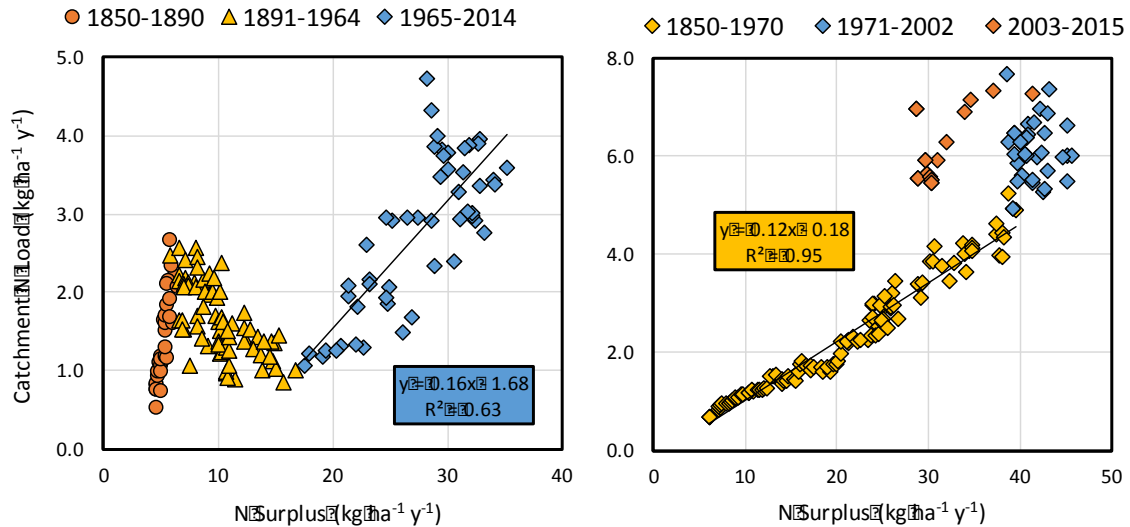
4.4.3.2 Regime Shifts in Soil Organic N Trajectories. For the MRB, the model results show a pattern of soil organic N (SON) depletion after initial cultivation of pristine landscapes (**Figure 4.7a**), followed by SON accumulation as net N inputs increase. This pattern is suggestive of three different functional states across the anthropogenically induced evolution of the landscape (Van Meter et al. 2016). In the first, under pristine or very low-impact conditions, SON levels were at steady state, with rates of immobilization and mineralization being equal to each other such that there is minimal net N flux out of the soil organic pool. In the second, which for the MRB began in the mid to late-1800s and which was triggered by the rapid westward expansion of settlement across the watershed, was characterized by a large regime shift, where the soil layer became a major source of mineralized N to surface and groundwater. These results are in line with many literature reports of rapid mineralization of soil organic matter after initial cultivation (Beniston et al. 2014; M.B. David et al. 2009; Davidson and Ackerman 1993b; Lal, Follett, and Kimble 2003;

Whitmore, Bradbury, and Johnson 1992), particularly in nutrient-rich soils like those found throughout the North American prairie region. Such rapid losses can be attributed to a loss of the physical protection provided by soil aggregates in undisturbed soils, as cultivation breaks up aggregate structures (Six et al. 2002b) and thus increases oxidation and mineralization rates (Lal, Follett, and Kimble 2003). Finally, in the third stage, we see another major shift, with the soil becoming an N sink as the N inputs to agricultural land increase with the start of more intensive agricultural use, and particularly the use of N fertilizers. For the MRB, this shift can be seen in the period between 1940 and 1960, with soils since that time consistently serving as a net N sink.

For the Susquehanna River Basin, the pattern is quite different, primarily due to the different levels of soil fertility in the SRB compared to the MRB (**Figure 4.7b**). In the MRB, median levels of SON, as indicated by NCSS soil sampling (NCSS), are currently on the order of 7580 kg ha^{-1} basin-wide, or 13,600 kg ha^{-1} in cropland, approximately three to four times those in the in the SRB (2065 kg ha^{-1}, basinwide; 4,600 kg ha^{-1} cropland). The MRB is dominated by Mollisols (U.S. Soil Taxonomh) or Chernozems (FAO System of Soil Classification), which are the soils of grassland systems and are characterized by a thick, dark surface horizon, high levels of fertility, and thus high levels of SON (Kellogg 1936). In contrast, the SRB is more dominated by Inceptisols (U.S. Soil Taxonomy) or Camibsols (FAO System of Soil Classification), which have minimal horizon development, lower levels of fertility, and thus lower levels of SON (Kellogg 1936). Upon first cultivation the N-poor soils of the SRB would have less N to lose than the N-rich soils of the MRB. Accordingly, although there was a net positive N flux from soils of the SRB from approximately 1800-1860, when the conversion of forests to cropland was at its height for the region, these fluxes were relatively small (0.6±0.1 kg ha^{-1}) compared to those for the MRB during this period (1.4±0.6 kg ha^{-1}). Our results show that the SRB then became a net sink for N beginning in the 1890s, although the magnitude of this sink decreased significantly after the 1920s, primarily due to decreases in the percent farmland and a trend toward reforestation. Currently, soil is again serving as a minor N source, with this pattern being attributable to conversion of agricultural land to non-agricultural uses

at the same time that atmospheric N deposition is on the decline (**Figure 4.5**), thus decreasing the net inputs to the land surface.

One caveat regarding these results is related to the assumptions we have made regarding the potential for N accumulation in non-agricultural soils. Although some research suggests that N is also accumulating in forested (de Vries et al. 2009) and suburban (Lewis et al. 2006b) areas beyond baseline levels due to both atmospheric N deposition and the use of lawn fertilizers, other work indicates that forested areas in particular may reach a point of N saturation, a condition in which N availability may exceed the capacity of the terrestrial system to further accumulate N (Lovett and Goodale 2011; Niu et al. 2016). Due to uncertainty associated with establishment of threshold values for N saturation, we have assumed that no N accumulation would occur beyond levels in the pristine system. In so doing, we likely provide an overly conservative estimate of N retention in soils and, thus may overestimate the flux to groundwater.

4.4.3.3 Groundwater N Accumulation. For both the MRB and SRB, the model results show a net positive flux of N to groundwater storage in response to both new cultivation of land and increases in N surplus values over time (**Figure 4.7**), an increase that is consistent with observed increases in groundwater nitrate concentrations at United States Geological Survey sites across the U.S. from 2 mg NO_3^--N mL^{-1} to approximately 15 mg NO_3^--N mL^{-1} between 1940 and 2003 (Puckett, Tesoriero, and Dubrovsky 2011b). In the MRB, annual model-estimated increases in groundwater N across the watershed were relatively small between 1800 and 1860, averaging 1.2±0.6 kg ha^{-1}, and then doubling to 2.8±0.9 kg ha^{-1} during the period of fast land-use change between 1860 and 1920. Although annual inputs to groundwater again leveled off to approximately pre-1860 levels after 1920, groundwater in the MRB is currently a N sink, with levels increasing on the order of 3.8 kg ha y^{-1} (1990-2013).

In the Susquehanna Basin, despite its smaller percentage of agricultural land, the rate of groundwater N accumulation has been consistently greater than that in the MRB, primarily due to the SRB's high atmospheric N deposition rates, nearly twice

those in the MRB (23.0±5.4 kg ha^{-1}, SRB; 10.6±1.1 kg ha^{-1}, MRB (1990-2013)). In the non-agricultural areas of the SRB, which make up approximately 80% of the watershed, there is no N removal from crop production and N uptake levels are relatively low (Lovett and Goodale 2011; Baker et al. 2001). With the low-nutrient soils of the region providing little buffering capacity, N from deposition sources passes quickly through the landscape and enter groundwater reservoirs. Such results are also expected based on the higher recharge rates in the SRB (~230 mm y^{-1}) than the MRB (~125 mm y^{-1}) (USGS 2010), as Liao et al. (2011) have consistently found a strong relationship between mass in groundwater and recharge rate at similar levels of applied N. Currently, the model predicts that increases in groundwater N in the SRB are occurring at a rate of approximately 11.6 kg ha y^{-1}.

Our results suggest that differences in land use and the high levels of industrial-driven N deposition in the SRB have led to a total N accumulation in the SRB of approximately 980±275 kg ha^{-1}, close to double that in the MRB (508±237 kg ha^{-1}). Although no consistent data is available to estimate or compare actual current magnitudes of nitrate-N in groundwater aquifers between the two watersheds due to the complexity of the underlying aquifer systems and the large areas covered by the watersheds, concentration data do suggest higher levels for the SRB. In particular, a USGS study of nitrate-N in groundwater of the lower SRB found median nitrate concentrations of 7.3 mg-N L^{-1} in agricultural areas of the Piedmont region (Lindsey et al. 1997). In the MRB, NAQWA data from selected aquifers (Lindsey and Rupert 2012) show median nitrate-N concentrations from 0.9 mg-N L^{-1} in alluvial aquifers of Arkansas and Tennesse to 2.5 mg/L in heavily agricultural areas of Iowa and 3.3 mg-N L^{-1} in the high plains aquifer in western portions of the MRB. These lower groundwater concentrations for the MRB are consistent with our model prediction of lower N loading to groundwater, as discussed in Section 4.4.3.1.

Figure 4.7. Nitrogen fluxes to and from subsurface reservoirs in the Mississippi and Susquehanna River Basins, 1800-2014.
For the MRB, soil organic N fluxes exhibit a major regime shift over the study period, from a depletion pattern from the 1880s to 1930s, to a pattern of N accumulation since the 1960s (**a**). For the SRB, soil N plays a more minor role in N dynamics (**b**), with groundwater functioning as a more significant N sink. Our modeling results show groundwater N accumulation in the SRB (**d**) to be approximately twice that in the MRB (**c**)
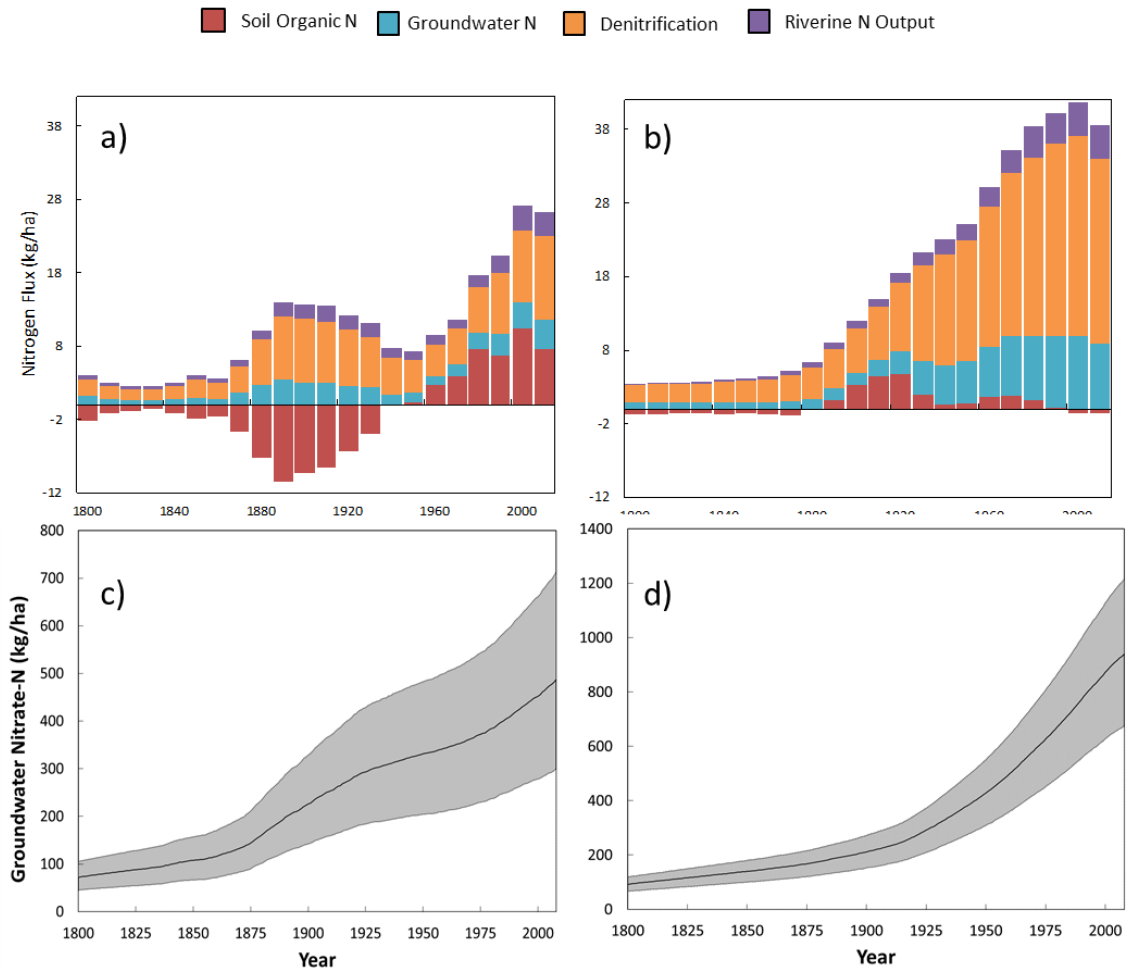
4.4.4. Nitrogen Age at the Catchment Outlet

Nitrogen age, which we define herein as the time elapsed from application of N at the land surface to the arrival of N at the catchment outlet, is calculated as a function of (1) travel times through groundwater pathways, and (2) the distribution of N residence times in the soil organic matter pools. We assumed exponential travel time distributions for the groundwater pathway (McGuire and McDonnell 2006a), and

84

our model calibration suggested mean groundwater travel times of approximately 16 years (16.0±5.7 y, MRB; 15.6±3.1, SRB) for the two study areas. Although the estimation of groundwater travel times through subsurface pathways is notoriously complex, particularly in varied geologic settings (Phillips, Focazio, and Bachman 1999), our modeled results are in line with literature reports. In particular, in subwatersheds within the SRB and MRB, groundwater travel times have been found to range from less than a year to more than 50 years (Sanford and Pope 2013; Phillips, Focazio, and Bachman 1999; Lindsey et al. 2003; Schilling et al. 2007).

As discussed in Section 4.2.2.2, isotope studies suggest that the majority of nitrate-N leaching from the soil profile has passed through the soil organic N pool (Haag and Kaupenjohann 2001; Spoelstra et al. 2001). Accordingly, N residence times within the soil profile, which are controlled by organic N mineralization rates, can be considered to represent a significant fraction of the time lag between N application on land and arrival at the catchment outlet. Organic matter in soil is mineralized to more mobile inorganic forms on timescales ranging from days to millennia (Torn et al. 1997; Gleixner et al. 2002; Jenkinson 1990). Within our modeling framework, residence times in soil organic matter are dependent on whether N is in the active pool or the protected pool. Based on our calibration results, the mean residence times of SON in the active pools for the two watersheds are less than 10 years (8.8 years, MRB; 7.6 years, SRB). For the protected pool, however, these times are two orders of magnitude greater (4280 years, MRB; 1636 years, SRB).

Based on the above, we found the N load at the catchment outlet in both of the study watersheds to be dominated by legacy N, which we consider here to be N greater than 1 year of age (**Figure 4.8**). For the MRB, we again see the strong signature of the plowing of pristine lands in the late-18th and early-19th centuries. During this period, previously protected soil organic N, with its very long residence times, was exposed to the stresses of climate and mechanical disruption, leading to rapid mineralization of older SON (Six et al. 2002b; Davidson and Ackerman 1993b). For the period between 1860 and 1920, more than 60% of the N flux at the MRB outlet would have entered the terrestrial system more than 50 years ago, with much of it originating from biological N-fixation during the pre-settlement period.

Currently, legacy N in the MRB accounts for approximately 85% of all the annual N load, with more than half of that 85% having originated from anthropogenic sources since 1960. For the SRB, 47% of the current load can be attributed to legacy sources, with the rest being attributed to current-year N surplus. Nearly all of the annual legacy N loading (>95%) is anthropogenic in origin, having been introduced into the terrestrial system since 1960.

Figure 4.8. Age of nitrogen at the catchment outlet.
The figure shows changes in the distribution of N age over the study period, by decade, for the Mississippi (left) and Susquehanna (right) River Basins.
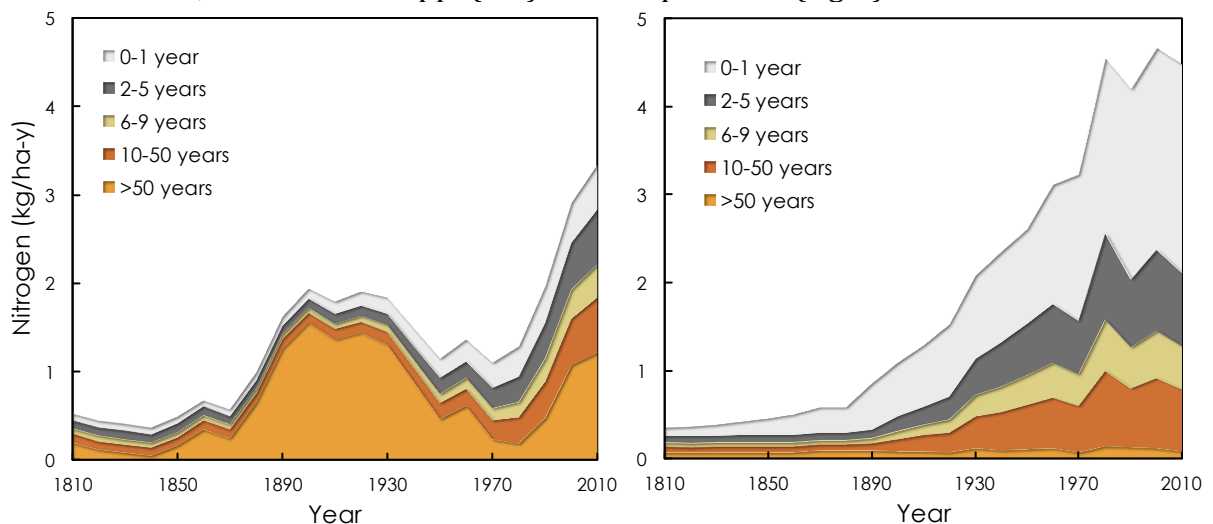
4.4.4.4 Characterization of Nitrogen Sources at the Catchment Outlet. As more aggressive nutrient reduction goals are being set for both Mississippi and Chesapeake Bay watersheds, much attention has focused on the implementation of new management practices and conservation measures (Rabotyagov et al. 2014 ; National Research Council 2011). To effectively meet such goals, it is crucial to understand the primary sources of nutrients reaching the catchment outlet. For both the MRB and SRB, changes in land use and management have led to changes over time in the relative importance of the different sources of N (**Figure 4.9**). As seen in the figure, the major change for the MRB has come with the use of N fertilizer, which now accounts for approximately 28% of total N loading. Although the use of commercial N fertilizer began in earnest in the 1940s, our results show that it took nearly two

decades for fertilizer to make a significant contribution to N loading. More specifically, fertilizer N accounted for a negligible portion of N loads in the 1940s; this percentage had increased to approximately 5% by the 1960s, then growing to 18% in the 1970s to 28% now.

In contrast, although N fertilizer use also saw a more than 100-fold increase between the 1950s and the present day in the SRB, fertilizer N makes up a much smaller portion of the N-loading budget, accounting for only 4% of total loads. Instead, N loading in the SRB has come to be dominated by atmospheric N deposition. In the 1950s, the relative importance of atmospheric deposition was comparable between the two basins (31% of N loading, MRB; 34%, SRB). However, due to urbanization and increased fossil fuel use as well as the density of livestock operations (National Research Council 2011) in the SRB, atmospheric N deposition continued to increase into the 1990s, accounting for as much as 350 ktons of annual N loading. The greater importance of N deposition in the SRB is also a result of the relatively smaller proportion of agricultural land in the watershed, which means that atmospheric N deposition is the only anthropogenic N input across approximately 85% of the watershed. Although atmospheric N deposition rates have begun to show a significant downward trend in the northeastern U.S. (Houlton et al. 2013), N deposition continues to account for approximately 40% of N loading in the SRB.

In the SRB, manure N also constitutes a large fraction of annual N loading (27%). Throughout the Chesapeake Bay region, not only is the density of livestock production relatively high, the small proportion of agricultural land leads to a lack of a local land base for spreading livestock manure (Guan and Holley 2011). Accordingly, there are higher per-area inputs of manure to agricultural land throughout the SRB, leading to over-saturation of land with surplus liquids and nutrients and higher levels of N runoff. Interestingly, for the MRB, although the magnitude of manure production has increased more than fivefold over the study period, it makes up only 10% of total N loading, a much lower proportion than in the SRB. It should be noted here, however, that approximately half of the atmospheric N deposition in both watersheds can be traced back to volatilization of a combination of fertilizer and animals waste (Hong, Swaney, and Howarth 2011; Schindler 2006). In addition, a large portion of

U.S. cropland is devoted to producing animal feed, e.g. more than 40% of corn and 80% of soybeans, meaning that livestock make a bigger contribution to watershed N loading than may be suggested by manure N production alone.

Figure 4.9. Sources of nitrogen at the catchment outlet.
The figure shows changes in the distribution of N age over the study period, by decade.
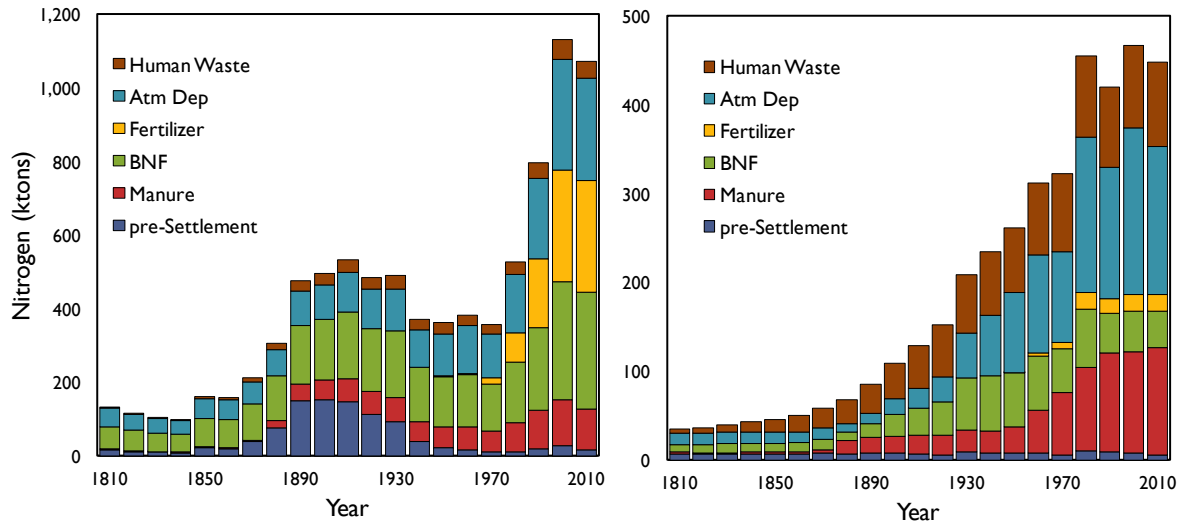
4.5   Implications and Significance

In 2008, the Mississippi River/Gulf of Mexico Watershed Nutrient Task Force released an "action plan" to reduce the size of the Gulf of Mexico's summer hypoxic zone to less than 5,000 km^2 by 2015 (S. S. Rabotyagov et al. 2014; USEPA 2008). With the 2014 and 2015 dead zones being measured at 2-3 times the targeted size (13,085 km^2 and 16,768 km^2, respectively (NOAA 2015)), the deadline for achieving this goal has now been extended to 2035. Similarly, the Chesapeake Bay Program (CBP) a broad partnership among multiple states and the U.S. Environmental Protection Agency, committed in 1987 to reducing "controllable" N and P loading to the Chesapeake Bay by 40% by the year 2000. A 2011 report evaluating the success of these efforts notes that progress has been limited and that the nutrient reduction goals have still not been attained (Reckhow et al. 2011).

Such delays in achieving reduction goals can be attributed to a number of causes, from institutional inertia (Berkes, Colding, and Folke 2008), to a lack of funding for needed interventions (USDA 2015), to evolving knowledge regarding the effectiveness of specific intervention strategies (Mitsch et al. 2001; Bouraoui and Grizzetti 2014). Increasingly, however, policymakers and researchers alike have pointed to the existence of legacy nutrients in human-impacted catchments as a cause for time lags in catchment response (Van Meter and Basu 2015; Worrall, Howden, and Burt 2015; Meals, Dressing, and Davenport 2010), time lags that present obvious challenges to meeting current nutrient reduction goals. Despite this growing recognition of the need for considering landscape-scale nutrient legacies when setting policy goals and implementing remediation strategies, there remains a lack of appropriate models that can capture land use change and water quality impacts over long time scales. In the present study, we have taken a long-term approach to exploring the possible impacts of legacy-related time lags within the MRB and SRB, pairing more than two centuries of watershed-scale N input data with the ELEMeNT modeling framework in order to more adequately take into account the development of legacy N stores within these watersheds and to quantify the role that these legacies play in multi-decadal trajectories of N loading.

Our results first show 7-fold and 14-fold increases in N loading for the MRB and SRB, respectively, since pre-industrial times. Although such increases are clearly linked to 20th-century increases in the use of commercial N fertilizers, N loading has also at times shown a decoupling from N inputs due to the influence of legacy N. For the MRB, this decoupling occurred most prominently with the release of large landscape-scale N legacies during the period of European settlement; for the SRB, however, it is most clearly seen as a function of more recent anthropogenic legacies in the SRB, as N surplus values have decreased, while N loading has remained elevated (**Figure 4.6**). The model results also demonstrate the development of large subsurface N legacies for both of the study watersheds, although the magnitudes and locations of the accumulation differ between the two watersheds. In particular, the lower-fertility soil of the SRB together with higher annual runoff leads to less N

accumulation in soil, but greater groundwater accumulation and higher levels of stream N loading compared to MRB.

Our results indicate that current annual N loading in both the MRB and SRB is strongly impacted by legacy sources, which, as described in 3.4, we define as N greater than 1 years of age (85%, MRB; 47%, SRB). Accordingly, to achieve both short-term and long-term success in reducing N loads to coastal areas, it may be necessary to take a two-pronged approach to nutrient management in these watersheds. For the fastest reductions in loading, it will be important to target current-year sources. For the MRB, which is the more legacy-driven system and thus more bound by inertia, short-term gains will be more difficult to achieve. In this case, a targeted short-term approach like the increased use of constructed wetlands to intercept runoff from tile drains and flooding streams (Mitsch et al. 2001) would need to be integrated with longer term approaches of reductions in N application rates, and modification of tile drainage networks to slow the transport of N to nearby waterbodies (Drury et al. 2014). In the SRB, where both animal manure and urban wastewater represent significant current-year sources, upgrades to WWTPs (Carey and Migliaccio 2009; Zimmerman and Dooley 2014) and more innovative forms of manure management, including the development of biogas reactors for both waste treatment and energy production (Weiland 2006), may have a larger short-term impact. Indeed, WWTP upgrades have accounted for a significant portion of nutrient reductions already achieved in the Chesapeake Bay region (Reckhow et al. 2011), and the wastewater treatment plant at Harrisburg, Pennsylvania, the largest point source of nitrogen to the Susquehanna River, is currently undergoing a major upgrade scheduled for completion in 2016 (CRW 2016).

For the remediation of legacy N sources, riparian buffers and wetlands, in areas where a significant portion of groundwater intersects the buffered area, may represent the best approach to preventing groundwater N from entering waterways (Messer et al. 2012). Although soil N legacies can serve as a long-term source to groundwater, opportunities may also be available to effectively utilize the legacy N through the planting of cover crops (Drury et al. 2014; Malone et al. 2014) or by the

conversion of areas currently in row crop to perennial vegetation, including biofuel crops such as switchgrass or Miscanthus (Costello et al. 2009; Wu and Liu 2012).

       The most important finding of the current study is that significant legacies of N have accumulated within the Mississippi and Susquehanna river basins. Moreover, plentiful evidence exists to suggest that these two heavily impacted watersheds are not unique, and that legacy nutrient stores likely play a dominant role throughout the world in controlling nutrient loading to coastal areas (Sharpley et al. 2013; Withers et al. 2014). As more stringent nutrient control measures continue to be put into place (Backer et al. 2010; USEPA 2008; Reckhow et al. 2011), our work underlines the necessity for further exploring the magnitudes and spatial distribution of legacy nutrient stores so as to better our ability to meet nutrient reduction goals and to reduce uncertainties regarding the timescales over which legacy nutrients will adversely affect water quality.

Chapter 5 - Time Lags in Watershed-Scale Nutrient Transport: An Exploration of Dominant Controls

5.1   Introduction

Nutrient-driven hypoxia is a continuing problem in near-coastal waters around the world, from the South China Sea in Asia (Wang et al. 2016) to the Baltic Sea in Europe (Caballero-Alfonso, Carstensen, and Conley 2015) and the Gulf of Mexico (R. E. Turner, Rabalais, and Justic 2008) and Chesapeake Bay (Diaz and Rosenberg 2008) in North America. Freshwater lakes and other surface water bodies also continue to be plagued by problems of eutrophication, with excess nutrient loading leading to reports of harmful cyanobacterial blooms in areas such as Lake Taihu in China and Lake Erie in North America (Xu et al. 2015; Michalak et al. 2013). Such nutrient enrichment poses a threat to drinking water quality and can disrupt the biogeochemical and ecological stability of freshwater and saltwater habitats.

For decades, attempts have been made at a range of scales to reduce the discharge of nutrients to surface and groundwater, from the upgrading of wastewater treatment plants to implementation of a variety of agricultural management practices, including reducing N application rates, constructing treatment wetlands, utilizing controlled drainage, and creating riparian buffer zones (Kronvang et al. 2008; D'Arcy and Frost 2001). Despite such interventions, however, measurable progress to achieving nutrient water quality goals has been limited (Meals, Dressing, and Davenport 2010). In the Netherlands, for example, a phased program to meet water quality goals for Nitrogen (N) and Phosphorus (P) was implemented in 1985 (Boers 1996); in 2009, however, more than 20 years later, it was reported that only 25% of surface waters in the Netherlands met the established standards for N and P (van Puijenbroek, Cleij, and Visser 2014). In Denmark it is

reported that after nearly four decades of combating nutrient pollution, only marginal progress is being made toward the goal of achieving approximately 50% reductions in N and P loading . Similarly, in North America, ambitious goals were set in the 1980s to reduce "controllable" N and P loading to the Chesapeake Bay by 40%, and in 2008 the Mississippi River/Gulf of Mexico Waters Nutrient task force set the goal of reducing the size of the summer hypoxic zone to 5000 km2 by 2015 (Rabotyagov et al. 2014; USEPA 2008). In neither of these cases have nutrient goals been achieved, and target dates have now been extended by up to two decades (Rabotyagov et al. 2014; Reckhow et al. 2011).

Based on such apparent failures, one might predict that policy groups and regulatory bodies would be moving toward the establishment of more conservative timelines for achieving nutrient goals. Recent announcements by the Great Lakes Commission (GLC), however, suggest otherwise ("Lake Erie Nutrient Reduction Plan Released" 2015). In an effort to diminish the problems associated with harmful algal blooms and anoxic zones in Lake Erie, the GLC has endorsed a plan to reduce P loading to the central and western basins by 40% by the year 2025, allowing just a 10-year period to implement and achieve the intended goal. In the action plan associated with the announcement, there is little mention of a science-based rationale for this 10-year time frame, except to say that the "timelines herein will be pursued using an adaptive management approach whereby they may be revised based on regular monitoring, new information, discussion and knowledge of the system" (Joint Action Plan for Lake Erie, 2015).

The establishment of ambitious targets for achieving needed improvements in water often may primarily reflect a basic optimism that the setting of targets will shape action in a way that long-term planning with less tangible short-term rewards may not (Langford and Winkler 2014). 6will scarcely accounts for lags in

The relatively short time periods proposed to achieve these water quality goals may attempt to account for institutional lags or lags in the implementation of new management practices, but they do not appear to account for physically-based time lags within watersheds, lags that can lead to significant delays between improvements in nutrient use efficiency or management and subsequent measurable improvements in water quality. The presence of such physically-based time lags, however, is increasingly recognized in the

scientific literature (Van Meter and Basu 2015; Fenton et al. 2011a; Hamilton 2012a; Meals, Dressing, and Davenport 2010). Such time lags can occur via a range of mechanisms across the landscape, from temporary storage of nutrients in soil or vegetation, to long hydrologic transport times through the subsurface, to retention of nutrients in surface water reservoirs and stream sediments. For example, it is now well understood that, for nitrate, hydrologic delays due to slow groundwater travel pathways may result in very slow improvements in water quality, even with significant improvements in N management (Van Meter and Basu 2015; Meals, Dressing, and Davenport 2010; Sanford and Pope 2013; Hamilton 2012a; Fenton et al. 2011a). A growing body of work is thus focusing on quantifying transit times of water and solutes both through the vadose zone and through complex aquifer systems, using experimental and modeling approaches (McGuire and McDonnell 2006b; van der Velde et al. 2010; Rinaldo et al. 2015; Sousa et al. 2013). It is also being recognized that while slow groundwater transit times lead to *hydrologic lags*, N and P retention in both soils and sediments might lead to an additional *biogeochemical time lag* that is relatively less studied and more complex to quantify (Van Meter and Basu 2015; Hamilton 2012a; Worrall, Howden, and Burt 2015).

Despite the importance of understanding and quantifying catchment-scale time lags with regard to setting reasonable and achievable goals for water quality improvement, we continue to lack appropriate techniques for quantifying these lags, particularly techniques that can take into account the diversity of landscape and management drivers that may impact these lags. Although nutrient mass balance approaches have been used to link the magnitude of current watershed nutrient surpluses with current N and P loading (Hong, Swaney, and Howarth 2011; Swaney et al. 2012b; Boyer et al. 2002), there has been little emphasis on validating the consistency of these input-output relationships over time. There has been increasing interest in calculating long-term N and P balance trajectories (Goyette et al. 2016; David, Drinkwater, and McIsaac 2010) as well as in quantifying long-term trends in N loading, but there has until now been no systematic attempt to link these long-term trajectories of nutrient inputs and outputs as a means of clarifying our understanding of catchment-scale time lags.

In the present study, we have focused specifically on nitrogen dynamics in an intensively managed watershed with the goal of quantifying N-related time lags and of identifying the primary physical and management controls on these lags. Using the Grand River Watershed in Southern Ontario, Canada, as a case study, we have attempted to answer the following questions:

1) What are the dominant controls on stream N loads?
2) Can long-term trajectories of N input and output be used to quantify time lags in catchment-scale N response?
3) Do time lags vary as a function of season?
4) What are the primary controls on time lags, and do these controls also vary as a function of season?

5.2 Methods

5.2.1 Study Area

The Grand River Watershed (GRW), located in southwestern Ontario, covers an area of approximately 6800 km^2 and is the largest Canadian watershed draining into Lake Erie (Loomer and Cooke 2011). Typical of many watersheds in the eastern U.S. and Canada, the GRW remains heavily influenced by agriculture but has also in recent decades been characterized by a loss of agricultural land, reforestation, and increasing urbanization (Ramankutty and Foley 1999). Although agriculture is the dominant land use in the watershed, the central portion of the watershed is also home to areas of intense urbanization. As such, population densities as well as the intensity of agricultural land use vary significantly across the watershed. The GRW's long history of intensive agriculture as well as its currently large urban footprint have led to significant changes in stream and groundwater nitrate concentrations over time and make it an ideal candidate for an analysis of catchment-scale time lags.

The GRW is spatially heterogeneous with regard to its surficial geology. As a result, some areas of the watershed more vulnerable to overland runoff and soil erosion, while other areas have sandier, more permeable soils, leading to faster movement of dissolved nutrients such as nitrate into the subsurface (Loomer and Cooke 2011). The watershed can be divided into three geologic zones, the upper till plain, the central gravel moraines, and the lower clay plain. The upper till plain, which encompasses the Upper

Grand as well as the upper Nith and Conestogo sub watersheds, is characterized by low levels of permeability and high levels of runoff (250-700 mm/year). In contrast, the central region of the watershed, which includes, among others, the Speed, lower Nith, and Whiteman's Creek sub watersheds, is highly permeable, with high levels of groundwater recharge. The lower Grand, which includes portions of the Fairchild subwatershed, has silt-dominated soil and very high levels of runoff. The hydrology of the GRW has been modified by both damming and by tile drainage. Constructed water control structures have led to the creation of 7 large reservoirs on both the main stem and tributaries of the Grand. Subsurface drains (tile drainage) are heavily utilized in the upper till plain to remove excess water from cropland and route it into nearby ditches and streams, thus reducing overland runoff and increasing the importance of subsurface pathways for nutrient transport. In the Conestoga and Canagagigue subwatersheds, fields with tile drainage encompass approximately 35% and 50% of the total watershed area, respectively (GRCA 2016).

For our analysis, we focus on 16 subwatersheds across the GRW, 9 of them tributaries to the Grand, and the other 7 along the river's main stem. A summary of these watersheds along with relevant station data is provided in **Table 5.1.**

Table 5.1. Water Quality Monitoring Stations used in the Analyses

River	Site Description	PWQMN ID Number	Area (ha)	Date Range
Grand River	Near Marsville	16018406702	65,821	1972-1996, 2007-2014
	Below Shand Dam	16018403702	78,512	1972-1998, 2001-2014
	West Montrose	16018410302	115,214	1980-1998, 2002-2014
	Brantford	16018402702	529,518	1964-2014
	Newport	16018402402	521,737	1970-2006
	Glen Morris	16018401002	355,972	1965-2014
	York	16018409202	602,943	1977-2013
Canagagigue Creek	Upper Canagagigue	16018405102	6,414	1973-2014
	Lower Canagagigue	16018401602	11,357	1973-2014
Speed River	Below Guelph	16018403602	62,853	1972-2014
	Eramosa River	16018410202	23,023	1979-2014
Conestogo River	Glen Allan	16018407702	56,660	1975-2014
Nith River	Upper Nith	16018403202	54,774	1970-2012
	Lower Nith	16018400902	110,174	1964-2013
Whiteman's Creek	Whiteman's Creek	16018410602	32,611	1981-2014
Fairchild Creek	Fairchild Creek	16018409302	38,073	1979-2014

Figure 5.1: Grand River Watershed showing the stations analyzed along both the main stem of the river (left) and its tributaries (right).

Grand River, Main Stem

A   Grand River near Marsville
B   Grand River Below Shand Dam
C   Grand River at West Montrose
D   Grand River at Glen Morris Bridge
E   Grand River at Brantford
F   Grand River at Newport
G   Grand River at York

Grand River, Tributaries

H   Conestogo River at Glen Allan
I   Upper Canagagigue Creek
J   Lower Canagagigue Creek
K   Speed River Below Guelph
L   Eramosa River
M   Upper Nith River
N   Lower Nith River
O   Fairchild Creek
P   Whiteman's Creek

5.2.2 N Surplus Calculations

Subwatershed-scale N surplus trajectories (*NS*) were calculated for the GRW utilizing long-term N surplus data calculated at the county scale, as reported by Zhang (2016). In these calculations, NS is the difference between N inputs and outputs, as described in the following equations:

$$NS = N_{inputs} - N_{outputs} \qquad (5.1)$$

$$N_{inputs} = FERT + BNF + DEP + MAN + W_h \qquad (5.2)$$

$$N_{outputs} = CROP \qquad (5.3)$$

In the above, *FERT* corresponds to annual inorganic N fertilizer inputs (kg ha^{-1}), *BNF* to biological N fixation, *DEP* to atmospheric N deposition (kg ha^{-1}), *MAN* to manure N inputs, W_h to N in human waste, and *CROP* to N outputs in crops.

Fertilizer N inputs (*FERT*) were calculated based on provincial fertilizer sales and use data (Korol et al. 2000; Statistics Canada 2016) as well as cropped area data from the Canadian Census of Agriculture (Statistics Canada). Biological N fixation (*BNF*), the process by which microbial organisms convert unreactive atmospheric nitrogen to reactive N (Galloway et al. 1995), was estimated by both area and yield-based methods (Han and Allan 2008; Hong, Swaney, and Howarth 2013) based on cropped area and annual yield data (Statistics Canada). Atmospheric N deposition (*DEP*) was calculated for the years 1977-2011 based on data from the NatCHEM database (Environment Canada 2016), while years prior to 1977 we used data obtained from Dentener et al. (2006). Manure N inputs (*MAN*) were estimated based on livestock data from the Census of Agriculture (Statistics Canada) and animal N intake and excrement parameters (Hong, Swaney, and Howarth 2011). N inputs from human waste (W_h) were calculated using population data from the Canada Census of Population (Statistics Canada) and estimates of human N consumption (Boyer et al. 2002; Hong, Swaney, and Howarth 2011). Crop N output was calculated based on crop yield data (Statistics Canada) and literature values for crop-specific N content (Hong et al. 2011; Bouwman et al. 2005). For further details regarding the N mass balance calculations, see Zhang (2016). ArcGIS software was used to translate the county-scale data to the watershed scale (ESRI 2010).

5.2.3 Trend Analysis in Stream Nitrate Data

5.2.3.1 Discharge and Water Quality Data. Daily discharge data was obtained online from the Water Survey of Canada, the national authority responsible for collecting, interpreting and disseminating standardized water resource data in Canada (Water Survey of Canada, wateroffice.ec.fc.ca). N concentration data was obtained from the Ontario Provincial Water Quality Monitoring Network (PWQMN; Ontario Ministry of Environment). The PWQMN has functioned as a partnership between the Ontario Ministry of the Environment (MOE) and local conservation authorities since the 1960s with the goal of carrying out long-term surface water quality monitoring throughout Ontario. All PWQMN monitoring stations within the GRW are sampled by the Grand River Conservation Authority

following a standardized protocol. Sites are currently sampled between 8 and 10 times per year (Loomer and Cooke 2011)(Loomer & Cooke, 2011). Sixteen water quality monitoring sites were chosen for the current analysis based on the following criteria: a) location with the GRW; b) proximity to a Ministry of Environment flow-monitoring station with discharge data available for the years corresponding to the sampling dates for the water quality samples; c) available sampling data over a period of at least 25 years. The longest record length for any of the stations was 48 years (1966-2014), and 87% of stations had data available over a period of at least 35 years. The PWQMN stations are provided in **Table 5.1.**

5.2.3.2 Estimation of Nitrate Load and Flow-averaged Concentrations (FAC). In order to understand long-term trends in riverine N fluxes, we used the weighted regression on time, discharge, and season (WRTDS) modeling approach (Hirsch 2010). WRTDS was developed as a means of estimating contaminant loads from sparse concentration data and has been applied previously to studies of the Mississippi River (Sprague et al. 2011; Lake Champlain (Medal et al. 2012), Iowa (Green et al. 2014) and Chesapeake Bay Watersheds (Zhang et al. 2013). WRTDS relies on the availability of daily stream discharge data together with periodic concentration data to develop weighted regression relationships that vary over time, season, and discharge regimes, allowing it to avoid biases that can arise when using time-constant parameters (Green et al. 2014; R. M. Hirsch and De Cicco 2014; Stenback et al. 2011). Daily concentration values were calculated in WRTDS via the following equation:

$$\ln(c) = \beta_0 + \beta_1 t + \beta_2 \ln(Q) + \beta_3 \sin(2\pi t) + \beta_4 \cos(2\pi t) + \varepsilon \qquad (5.4)$$

where, c is the concentration [ML^{-3}], $\beta_0, \beta_1, \beta_2, \beta_3, \beta_4$ are fitted regression coefficients, Q [$L^3 T^{-1}$] is daily streamflow, t [T] is time, and ε is an error term. Based on the WRTDS methodology, we utilized Matlab to create a matrix of regression relationships for every year across the full record of concentration data, for each month, and across 20 levels of discharge equally spaced in log space, spanning the full range of discharge values for each flow station (Hirsch, et al. 2010). When discharge values fell between these levels,

coefficient values were calculated based on interpolation between the matrix values.

In Supplemental Figure A3.1, we provide an example of the relationship between nitrate concentrations estimated via the WRTDS methodology and observed concentrations, as obtained from the PWQMN data described in section 2.3.1. As expected, the points show a close to 1:1 relationship (mean error = -0.01 mg NO_3-N/L). Supplemental Figure A3.2, which shows the ratio of observed to predicted nitrate concentrations in relation to observed discharge, demonstrates that errors in the predicted concentrations are not biased by discharge. The mean percent bias for all of the stations is -0.01. A complete summary of multiple error statistics is provided in supplemental Table A3.1.

Seasonal and annual flow-weighted concentrations were calculated from the measured daily discharge and the estimated daily concentrations (EQ 5.4) using the following equation:

$$C_f = \frac{\sum_{i=1}^{n} Q_i C_i}{\sum_{i=1}^{n} Q_i} \tag{5.5}$$

Annual FAC values were calculated using streamflow data for the entire year, while the seasonal data was estimated for the winter (December, January, February), spring (March, April, May), summer (June, July, August) and fall (September, October, November) seasons. Note that the numerator in Equation 5.5 is the annual N load. For our regression and cross correlation analyses described below, we used the flow-averaged concentration estimates instead of the most commonly used approach of using the N load. We have used this approach because the N load is strongly affected by year-to-year variations in mean annual discharge and thus climatic controls (Nandita B. Basu, Rao, et al. 2010), while FAC is a truer biogeochemical signature of the watershed that is impacted by land use and land management.

5.2.4 Regression Analysis to Understand Spatial Patterns

Correlation analyses were used to assess the relationships between a range of physical and management-related watershed characteristics (independent variables) and the mean annual flow-averaged nitrate concentrations (dependent variable) averaged over the period 2000-2010. Standardized regression coefficient values were calculated for each of the relationships, as follows (Muleta & Nicklow 2005):

$$SRC = \frac{s_x}{s_y} \tag{5.6}$$

where *SRC* is the standardized regression coefficient and s_x and s_y are the standard deviations of the independent and dependent variables, respectively. SRC values allow the strengths of the correlations between independent and dependent variables to be easily compared across a range of different variables.

Spatial data for the correlation analysis was obtained from the Grand River Information Network made available by the Grand River Conservation Authority (GRCA 2016). Management data, including annual N surplus values, fertilizer and manure application, and population density were derived from the N surplus calculations described in Section 5.2.2

5.2.5 Cross Correlation Analysis to Quantify Time Lags

Cross-correlation analysis is a standard statistical technique to quantify the correlation between two time series that are lagged in time with respect to each other (D. Chen et al. 2014; Hipel and McLeod 1994). We used this technique to quantify time lags between annual N surplus (ANS) and the flow-averaged nitrate concentrations at outlet. Time lag values for each watershed were selected based on the lag time with the highest positive correlation ($p<0.05$) between N surplus values and flow-averaged concentrations. The analysis was carried out in Matlab. Annual time lags were estimated based on annual FAC timeseries, while seasonal time lags were estimated based on seasonal FAC timeseries. As discussed in Section 1.0, time lags can occur due to temporary storage of N in vegetation, in soil and groundwater as well as in surface water reservoirs. Accordingly, the time lags calculated herein reflect the sum of all biogeochemical and hydrologic lags in N transport across the watersheds.

5.2.6 Multiple Linear Regression Analysis to Quantify Dominant Controls on Time Lags

A multiple linear regression (MLR) model was utilized to identify the dominant controls on the annual and seasonal time lags for the 16 study watersheds. First, simple regression analysis was used to identify watershed variables having a significant relationship with annual and seasonal time lag values. The watershed variables tested in this analysis were watershed area (AREA), % very fine sand (SAND_VF), soil type (%

SAND, SILT and CLAY), % soil organic matter (SOM), mean % slope (SLOPE), cropped area (CRP_AREA), % fractional tile-drained area (TILE), % wetland (WETLAND), depth to the water table (WAT_TBL), fertilizer application rate (FERT), watershed manure production (MAN), population density (POP_DEN), and the annual nitrogen surplus (ANS). Of these, for the last four variables, the mean values over the 2000 – 2010 timeframe was used for the analyses. It should be noted that N-related lag times in watersheds are widely considered to be dependent on the long travel times for mineral N through both unsaturated zone and groundwater pathways (Sousa et al. 2013). We therefore attempted to quantify this dependence in our analysis, considering soil type (percent sand, silt, clay, organic matter) and depth to the water table as proxy values for travel times through the unsaturated zone and the landscape gradient (slope) as a proxy for travel times through the saturated zone (Lindsey et al. 2003). The dominant variables thus identified were used to develop an MLR model. We developed a total of 5 MLR models (annual and four seasons) that explained the seasonal and annual variations in lag times across the 16 subwatersheds.

5.3.0 Results and Discussion

The objective of the present study was to clarify the spatial and temporal relationships between annual N surplus values and catchment-scale N loading. In particular, we have attempted to quantify time lags between changes in N inputs and subsequent catchment-scale changes in water quality and to identify the primary controls on such lags. We have also explored the seasonality of N-related time lags and have attempted to identify at what times of year N loading may be more legacy-driven and at what time dependent on current-year inputs. We describe the results of these explorations below.

5.3.1 Spatial Patterns and Dominant Controls on the Mean Annual FAC in the Stream

Regression analysis was used to evaluate the relationship between annual N surplus values and annual flow-averaged nitrate concentrations as well as 14 other watershed attributes (**Table 5.2**). As shown in Figure 5.2a, mean N surplus values (2000-2010) were found to be significantly correlated with mean FAC values (2000-2010) (**Table 5.2**) for the 16

subwatersheds of the GRW (SRC=0.82, p<0.001), as shown in **Figure 5.2a**. These results are consistent with the linear relationships between N inputs and outputs observed in multiple watersheds across the world (Mayer et al. 2002; Hong, Swaney, and Howarth 2013; Swaney et al. 2012a; G. Billen, Garnier, and Lassaletta 2014). Two major drivers of N surplus values (manure production and population density) also show strong (manure, SRC=0.63; population density, SRC=0.74), significant (p<0.05) relationships with the flow-averaged concentration values (**Figure 5.2b and 5.2c**), whereas a weaker relationship is seen between fertilizer application and nitrate concentrations. The organic carbon content of the soil was found to be significantly *negatively* correlated with FAC, which is consistent with observations that drainage paths with higher organic matter content are associated with higher denitrification rates, thus leading to decreased N loading to surface and groundwater (Speiran 2010; Brettar & Hofle 2002). The only watershed variable more strongly correlated with flow-averaged concentration values than the annual N surplus is the fractional tile-drained area (SRC=0.95, p<0.001), which is consistent with studies showing the positive relationship between tile drainage and N loads (M.B. David et al. 2008) (**Figure 5.2d**).

Table 5.2. Standardized Regression Coefficient (SRC) values, correlation coefficients and p values between mean annual FAC (2000 – 2010) and Watershed Attributes for the 16 watersheds considered in this chapter

	SRC	p-value	R^2
Watershed Area	0.02	0.956	0.00
Percent Sand	-0.28	0.301	0.09
Percent Silt	0.16	0.546	0.04
Percent Clay	0.41	0.115	0.16
Percent Org Matter	-0.72	0.002	0.47
Slope	-0.57	0.023	0.33
Percent Cropped Area	0.53	0.035	0.24
Fractional Tile-Drained Area	0.95	<0.001	0.88
Fractional Wetland Area	-0.86	<0.001	0.70
Depth to Water Table	0.41	0.111	0.15
Fertilizer Application	0.38	0.145	0.14
Manure	0.63	0.009	0.39
Population Density	0.74	0.001	0.51
Annual N Surplus	0.82	<0.001	0.64

Figure 5.2. Spatial analyses exploring correlations between mean annual flow-averaged nitrate concentrations (FACs) (2000-2010) and various watershed attributes for the 16 subwatersheds in the GRW: (a) mean annual NS (2000 – 2010) vs. FAC (b) Manure N vs. FAC (c) Population Density vs. FAC (d) fractional tile drainage vs. FAC
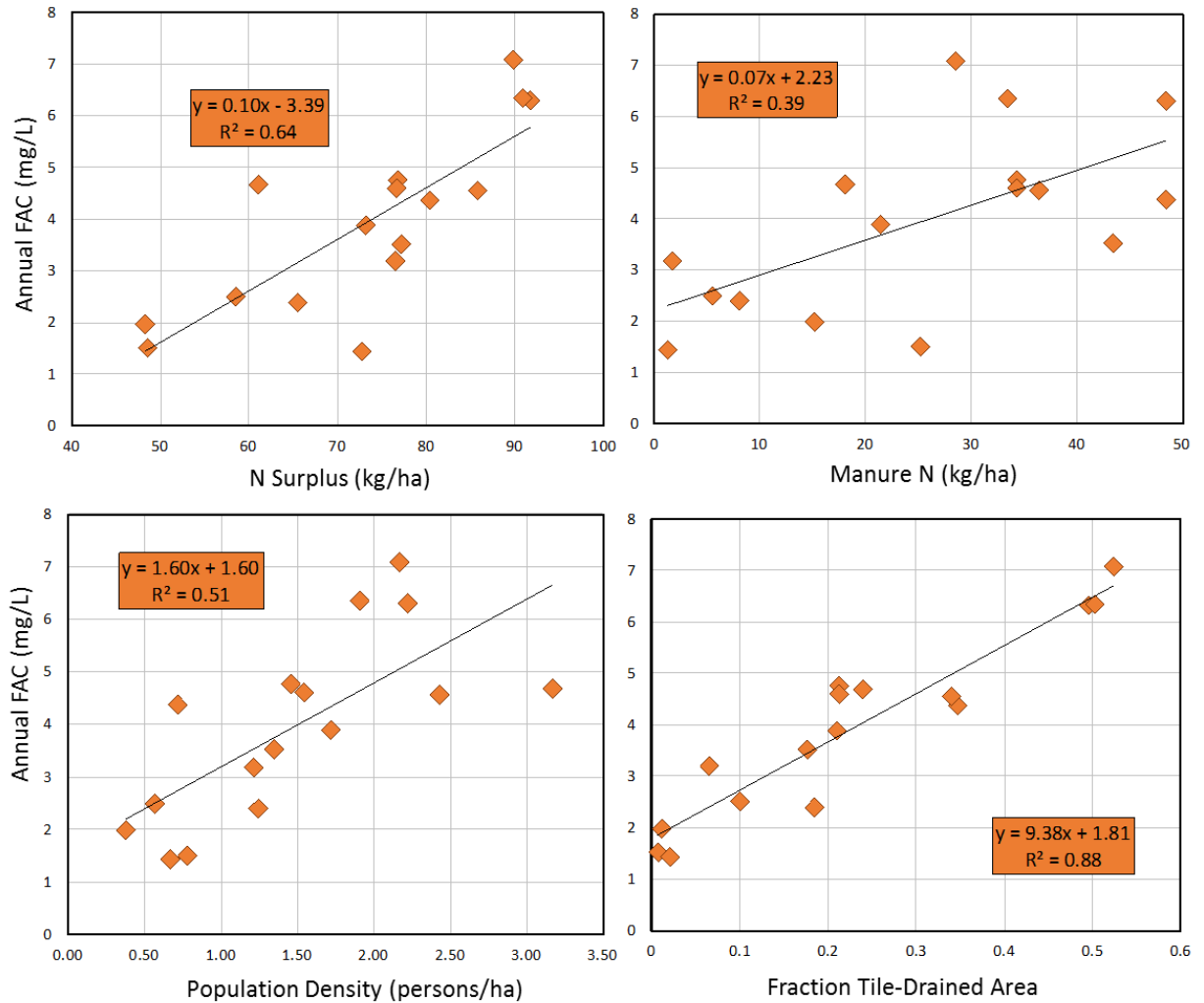
5.3.2   Temporal Trends in Annual N Surplus and Stream N Loading

5.3.2.1 N Surplus Trajectories. The positive correlation between mean annual flow-averaged nitrate concentrations and the mean annual N surplus (**Figure 5.2a**) suggests that reductions in the N surplus would lead to a reduction in the riverine N loads. To explore this question further, we utilized N surplus trajectories developed by Zhang (2016) across

the GRW over a 100-year timeframe, using agricultural census and other databases. In the GRW as a whole, the nitrogen surplus increased approximately two-fold from 46 kg N/ha/yr to 87 kg N/ha/yr between 1901 and 1976, and then decreased to 72 kg N/ha/yr by 2011 (**Figure 5.3a**). The N surplus trajectories for the 16 GRW subwatersheds show similar patterns, with peaks being reached between 1976 and 1980 (**Figure 5.3b**). In the figure, N surplus trajectories for the tributaries are represented by dotted lines, while those for the main stem of the Grand River are represented by solid lines. Although population densities are higher for the main stem watersheds (1.7 ± 0.3 persons ha^{-1}) than for the tributaries (1.1 ± 0.2 persons ha^{-1}), mean N surplus values are on the whole higher for the tributaries (tributaries: 79.4 ± 5.1 kg ha^{-1}; main stem: 65.6 ± 3.8 kg ha^{-1}). These higher N surplus values are primarily associated with the higher percent cropland in the tributaries (tributaries: $45.0 \pm 4.2\%$; main stem: $38.3 \pm 1.9\%$) and the associated higher rates of N fertilizer use (tributaries: 13.8 ± 3.1 kg ha^{-1}; main stem: 16.9 ± 2.5 kg ha^{-1}).

As noted above, N surplus values for all of the watersheds peaked in the mid- to late 1970s and have in general continued to decrease since that time. The extent of that decrease has ranged from 10.5-39.8% for the different sub-watersheds, with a median percent decrease of 16.5%. Decreases for the main stem have not differed significantly from those of the tributaries, with the exception of the Grand River at Marsville and the Grand River at Shand Dam, the two northernmost watersheds along the Grand. For these two nested subwatersheds, the percent decreases in N surplus values were 39.8% and 38.9%, respectively. These large decreases are primarily due to changes in cropping patterns and livestock density; in particular, these areas were net importers of food and feed in the mid-20th century but are now net exporters (X. Zhang 2016), thus decreasing the N surplus.

Figure 5.3 (a) Annual N surplus values and its sub-components over the GRW, adapted from Zhang et al. (in prep). (b) Annual N surplus values across the 16 subwatersheds used in our analyses. N surplus trajectories for the tributaries are represented by dotted lines, while those for the main stem of the Grand are represented by solid lines.
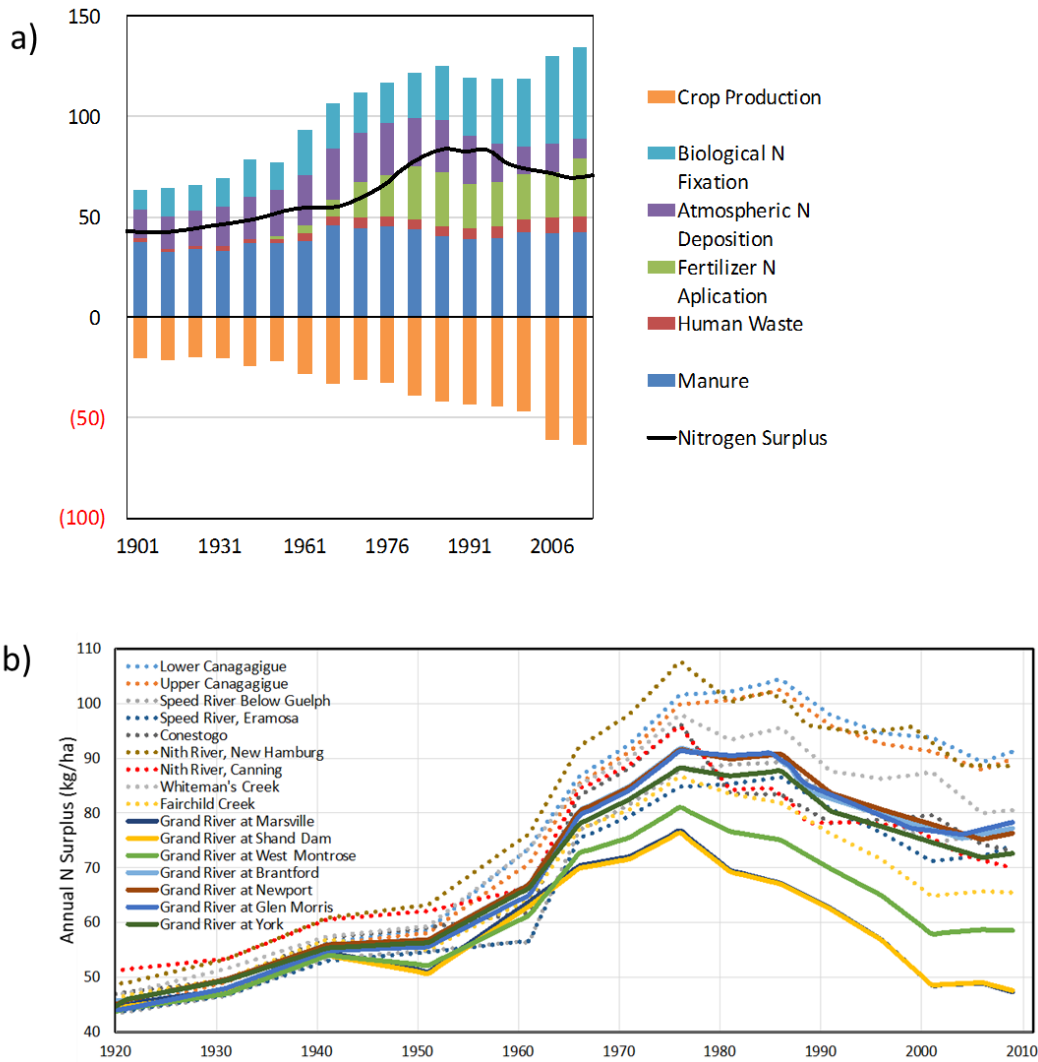
5.3.2.2 Nitrate Concentration Trajectories. Flow-averaged nitrate concentrations show an increasing temporal trend in the 1946-1992 timeframe across all the 16 sub-watersheds analyzed in this paper (**Table 5.3**). These increases were significant at a 99% confidence level ($p<0.01$) for all of the subwatersheds except Whiteman's Creek, the Eramosa River and the Grand River at West Montrose. The lack of significance for these three subwatersheds is likely due to a lack of data availability before 1980 rather than any actual

difference in trends. For the period 1993-2011, however, concentration trends have varied across the GRW. For this period, three of the 16 subwatersheds show a decreasing trend for flow-averaged nitrate concentrations, with the trend being significant (p<0.01) for only two of these, the Lower Canagagigue and Fairchild Creek tributaries. Of the remaining watersheds, all show an increasing trend, with this trend being significant (p<0.01) for three sites, all along the main stem of the Grand.

Table 5.3. Trends in FAC over two time periods: 1966 – 1992 and 1993 – 2010.
FAC concentrations show a consistently increasing and mostly significant (p<0.05) trends in the earlier time period. In contrast, FAC values in the later time period show both increasing and decreasing trends, and many of the trends are not significant

Station Name	pre-1993			1993-2014		
	slope	p-value	R-squared	slope	p-value	R-squared
Grand River Near Marsville	0.020	0.001	0.54	0.021	0.040	0.53
Grand River Below Shand Dam	0.024	0.000	0.79	0.006	0.391	0.05
Grand River at West Montrose	0.010	0.379	0.07	0.004	0.743	0.01
Grand River at Brantford	0.078	0.000	0.98	0.022	0.010	0.35
Grand River at Newport	0.081	0.000	0.97	0.074	0.000	0.75
Grand River at Glen Morris	0.092	0.000	0.97	0.032	0.000	0.61
Grand River at York	0.073	0.000	0.92	0.013	0.056	0.21
Upper Canagagigue	0.056	0.001	0.48	-0.010	0.796	0.00
Lower Canagagigue	0.150	0.000	0.91	-0.120	0.000	0.75
Speed River Below Guelph	0.088	0.000	0.79	0.017	0.409	0.04
Eramosa River	0.011	0.159	0.16	0.001	0.813	0.00
Conestogo River at Glen Allan	0.094	0.000	0.90	0.063	0.003	0.43
Upper Nith	0.079	0.000	0.87	-0.004	0.835	0.00
Lower Nith	0.121	0.000	0.98	0.004	0.686	0.01
Whiteman's Creek	0.035	0.149	0.20	0.028	0.036	0.25
Fairchild Creek	0.041	0.002	0.58	-0.031	0.000	0.63

5.3.2.3 Hysteresis in N Input-Output Trajectories

As described in Section 5.3.1, our spatial analysis of the GRW shows a strong correlation between flow-averaged nitrate concentrations and annual N surplus values (R^2=0.64, p<0.001). However, a look at relationships between inputs (N surplus values) and outputs (nitrate FAC values) over time for individual subwatersheds indicates a disruption in the linearity of the input/output relationship.

For example, as seen in **Figure 5.4a,** N surplus values for the Grand River at Brantford began to decrease in the late 70s and early 80s, but there has been no apparent decrease in FAC values since that time, although the slope value for FAC vs time for the post-1993 period (0.022 ± 0.007 mg L^{-1} y^{-1}, R^2=0.35) has decreased somewhat from that before 1993 (0.078 ± 0.002 mg L^{-1} y^{-1}, R^2=0.98). For the Lower Canagagigue, however (**Figure 5.4b)**, the response to changes in N surplus values has been faster, with a peak for flow-averaged nitrate concentrations being seen in 1997 at 8.3 mg L^{-1}, and then with significant decreases in FAC values for the post-1993 period of 0.120 ± 0.017 mg L^{-1} y^{-1}.

The results described above are suggestive of a mismatch between N surplus values and current-year N loading. For example, in **Figure 5.4c** we see a positive linear relationship between N surplus values and N outputs for the slower-responding main stem of the Grand up until approximately 1978 (R^2=0.93). From 1979-1986, however, there is a period of nonlinearity, where N surplus values remain relatively constant, while FAC values continue to increase. Beginning in 1987, we see the development of a *negative* relationship between current-year N surplus values and flow-averaged nitrate concentrations. This negative relationship between current inputs and outputs indicates a potentially *lagged* relationship and thus a visible hysteresis effect in the response curve of N surplus vs FAC values. For the Lower Canagagigue (**Figure 5.4d**), the hysteresis loop is tighter than that for the Grand River at Brantford, and by 2010 shows a return to late 1970s-level flow-averaged nitrate concentrations. The tighter hysteresis loop for the Lower Canagagigue suggests that this smaller tributary responds more quickly to changes in N inputs than the main stem of the Grand, meaning that current nutrient dynamics in the watershed are less driven by N legacies and thus that time lags will be shorter.

Figure 5.4. Temporal trajectories of Annual N surplus (ANS) and annual FAC values from 1940 – 2010 for two subwatersheds of the GRW: (a) the Grand River at Brantford, and (b) the Lower Canagagigue. The ANS trajectories for the two subwatersheds are quite similar, while the FAC trajectories are dramatically different, with the Lower Canagagigue watershed showing a much quicker response. These differences are also apparent when plotting the FAC against ANS, with the Lower Canagagigue (d) showing a tighter hysteresis loop than the Grand River at Brantford (c).
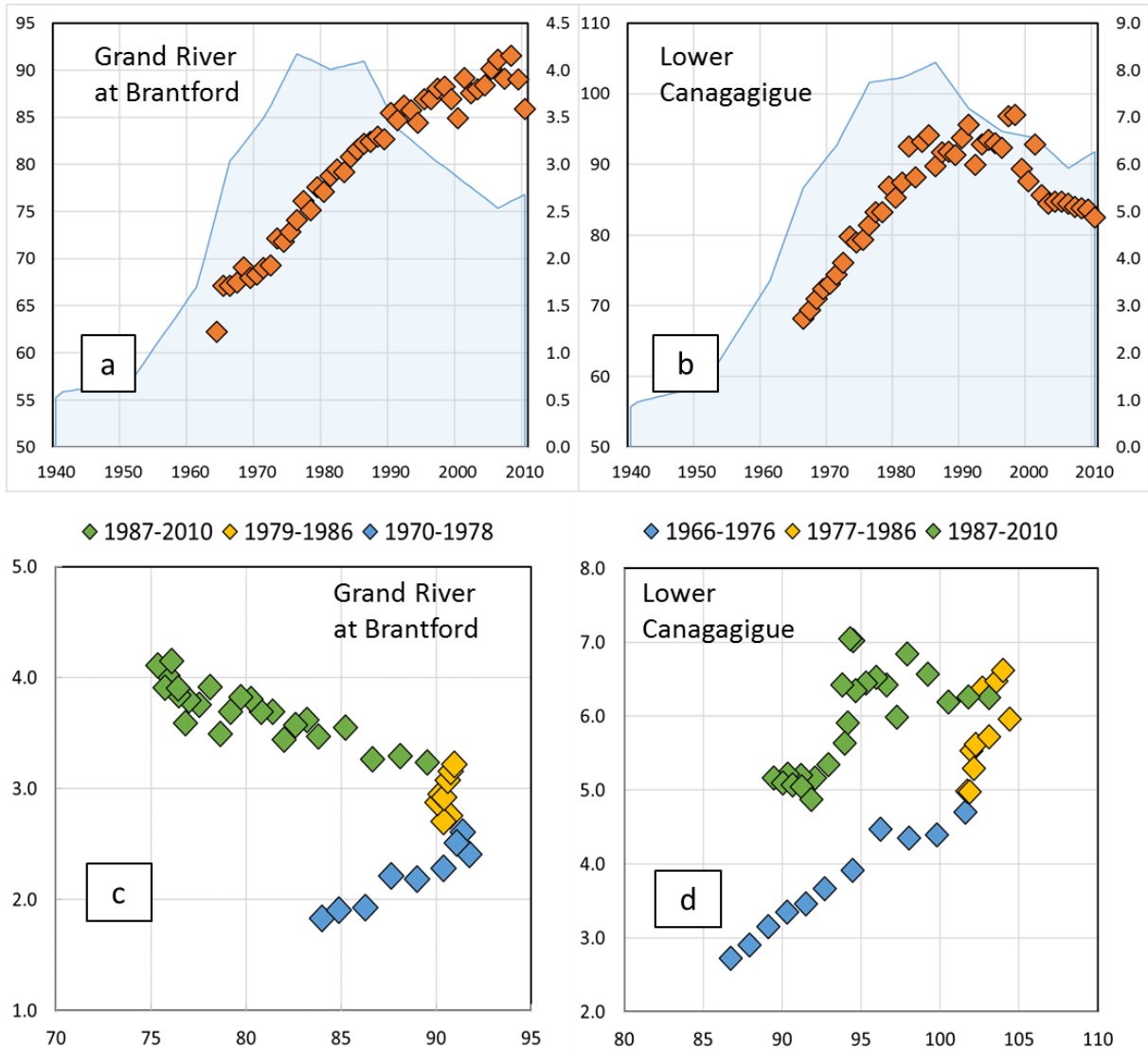
5.3.4   Quantification of Annual and Seasonal Time Lags

The results of the cross-correlation analysis provide us with estimates of time lags between changes in annual N surplus values and subsequent changes in flow-averaged

nitrate concentrations. Annual nitrogen lag times for the 16 study watersheds were found to range from 15 – 33 years, with a median value of 24.3 years (**Table 5.4**).

Table 5.4. Annual and Seasonal Lag Times for the 16 Sub-watersheds in the GRW

Station Name	Time Lags (years)				
	Annual	Winter	Spring	Summer	Fall
Grand River Near Marsville	26	23	27	34	26
Grand River Below Shand Dam	30	30	28	29	24
Grand River West Montrose	19	19	20	18	16
Grand River at Glen Morris	19	14	22	24	15
Grand River at Brantford	29	25	30	30	25
Grand River at Newport	25	27	28	25	23
Grand River at York	22	22	22	27	27
Canagagigue Creek (upper)	19	17	20	26	6
Canagagigue Creek (lower)	15	11	19	14	6
Speed River below Guelph	22	22	17	18	25
Speed River (Eramosa River)	24	22	15	31	25
Conestogo River at Glen Allan	25	22	22	26	26
Nith River (Upper)	30	30	30	19	19
Nith River (Lower)	19	19	21	20	17
Whiteman's Creek	33	37	33	26	28
Fairchild Creek	31	-	24	33	23

Interestingly, the distribution of lags also shows a distinct seasonal pattern. To illustrate this point, we show in **Figure 5.5** the trajectories for monthly flow-averaged nitrate concentrations superimposed against the annual N surplus values for the Grand River at Glen Morris Bridge. Our cross-correlation analysis of annual lag values indicates a lag time of 19 years for this site. The monthly trajectories shown in the figure, however, show a range of behaviors across the year. In the summer months (June-August), for example, FAC values have been increasing consistently, and there is little or no response to decreasing N surplus values over time.   In the fall and winter months, however, the watershed appears much more responsive to changes in N surplus values, with distinct peaks and subsequent decreases in the N concentration trajectories. In November and December, for example, the slope values for the pre-1993 period (0.084 ± 0.005 mg L^{-1} y^{-1}, November; 0.095 ± 0.006 mg L^{-1} y^{-1}, December) are significantly different from those for

112

the period after 1993 (-0.023 $\pm$ 0.036 mg L^{-1} y^{-1}, R^2=0.03, November; -0.019 $\pm$ 0.041 mg L^{-1} y^{-1}, R^2=0.02, December). In July, however, the slope values for the pre- and post-1993 periods are statistically indistinguishable (0.054 $\pm$ 0.002 mg L^{-1} y^{-1}; pre-1993; 0.042 $\pm$ 0.030 mg L^{-1} y^{-1}, post-1993). Seasonal time lags are provided for all 16 subwatersheds of the GRW in **Table 5.4**. In the mean, seasonal cross-correlation analysis shows that N-related time lags are the longest in summer (25.4 $\pm$ 1.6 y) and the shortest in fall (21.1 $\pm$ 1.8 y) (**Figure 5.6**). In the following section we explore the dominant controls on the annual as well as the seasonal time lags.

Figure 5.5. Monthly trends in Watershed-Scale N Surplus and FAC trajectories for the Grand River at Glenn Morris Bridge
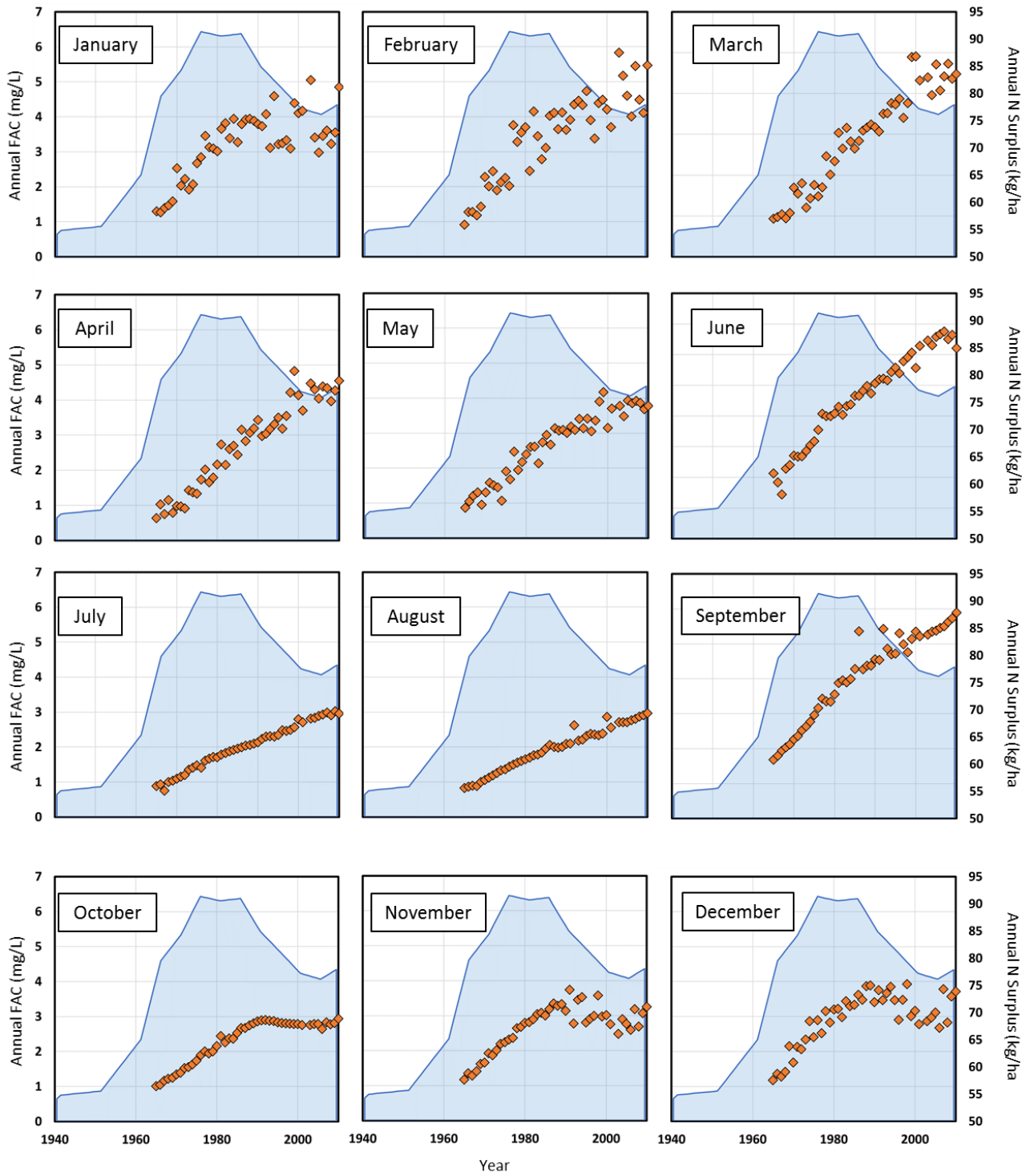
Figure 5.6. Seasonal Time Lags for the 16 GRW Subwatersheds
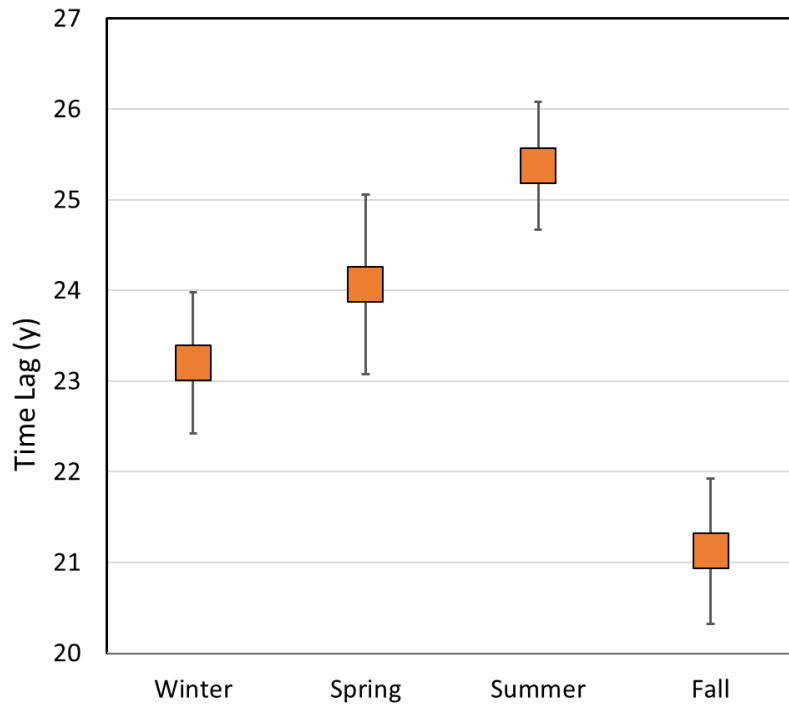
Spatially, lag times were the longest in the northern sub-watersheds (22- 24 years), decreased in the Middle Grand, and then again increased for the Lower Grand (**Figure 5.7**). The longer lag time in the northern watersheds can be most likely attributed to the smaller percent tile drained and greater fraction wetland area, while the decrease in lags in the central Grand can most likely be attributed to the higher fraction of area under tile drainage. There was no statistically significant difference between the lag times for the main steam and the tributaries of the Grand, indicating that watershed area is possibly not as strong a control in lag times.

Figure 5.7. Spatial Patterns in Annual Lag times across the Grand River Watershed
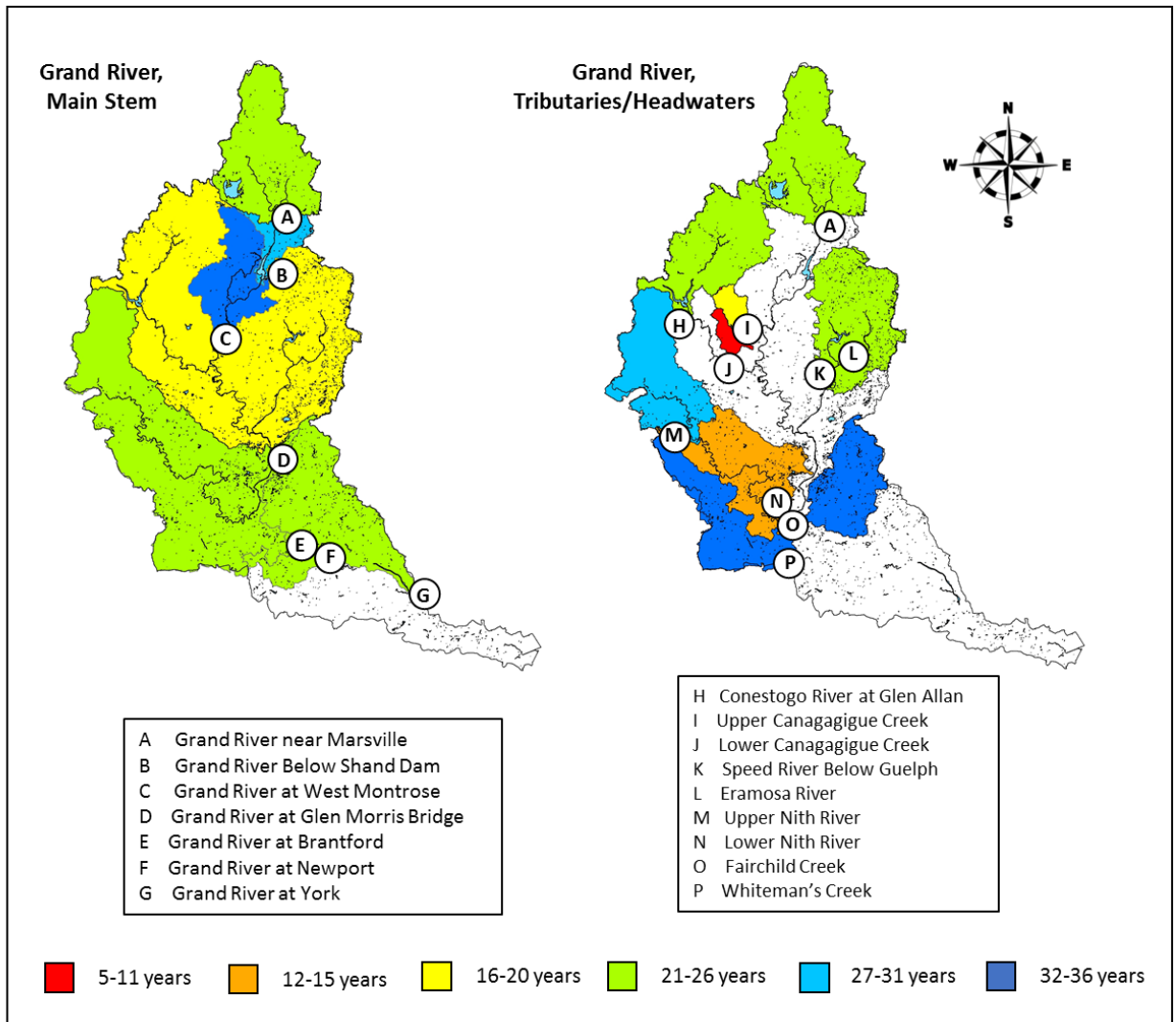
5.3.5 Dominant Controls on Annual and Seasonal Time Lags

As described in Section 5.2.6, we carried out a correlation analysis to identify key relationships between watershed characteristics, management practices and N-related time lags for the study watersheds. The results of this analysis are shown in Table 5.5, which provides p-values for each of the variables included in the analysis.

Table 5.5. Results of correlation analysis to evaluate explanatory variables for inclusion in the multiple linear regression model

| | Time Lags | | | | |
| | Annual | Spring | Summer | Fall | Winter |
	p-value	p-value	p-value	p-value	p-value
Sand	0.827	0.702	0.292	0.914	0.578
Silt	0.412	0.454	0.206	0.514	0.443
Clay	0.387	0.667	0.617	0.314	0.878
Organic Matter	0.700	0.846	0.010	0.774	0.769
Depth to Water Table	0.959	0.868	0.934	0.802	0.299
Tile Drained Area	0.434	0.045	0.585	0.009	0.415
Wetland Area	0.458	0.834	0.611	0.493	0.268
Watershed Slope	0.409	0.001	0.478	0.343	0.308
Fertilizer	0.894	0.988	0.565	0.716	0.669
Manure	0.976	0.900	0.501	0.929	0.342
Population Density	0.330	0.870	0.861	0.508	0.574
N Surplus	0.081	0.759	0.755	0.773	0.115
Watershed Area	0.996	0.466	0.507	0.413	0.944

The MLR model based on the correlation analyses is as follows:

$$LAG = \beta_0 + \beta_1(ANS) + \beta_2(TILE) + \beta_3(SLOPE) + \beta_4(OM) + \varepsilon \qquad (5.7),$$

where, LAG is the annual or seasonal time lag, ANS is the annual N surplus, TILE is the fractional tile-drained area, SLOPE is the mean percent slope value, OM is the percent soil organic matter, ε is the error term, and $\beta_0, \beta_1, \beta_2, \beta_3, \beta_4$ are regression coefficients. The obtained coefficient values for the MLR model are given in **Table 5.6.**

Table 5.6. Coefficients for multiple linear regression analysis of both annual and seasonal time lags between changes in annual N surplus values and flow-averaged nitrate concentrations for the 16 study watersheds. Blank spaces indicate no significant relationship

Lag	β_0 (INTERCEPT)	β_1 (ANS)	SRC (ANS)	β_2 (TILE)	SRC (TILE)	β_3 (SLOPE)	SRC (SLOPE)	R^2	p-value
Annual	45.1	-0.28	0.62	-	-	-	-	0.61	0.010
Spring	46.2	-0.19	0.48	-		-1.3	0.55	0.53	0.015
Summer	50.6	-0.34	0.73	-		-		0.46	0.001
Fall	27.6	-		-28.3		-		0.54	0.004
Winter	-	-		-		-		-	-

For both annual and summer time lags, the only variable with a statistically significant correlation is the annual N surplus, which is negatively correlated with lag time (SRC=0.62, p=0.010, annual; SRC=0.74, p=0.001, summer). In spring, lag times are also negatively correlated with both the annual N surplus; in addition, they are correlated with the mean percent slope for the watershed (p=0.015), with the two together accounting for approximately 53% of variation in spring lag times across the watersheds. In fall, the fraction of the watershed under tile drainage is the only significant driver of differences in lag times (p =0.004), explaining approximately 54% of variation across the study watersheds.

The negative relationship in fall between tile drainage and time lags (negative β_2) is consistent with previous analyses (Basu et al. 2013; Schilling et al. 2012) demonstrating decreases in groundwater travel times with increases in the percent of the watershed that is tiled. Tile drains speed the delivery of water from the landscape to streams, thus leading to shorter lag times. Similarly, greater landscape slope leads to faster delivery of water and thus shorter lag times (Schilling and Wolter 2007; Basu et al. 2012). Interestingly, the present analysis showed no significant relationship (p<0.05) between soil texture (sand, silt, and clay content) or water table depth with either annual or seasonal time lags (**Table 5.5**), despite the accepted role of these watershed variables in controlling unsaturated zone travel times. Such lack of correlation is likely due to the strong influence of tile drainage, which appears to fundamentally change the hydrologic behavior of the watershed and thus

trump the influence of natural-system controls. The present results suggest that time lags in spring and fall, time periods characterized by snowmelt and heavy rains, are primarily hydrology driven, with tile drainage playing the most significant role during fall rains and surface runoff playing a more important role in the spring snowmelt period. In the summer, however, when streamflow is at its lowest within the GRW, lags are relatively independent of hydrology and more dependent on the N inputs themselves.

But how does the size of the N surplus impact the lag time? An answer to this question may lie in what has been called the N saturation hypothesis. In 1989, Aber et al. (1998) published a review of the known impacts of N deposition on forest ecosystems. In this review, it was hypothesized that temperate forests would reach a saturation point in response to chronic additions of atmospheric N, after which N leaching and N_2O emissions would increase exponentially. Since then, the N saturation hypothesis has been refined to emphasize that N saturation is an issue of *kinetics* (Lovett and Goodale 2011). In other words, N losses from an ecosystem will occur when the rate at which N is added to the system exceeds the rates at which available sinks (soil and vegetation) are able to incorporate the added N. We propose that a similar kinetic saturation effect is likely at work in agricultural systems. Previous N isotope work has shown that the majority of leached nitrate is microbial in origin (Spoelstra et al. 2001). These findings suggest that the mineral N added to the soil surface via atmospheric deposition or N fertilizer, if not directly taken up by plants, will cycle through the organic pool before being re-nitrified and ultimately lost from the soil system to underlying groundwater. Indeed, it was found in a more recent study that 12-15% of isotopically labeled N fertilizer was still present in the soil organic matter more than 25 years after tracer application (Sebilo et al. 2013). However, if N inputs exceed the rate at which N can be taken up by plants or taken up by biomass, the residence time distribution of N within the soil profile may be skewed toward shorter residence times. Thus with higher N inputs, the importance of biogeochemical lags may be reduced, and overall lag times will decrease.

Also to be considered with regard to summer concentration trajectories is the relative importance of wastewater treatment plant inputs. Population in the GRW as a whole increased by approximately 55% between 1976 and 2011. Therefore, while the overall N surplus has decreased by 15 kg/ha, the portion of the N budget directly associated

with human population has *increased* on the order of 2-3 kg/ha. In the GRW, wastewater inputs constitute a larger portion of stream N than in other parts of the year due to lower levels of runoff and higher uptake of nutrients via crop growth. In the Grand River at Glen Morris Bridge, for example (Fig. 5.5), summer flow-averaged nitrate concentrations are approximately 3.0 mg /L, with approximately 22% of that summer nitrate mass being associated with human waste. In contrast, wastewater N during the higher spring flows would account for only approximately 5% of the total nitrate mass. The increases in wastewater N since the mid-1970s, therefore, may be a confounding factor in assessing summer time lags. It should be noted, however, that although population, and thus potentially wastewater N, has increased by 55% since 1976, summer flow-averaged nitrate concentrations have increased by more than 100% during that time, thus indicating that landscape-related time lags are still a major determinant of summer concentration trajectories.

4.0   Conclusion

A statistical approach was used to quantify N-related time lags and to identify dominant controls on these lags, using the approximately 7000 km^2 Grand River Watershed (GRW) in Ontario, Canada as a case study. In this work, long-term N surplus trajectories were established for 16 subwatersheds across the GRW, and these trajectories were paired with multi-decadal flow-averaged nitrate concentration data to statistically quantify mean annual and seasonal time lags. The results of this work indicate that annual N-related time lags across this intensively managed watershed range from 15 to more than 30 years. In addition, it was found that these time lags vary seasonally, with the shortest lag times being seen in fall and the longest during the summer months. Tile drainage was found to be a major control on both fall N-related time lags, with greater areas under tile drainage being positively correlated with shorter time lags. In spring, however, watershed slope was found to be the primary control on time lags, with steeper slopes being significantly associated with shorter time lags. Both summer and annual time lags were found to be correlated with annual N surplus values, suggesting that at higher N surplus values,

120

kinetics may limit opportunities for uptake into soil and vegetation and thus lead to shorter biogeochemical time lags within the watershed.

Chapter 6 - Conclusions and Recommendations

6.1 Major Findings of this Research

      The overall goal of my thesis was to explore N dynamics in human-impacted watersheds across a range of spatial scales, from the individual soil-pedon scale in Chapter 2, to the small (< 10 km^2) and the intermediate (6800 km^2) watershed scales in Chapter 3 and 5, to the Mississippi Basin (3 million square km) and the Susquehanna River Basin scale (xx) in Chapters 2 and 4. The prevailing paradigm about nitrogen is that it is a leaky, quickly moving solute with fast and far-reaching impacts on surface and groundwater quality. Although it is commonly known that the concentration trajectories of nitrate in surface waters may be slow to respond to landscape changes in inputs due to time lags associated with slow groundwater pathways, there has been little understanding of potential biogeochemical time lags for N associated with the uptake of N into vegetation, soil organic matter and sediments. The present work was begun with the hypothesis that intensively managed catchments have legacy stores of N that have built up over years of increased anthropogenic N inputs in the form of fertilizer, manure, and atmospheric N, and that such legacies contribute to time lags between changes in land use and management and measurable changes in water quality. These legacy stores were hypothesized to include both hydrologic legacies, with N occurring in a dissolved, mineral form, and biogeochemical legacies, with N in occurring in a sorbed form as soil organic N, primarily within the soil profile. The results of this work are summarized below.

      In my analysis of long-term soil data (1957 – 2010) from 2069 sites across the Mississippi River Basin (MRB) presented in Chapter 2, I found N accumulation, possibly as soil organic nitrogen (SON), in the root zone of cropland soils that led to a watershed scale accumulation in MRB on the order of 3.8 ± 1.8 Mt y^{-1}. This finding made a critical contribution towards identifying the fate of the 'missing N' often referred to watershed-scale N mass balance studies. Although caution must be exercised in relying upon the precise magnitude of accumulation due to large

uncertainties in the data, these results represent considerable progress toward the closing of N budgets, from the watershed to the global scale. I developed a simple modeling framework to capture N accumulation and depletion dynamics driven by anthropogenic perturbations across the landscape. Using the model, I showed that the observed accumulation of SON in the MRB over a 30-year period would lead to a biogeochemical lag time of 35 years to deplete 99% of legacy SON, even with a complete cessation of fertilizer application. Note that the overall lag time would need to include the hydrologic lag time in addition to the biogeochemical lag time.

In the next step of this research (Chapter 3), I narrowed my focus to the small watershed scale, focusing on a <10 km^2 watershed in the Iowa, at the heart of the North American corn belt. In this work, I extended the simple modeling framework presented in Chapter 2 to include the hydrologic lag time. Specifically, I developed a spatially explicit process-based model capable of quantifying concentration reduction benefits associated with watershed restoration efforts, with a particular focus on exploring the impacts of different spatial patterns of landscape conversion. The model allowed us to quantify economic and environmental tradeoffs associated with the implementation of conservation measures. In particular, it allowed us to demonstrate that the time required to achieve 25-50% reductions in N loading, a commonly held goal of many nutrient reduction programs, could range from 5 to more than 30 years, even with an immediate removal of substantial proportions of cropland (25-75%) from agricultural production. It also showed that the spatial placement of best management practices within a watershed can have a significant impact on time scales for improvements in water quality, with interventions close to the stream having a potentially much greater effect on stream nitrate concentrations than those in upland areas.

To further explore the time scales of N accumulation and depletion dynamics in heavily impacted watersheds, the process-based model described above was expanded to include long-term changes in N inputs (Chapter 4). Out of this work came the new ELEMeNT modeling framework, designed to explore long-term nutrient trajectories and the development of legacy nutrient scores across the landscape. In this phase of my research, I applied the ELEMeNT model to two large watersheds, the

Mississippi River Basin (MRB) and Susquehanna River Basin (SRB). The results of this work show that both the MRB and SRB are strongly impacted by legacy sources, which I define herein as N greater than 1 years of age. The MRB was found to be the more legacy-driven system, with current annual loads consisting of 85% legacy N, while the SRB is somewhat faster-responding (47% legacy). Accordingly, short-term gains will likely be harder to achieve within the MRB. The model results do, however, show significant accumulations of legacy N within both basins. In particular, the present results suggest that groundwater N accumulation in the MRB and SRB is on the order of 500 kg ha^{-1} and 1000 kg ha^{-1}, respectively.

Finally, a statistical approach was used to quantify N-related time lags and to identify dominant controls on these lags, using the approximately 7000 km^2 Grand River Watershed (GRW) in Ontario, Canada as a case study (Chapter 5). In this work, long-term N surplus trajectories were established for 16 subwatersheds across the GRW, and these trajectories were paired with multi-decadal flow-averaged nitrate concentration data to statistically quantify mean annual and seasonal time lags. The results of this work indicate that annual N-related time lags across this intensively managed watershed range from 15 to more than 30 years. In addition, it was found that these time lags vary seasonally, with the shortest lag times being seen in fall and the longest during the summer months. Tile drainage was found to be a major control on both fall and spring N-related time lags, with greater areas under tile drainage being positively correlated with shorter time lags. Watershed slope was also found to be a primary control in spring, with steeper slopes being significantly associated with shorter time lags. In the summer months, soil organic matter was found to be positively correlated with longer time lags, thus supporting our hypothesis that N retention in soil organic matter likely serves as a major reservoir for anthropogenic N.

To summarize, (a) I validated my hypothesis of existence of biogeochemical legacies in the root zone of agricultural using a combination of data synthesis and modeling approach, (b) developed a process based parsimonious model that can predict stream nitrate concentrations as well as N pools and fluxes in the landscape, as a function of long term input trajectories of N, and (c) developed a statistical technique to quantify watershed-scale lag times as a function of N input and output

trajectories. My work thus makes a critical contribution to watershed science in human impacted landscapes by developing an explicit understanding of the long-term impacts of legacy nutrient stores, as well as the transport and transformations of these nutrients along the field-plot to watershed continuum. Only with such understanding can relevant policy goals and cost-effective and efficient adaptive management strategies be developed to improve water quality in intensively managed agricultural landscapes.

6.2   Limitations and Recommendations for Future Work

Although the results of the present work satisfy my primary objective of using data synthesis, process-based modeling and statistical approaches to quantify and explore the long-term impacts of legacy N accumulation in human-impacted watersheds, they also raise many additional questions regarding long-term nutrient dynamics, from the local to the global scale.

Our finding of N stores in root zones of agricultural soils of the MRB leads to questions regarding the mechanism of such accumulation and its depletion, as a function of climate and landscape controls. Future work would involve both exploring the existence of such legacies in watersheds around the world, as well as using experimental and modeling approaches to quantifying the magnitudes of N accumulation in subsurface reservoirs, and better constrain the time periods over which legacy N may impact water quality. Understanding of agricultural legacies and catchment-scale time lags can be leveraged to design BMPs that target legacy reduction, for example, cover crops that increase N uptake or controlled drainage that enhance the landscape denitrification potential. It is also critical to better incorporate uncertainty calculations into our predictions regarding legacy accumulation and time scales for recovery.

Furthermore, it should be noted that a nutrient such as nitrogen cannot be considered in isolation, but must be understood as one component in a finely tuned symphony of interacting parts. As N loading has changed over time in watersheds from the smallest to the largest scale, so has that of carbon, phosphorus and silica. While N may accumulate preferentially in one landscape reservoir, phosphorus or other nutrients may accumulate in others, and mechanisms of release, transport and

retention for these nutrients may vary from the seasonal to the decadal scale. As nutrient ratios shift and nutrient cycling is disrupted across the landscape at a range of scales, it is critical to extend our analysis from individual nutrients to a host of key nutrients at a range of reactive interfaces, and understand how coupling of the elements impacts their individual response.

In addition, while the present work has focused on watershed-scale *physical* tine lags, there are also *social* lags in policy and implementation, and *ecological* lags in how fast a receiving water body responds to changing inputs. Future work would involve integrating our model with climate and land use change models on one hand, and lake, coastal and reservoir models on the other, understand the impact of changing climate, land use and land-management on water quality. The framework introduced in the current work, a framework that explicitly takes into account temporal trajectories of nutrient use, retention and transport, can be used to address these larger-scale time lag questions, and thus be instrumental in closing critical gaps in our scientific understanding of the long-term impacts of radical, anthropogenically driven changes in nutrient dynamics.

Finally, it should be noted that the present work, particularly in relation to development of the ELEMeNT modeling framework, relies on numerous assumptions that are necessary to current model functionality but that which, of necessity, may limit the accuracy with which the model represents watershed processes. Indeed, all modeling attempts, whether they be parsimonious or densely parameterized, are based on fundamental assumptions regarding the system being modeled. In the present work, a range of assumptions have been employed. For example, in both the simple model introduced in Chapter 3 and in the somewhat more complex ELEMeNT model, denitrification is modeled as a first-order process. Denitrification, however, is dependent on the availability of organic carbon and is also controlled by the presence or absence of oxygen. Isotope tracer experiments across a range of regions and biome types have shown that while both denitrification and biotic uptake do increase with increases in nitrate concentrations, the efficiencies of these removal processes also begin to decline at higher concentrations, thus confirming that N removal does not either intrinsically occur a first-order process (Mulholland et al. 2008). Moreover,

much recent work has revealed that the biogeochemical and hydrologic processes that regulate denitrification and biotic uptake are both spatially and temporally heterogeneous, leading to hot spots and hot moments of retention, degradation, and production (Vidon et al. 2010).

Other assumptions are also made as a part of the ELEMeNT modeling approach. Similar to the first-order denitrification assumption, I assume first-order soil degradation dynamics. Stream and reservoir nutrient retention dynamics are not explicitly included in the mode. In addition, although ELEMeNT considers a distribution of land-use trajectories across the watershed, it does not utilize a fully spatially distributed approach, meaning that assumptions are made regarding a homogeneity of soil types and climate dynamics across the watershed that clearly do not reflect the "reality" of the system.

Of course, such simplifications are common in attempts at modeling over long time scales and across large spatial scales. In their review of soil carbon models, for example, Manzoni & Porporato (2009), found a clear inverse relationship between model complexity and the temporal and spatial scale of the modeling frameworks. Indeed, they note that higher levels of parameterization may be more appropriate at smaller scales, where it is more necessary to describe highly dynamic small-scale processes with a high level of detail. Conversely, reductions in complexity may not only be "convenient" when applying models a large spatial and temporal scales, but may also be critical to large-scale simulations (Lischke et al. 2007).

Ultimately, questions regarding scale and model complexity are at the heart of attempts to model environmental and ecological processes. Our understandings of fundamental processes may, of necessity, develop at very fine scales, whereas our need to manage and develop policy surrounding these processes must involve consideration of systems at larger scales (Urban 2005). As models move to representations at larger scales, simplifications are routinely employed as part of the tradeoff between model complexity or "realism" and model reliability (Peters and Herrick (2004). Although it may be considered desirable to make a model more *accurate* by adding additional processes and controls, we may actually see concomitant decreases in precision with these additions due to error associated with

the additional parameterization of the model. Peters and Herrick (2004) have characterized this tension between simple and complex approaches as the difference between sins of omission and sins of commission. In other words, while simple modeling approaches may exclude key processes, thus resulting in potentially unknown prediction biases, complex approaches may reduce these biases but at the same time introduce additional estimation and measurement error. Accordingly, attempts at large-scale extrapolation are often best achieved via appropriate simplification of a fine-scale model (Urban 2005).

That being said, it will be important to explore further whether the assumptions and simplifications utilized in the ELEMeNT model have been appropriately applied, and to identify where more complexity may be introduced to represent landscape-scale processes at a scale appropriate to answer pending research questions. For example, as noted above, long-term N dynamics may be best considered not in isolation, but in relation to other key nutrients, including carbon, phosphorus, and silica. Many questions remain regarding the impacts of changing nutrient ratios over time and across seasons. To answer such questions, it will be necessary to explicitly include stream, lake and reservoir processes in the modeling framework, as well as key feedback processes among the different nutrients, in order to explore changing nutrient dynamics over time and the ways in which these changes may be impacting biota and eutrophication responses in receiving water bodies.

References

Aber, John, William McDowell, Knute Nadelhoffer, Alison Magill, Glenn Berntson, Mark Kamakea, Steven McNulty, William Currie, Lindsey Rustad, and Ivan Fernandez. 1998. "Nitrogen Saturation in Temperate Forest Ecosystems." *BioScience* 48 (11): 921–34. doi:10.2307/1313296.

"AFBF: Balance the Budget - DTN/The Progressive Farmer." 2014. Accessed September 10. http://www.dtnprogressivefarmer.com

Alam, M.J., and J.L. Goodall. 2012. "Toward Disentangling the Effect of Hydrologic and Nitrogen Source Changes from 1992 to 2001 on Incremental Nitrogen Yield in the Contiguous United States." *Water Resources Research* 48 (4).

ys, Dominique, and Philippe Pelissier. 1994. "Changes in Carbon Storage in Temperate Humic Loamy Soils after Forest Clearing and Continuous Corn Cropping in France." *Plant and Soil* 160 (2): 215–223.

Aulenbach, Brent T. 2006. "Annual Dissolved Nitrite plus Nitrate and Total Phosphorous Loads for the Susquehanna, St. Lawrence, Mississippi-Atchafalaya, and Columbia River Basins, 1968-2004."

Ayres, R.U., W.H. Schlesinger, and R.H. Socolow. 1996. "Human Impacts on the Carbon and Nitrogen Cycles." In *Industrial Ecology and Global Change*, 5:121–55. Cambridge: Cambridge University Press.

Backer, Hermanni, Juha-Markku Leppänen, Anne Christine Brusendorff, Kaj Forsius, Monika Stankiewicz, Jukka Mehtonen, Minna Pyhälä, et al. 2010. "HELCOM Baltic Sea Action Plan – A Regional Programme of Measures for the Marine Environment Based on the Ecosystem Approach." *Marine Pollution Bulletin* 60 (5): 642–49. doi:10.1016/j.marpolbul.2009.11.016.

Baily, A., L. Rock, C.J. Watson, and O. Fenton. 2011. "Spatial and Temporal Variations in Groundwater Nitrate at an Intensive Dairy Farm in South-East Ireland: Insights from Stable Isotope Data." *Agriculture, Ecosystems & Environment* 144 (1): 308–18. doi:10.1016/j.agee.2011.09.007.

Baker, J.M., and T.J. Griffis. 2005. "Examining Strategies to Improve the Carbon Balance of Corn/Soybean Agriculture Using Eddy Covariance and Mass Balance Techniques." *Agricultural and Forest Meteorology* 128 (3–4): 163–77. doi:10.1016/j.agrformet.2004.11.005.

Baker, John M., Tyson E. Ochsner, Rodney T. Venterea, and Timothy J. Griffis. 2007. "Tillage and Soil Carbon sequestration—What Do We Really Know?" *Agriculture, Ecosystems & Environment* 118 (1–4): 1–5. doi:10.1016/j.agee.2006.05.014.

Baker, Lawrence A., Diane Hope, Ying Xu, Jennifer Edmonds, and Lisa Lauver. 2001. "Nitrogen Balance for the Central Arizona-Phoenix (CAP) Ecosystem." *Ecosystems* 4 (6): 582–602. doi:10.1007/s10021-001-0031-2.

Bartoli, M., E. Racchetti, C. A. Delconte, E. Sacchi, E. Soana, A. Laini, D. Longhi, and P. Viaroli. 2012. "Nitrogen Balance and Fate in a Heavily Impacted Watershed (Oglio River, Northern Italy): In Quest of the Missing Sources and Sinks." *Biogeosciences* 9 (1): 361–73. doi:10.5194/bg-9-361-2012.

Barton, L., C.D.A. McLay, L.A. Schipper, and C.T. Smith. 1999. "Annual Denitrification Rates in Agricultural and Forest Soils: A Review." *Soil Research* 37 (6): 1073–94.

Basu, Nandita B., Georgia Destouni, James W. Jawitz, Sally E. Thompson, Natalia V. Loukinova, Amélie Darracq, Stefano Zanardo, et al. 2010. "Nutrient Loads Exported from Managed Catchments Reveal Emergent Biogeochemical Stationarity." *Geophysical Research Letters* 37 (23). doi:10.1029/2010GL045168.

Basu, Nandita B., Priyanka Jindal, Keith E. Schilling, Calvin F. Wolter, and Eugene S. Takle. 2012. "Evaluation of Analytical and Numerical Approaches for the Estimation of Groundwater Travel Time Distribution." *Journal of Hydrology* 475 (December): 65–73. doi:10.1016/j.jhydrol.2012.08.052.

Basu, Nandita B., P. S. C. Rao, H. Edwin Winzeler, Sanjiv Kumar, Phillip Owens, and Venkatesh Merwade. 2010. "Parsimonious Modeling of Hydrologic Responses in Engineered Watersheds: Structural Heterogeneity versus Functional Homogeneity." *Water Resources Research* 46 (4). doi:10.1029/2009WR007803.

Basu, N.B., P. Jindal, K.E. Schilling, C.F. Wolter, and E.S. Takle. 2012. "Evaluation of Analytical and Numerical Approaches for the Estimation of Groundwater Travel Time Distribution." *Journal of Hydrology* 475: 65–73.

Beniston, Joshua W., S. Tianna DuPont, Jerry D. Glover, Rattan Lal, and Jennifer A. J. Dungait. 2014. "Soil Organic Carbon Dynamics 75 Years after Land-Use Change in Perennial Grassland and Annual Wheat Agricultural Systems." *Biogeochemistry* 120 (1–3): 37–49. doi:10.1007/s10533-014-9980-3.

Berkes, Fikret, Johan Colding, and Carl Folke. 2008. *Navigating Social-Ecological Systems: Building Resilience for Complexity and Change*. Cambridge University Press.

Beusen, Arthur H. W., Alexander F. Bouwman, Ludovicus P. H. Van Beek, José M. Mogollón, and Jack J. Middelburg. 2016. "Global Riverine N and P Transport to Ocean Increased during the 20th Century despite Increased Retention along the Aquatic Continuum." *Biogeosciences* 13 (8): 2441–51. doi:10.5194/bg-13-2441-2016.

Biggs, T. W., T. Dunne, and L. A. Martinelli. 2004. "Natural Controls and Human Impacts on Stream Nutrient Concentrations in a Deforested Region of the Brazilian Amazon Basin." *Biogeochemistry* 68 (2): 227–257.

Billen, G., J. Garnier, and L. Lassaletta. 2014. "The Nitrogen Cascade from Agricultural Soils to the Sea: Modeling N Transfers at Regional Watershed and Global Scales - Supplementary Material." Accessed October 16. http://rstb.royalsocietypublishing.org.proxy.lib.uwaterloo.ca/content/suppl/2013/05/18/rstb.2013.0123.DC1/rstb20130123supp1.pdf.

Billen, Gilles, Vincent Thieu, Josette Garnier, and Marie Silvestre. 2009a. "Modelling the N Cascade in Regional Watersheds: The Case Study of the Seine, Somme and Scheldt Rivers." *Agriculture, Ecosystems & Environment* 133 (3–4): 234–46. doi:10.1016/j.agee.2009.04.018.

———. 2009b. "Modelling the N Cascade in Regional Watersheds: The Case Study of the Seine, Somme and Scheldt Rivers." *Agriculture, Ecosystems & Environment* 133 (3–4): 234–46. doi:10.1016/j.agee.2009.04.018.

Boers, Paul C. M. 1996. "Nutrient Emissions from Agriculture in the Netherlands, Causes and Remedies." *Water Science and Technology* 33 (4–5): 183–89.

Bouraoui, Fayçal, and Bruna Grizzetti. 2014. "Modelling Mitigation Options to Reduce Diffuse Nitrogen Water Pollution from Agriculture." *Science of The Total Environment* 468–469 (January): 1267–77. doi:10.1016/j.scitotenv.2013.07.066.

Bouwman, A.F. 2005. "Global and Regional Surface Nitrogen Balances in Intensive Agricultural Production Sysems for the Period 1970-2030." *Pedosphere* 15 (2): 137–55.

Bouwman, A.F., K.W. Van der Hoek, B. Eickhout, and I. Soenario. 2005. "Exploring Changes in World Ruminant Production Systems." *Agricultural Systems* 84 (2): 121–53. doi:10.1016/j.agsy.2004.05.006.

Bouwman, A.F., G. Van Drecht, and K.W. Van der Hoek. 2005. "Global and Regional Surface Nitrogen Balance in Intensive Agricultural Production Systems for Hte Period 1970-2030." *Pedosphere* 15 (2): 137–55.

Boyer, E W, CL Goodale, NA Jaworski, and R W Howarth. 2002. "Anthropogenic Nitrogen Sources and Relationships to Riverine Nitrogen Export in the Northeastern U.S.A." *Biogeochemistry* 57 (1): 137–69.

Buell, Gary R., and Helaine W. Markewich. 2003. *Data Compilation, Synthesis, and Calculations Used for Organic-Carbon Storage and Inventory Estimates for Mineral Soils of the Mississippi River Basin*. US Geological Survey. http://pubs.usgs.gov/pp/2004/1686a/p1686a.pdf.

Burke, Ingrid C., William K. Lauenroth, Geoff Cunfer, John E. Barrett, Arvin Mosier, and Petra Lowe. 2002. "Nitrogen in the Central Grasslands Region of the United States." *BioScience* 52 (9): 813–823.

Burt, R. 2009. "Soil Survey Field and Laboratory Methods Manual." 51. Soil Survey Investigations. Lincoln, NE: National Soil Survey Center, Natural Resources Conservation Service. http://www.nrcs.usda.gov/Internet/FSE_DOCUMENTS/nrcs142p2_052249.pdf.

Caballero-Alfonso, Angela M., Jacob Carstensen, and Daniel J. Conley. 2015. "Biogeochemical and Environmental Drivers of Coastal Hypoxia." *Journal of Marine Systems*, Biogeochemistry-ecosystem interaction on changing continental margins in the Anthropocene, 141 (January): 190–99. doi:10.1016/j.jmarsys.2014.04.008.

Canadell, J., R.B. Jackson, J.R. Ehleringer, H.A. Mooney, O.E. Sala, and E.D. Schulze. 1996. "Maximum Rooting Depth of Vegetation Types at the Global Scale." *Oecologia*, f, 108: 583–95.

Canfield, D. E., A. N. Glazer, and P. G. Falkowski. 2010. "The Evolution and Future of Earth's Nitrogen Cycle." *Science* 330 (6001): 192–96. doi:10.1126/science.1186120.

Carey, Richard O., and Kati W. Migliaccio. 2009. "Contribution of Wastewater Treatment Plant Effluents to Nutrient Dynamics in Aquatic Systems: A Review." *Environmental Management* 44 (2): 205–17. doi:10.1007/s00267-009-9309-5.

Carpenter, Stephen R, Carl Folke, Albert Norström, Olof Olsson, Lisen Schultz, Bina Agarwal, Patricia Balvanera, et al. 2012. "Program on Ecosystem Change and Society: An International Research Strategy for Integrated Social–ecological Systems." *Current Opinion in Environmental Sustainability* 4 (1): 134–38. doi:10.1016/j.cosust.2012.01.001.

Carpenter, Stephen R., Emily H. Stanley, and M. Jake Vander Zanden. 2011. "State of the World's Freshwater Ecosystems: Physical, Chemical, and Biological Changes." *Annual Review of Environment and Resources* 36 (1): 75–99. doi:10.1146/annurev-environ-021810-094524.

Chen, Dingjiang, Minpeng Hu, and Randy A. Dahlgren. 2014. "A Dynamic Watershed Model for Determining the Effects of Transient Storage on Nitrogen Export to Rivers." *Water Resources Research* 50 (10): 7714–30. doi:10.1002/2014WR015852.

Chen, Dingjiang, Hong Huang, Minpeng Hu, and Randy A. Dahlgren. 2014. "Influence of Lag Effect, Soil Release, And Climate Change on Watershed Anthropogenic Nitrogen Inputs and Riverine Export Dynamics." *Environmental Science & Technology* 48 (10): 5683–90. doi:10.1021/es500127t.

Chen, N., H. Hong, L. Zhang, and W. Cao. 2008. "Nitrogen Sources and Exports in an Agricultural Watershed in Southeast China." *Biogeochemistry* 87 (2): 169–79.

Clair, Thomas A., Nathan Pelletier, Shabtai Bittman, Adrian Leip, Paul Arp, Michael D. Moran, Ian Dennis, et al. 2014. "Interactions between Reactive Nitrogen and the Canadian Landscape: A Budget Approach: Canadian Nitrogen Budget." *Global Biogeochemical Cycles* 28 (11): 1343–57. doi:10.1002/2014GB004880.

Cleveland, C.C., A.R. Townsend, D.S. Schimel, H. Fisher, R.W. Howarth, L.O. Hedin, S.S. Perakis, et al. 1999. "Global Patterns of Terrestrial Biological Nitrogen (N2) Fixation in Natural Ecosystems." *Global Biogeochemical Cycles* 13 (2): 623–45.

Conant, Richard T., Gordon R. Smith, and Keith Paustian. 2003. "Spatial Variability of Soil Carbon in Forested and Cultivated Sites." *Journal of Environmental Quality* 32 (1): 278–286.

Conley, Daniel J., Hans W. Paerl, Robert W. Howarth, Donald F. Boesch, Sybil P. Seitzinger, Karl E. Havens, Christiane Lancelot, and Gene E. Likens. 2009. "Controlling Eutrophication: Nitrogen and Phosphorus." *Science* 323 (5917): 1014–1015.

Costello, Christine, W. Michael Griffin, Amy E. Landis, and H. Scott Matthews. 2009. "Impact of Biofuel Crop Production on the Formation of Hypoxia in the Gulf of Mexico." *Environmental Science & Technology* 43 (20): 7985–7991.

CRW. 2016. "AWTF Improvement Project #crwimprove | Capital Region Water." http://capitalregionwater.com/awtf-update/#sthash.oHydYCiu.dpbs.

D'Arcy, B., and A. Frost. 2001. "The Role of Best Management Practices in Alleviating Water Quality Problems Associated with Diffuse Pollution." *Science of the Total Environment* 265 (1): 359–367.

David, Mark B., Laurie E. Drinkwater, and Gregory F. McIsaac. 2010a. "Sources of Nitrate Yields in the Mississippi River Basin." *Journal of Environment Quality* 39 (5): 1657. doi:10.2134/jeq2010.0115.

———. 2010b. "Sources of Nitrate Yields in the Mississippi River Basin." *Journal of Environment Quality* 39 (5): 1657. doi:10.2134/jeq2010.0115.

David, Mark B., Gregory F. McIsaac, Robert G. Darmody, and Rex A. Omonode. 2009. "Long-Term Changes in Mollisol Organic Carbon and Nitrogen." *Journal of Environment Quality* 38 (1): 200. doi:10.2134/jeq2008.0132.

David, M.B., Stephen J. Del Grosso, Xuetao Hu, Elizabeth P. Marshall, Gregory F. McIsaac, William J. Parton, Christina Tonitto, and Mohamed A. Youssef. 2008.

"Modeling Denitrification in a Tile-Drained, Corn and Soybean Agroecosystem of Illinois, USA." *Biogeochemistry* 93 (1–2): 7–30. doi:10.1007/s10533-008-9273-9.

David, M.B., L.E. Drinkwater, and G.F. McIsaac. 2010. "Sources of Nitrate Yields in the Mississippi River Basin David.pdf." *Journal of Environmental Quality* 39: 1657–67.

David, M.B., G. McIsaac, R. Darmody, and R.A. Omonode. 2009. "Long-Term Changes in Mollisol Organic Carbon and Nitrogen." *Journal of Environment Quality* 38 (1): 200. doi:10.2134/jeq2008.0132.

Davidson, Eric A., and Ilse L. Ackerman. 1993a. "Changes in Soil Carbon Inventories Following Cultivation of Previously Untilled Soils." *Biogeochemistry* 20 (3): 161–193.

———. 1993b. "Changes in Soil Carbon Inventories Following Cultivation of Previously Untilled Soils." *Biogeochemistry* 20 (3): 161–193.

de Vries, W., S. Solberg, M. Dobbertin, H. Sterba, D. Laubhann, M. van Oijen, C. Evans, et al. 2009. "The Impact of Nitrogen Deposition on Carbon Sequestration by European Forests and Heathlands." *Forest Ecology and Management* 258 (8): 1814–23. doi:10.1016/j.foreco.2009.02.034.

De Vries, Wim, Gert Jan Reinds, Per Gundersen, and Hubert Sterba. 2006. "The Impact of Nitrogen Deposition on Carbon Sequestration in European Forests and Forest Soils." *Global Change Biology* 12 (7): 1151–73. doi:10.1111/j.1365-2486.2006.01151.x.

D'elia, Christopher F., Walter R. Boynton, and James G. Sanders. 2003. "A Watershed Perspective on Nutrient Enrichment, Science, and Policy in the Patuxent River, Maryland: 1960–2000." *Estuaries* 26 (2): 171–185.

Di, H.J., and K.C. Cameron. 2002. "Nitrate Leaching in Temperate Agroecosystems: Sources, Factors and Mitigating Strategies." *Nutrient Cycling in Agroecosystems* 46: 237–56.

Diaz, Robert J., and Rutger Rosenberg. 2008. "Spreading Dead Zones and Consequences for Marine Ecosystems." *Science* 321 (5891): 926–929.

Drobney, P.M. 1994. "Iowa Prairie Rebirth Rediscovering Natural Heritage at Walnut Creek National Wildlife Refuge." *Ecological Restoration* 12 (1): 16–22.

Drummond, Mark A., and Thomas R. Loveland. 2010. "Land-Use Pressure and a Transition to Forest-Cover Loss in the Eastern United States." *BioScience* 60 (4): 286–98. doi:10.1525/bio.2010.60.4.7.

Drury, C. F., C. S. Tan, T. W. Welacky, W. D. Reynolds, T. Q. Zhang, T. O. Oloya, N. B. McLaughlin, and J. D. Gaynor. 2014. "Reducing Nitrate Loss in Tile Drainage Water with Cover Crops and Water-Table Management Systems." *Journal of Environment Quality* 43 (2): 587. doi:10.2134/jeq2012.0495.

Ellert, B. H., and J. R. Bettany. 1995. "Calculation of Organic Matter and Nutrients Stored in Soils under Contrasting Management Regimes." *Canadian Journal of Soil Science* 75 (4): 529–538.

Erisman, Jan Willem, Nelleke Domburg, Wim de Vries, Hans Kros, Bronno de Haan, and Kaj Sanders. 2005. "The Dutch N-Cascade in the European Perspective." *Science in China Series C: Life Sciences* 48 (S2): 827–42. doi:10.1007/BF03187122.

Fenn, Mark E., Mark A. Poth, John D. Aber, Jill S. Baron, Bernard T. Bormann, Dale W. Johnson, A. Dennis Lemly, Steven G. McNulty, Douglas F. Ryan, and Robert

Stottlemyer. 1998. "Nitrogen Excess in North American Ecosystems: Predisposing Factors, Ecosystem Responses, and Management Strategies." *Ecological Applications* 8 (3): 706. doi:10.2307/2641261.

Fenton, Owen, Rogier P. O. Schulte, Philip Jordan, Stanley T. J. Lalor, and Karl G. Richards. 2011a. "Time Lag: A Methodology for the Estimation of Vertical and Horizontal Travel and Flushing Timescales to Nitrate Threshold Concentrations in Irish Aquifers." *Environmental Science & Policy* 14 (4): 419–31. doi:10.1016/j.envsci.2011.03.006.

Fenton, Owen, Rogier P.O. Schulte, Philip Jordan, Stanley T.J. Lalor, and Karl G. Richards. 2011b. "Time Lag: A Methodology for the Estimation of Vertical and Horizontal Travel and Flushing Timescales to Nitrate Threshold Concentrations in Irish Aquifers." *Environmental Science & Policy* 14 (4): 419–31. doi:10.1016/j.envsci.2011.03.006.

Filoso, S., L.A. Martinelli, M.R. Williams, L.B. Lara, A. Krusche, M.V. Ballester, V. Reynaldo, and P.B. De Camargo. 2003. "Land Use and Nitrogen Export in the Piracicaba River Basin, Southeast Brazil." *Biogeochemistry* 65: 275–94.

Fonseca, Bárbara Medeiros, Luciana de Mendonça-Galvão, Claudia Padovesi-Fonseca, Lucijane Monteiro de Abreu, and Adriana Cristina Marinho Fernandes. 2014. "Nutrient Baselines of Cerrado Low-Order Streams: Comparing Natural and Impacted Sites in Central Brazil." *Environmental Monitoring and Assessment* 186 (1): 19–33. doi:10.1007/s10661-013-3351-8.

Foster, Gregory D., Katrice A. Lippa, and Cherie V. Miller. 2000. "Seasonal Concentrations of Organic Contaminants at the Fall Line of the Susquehanna River Basin and Estimated Fluxes to Northern Chesapeake Bay, USA." *Environmental Toxicology and Chemistry* 19 (4): 992–1001.

Foufoula-Georgiou, Efi, Zeinab Takbiri, Jonathan A. Czuba, and Jon Schwenk. 2015. "The Change of Nature and the Nature of Change in Agricultural Landscapes: Hydrologic Regime Shifts Modulate Ecological Transitions: Hydrology Modulates Ecological Transitions." *Water Resources Research* 51 (8): 6649–71. doi:10.1002/2015WR017637.

Fowler, D., M. Coyle, U. Skiba, M. A. Sutton, J. N. Cape, S. Reis, L. J. Sheppard, et al. 2013. "The Global Nitrogen Cycle in the Twenty-First Century." *Philosophical Transactions of the Royal Society B: Biological Sciences* 368 (1621): 20130164–20130164. doi:10.1098/rstb.2013.0164.

Fowler, D., J. A. Pyle, J. A. Raven, and M. A. Sutton. 2013. "The Global Nitrogen Cycle in the Twenty-First Century: Introduction." *Philosophical Transactions of the Royal Society B: Biological Sciences* 368 (1621): 20130165–20130165. doi:10.1098/rstb.2013.0165.

Francis, Marcie. 2000. *Background Report on Fertilizer Use, Contaminants and Regulators*. DIANE Publishing.

Gál, Anita, Tony J. Vyn, Erika Michéli, Eileen J. Kladivko, and William W. McFee. 2007. "Soil Carbon and Nitrogen Accumulation with Long-Term No-till versus Moldboard Plowing Overestimated with Tilled-Zone Sampling Depths." *Soil and Tillage Research* 96 (1–2): 42–51. doi:10.1016/j.still.2007.02.007.

Galloway, J. N. 2003. "The Global Nitrogen Cycle." In *Treatise on Geochemistry 8*, 557–83.

http://www.ic.ucsc.edu/~mdmccar/ocea213/readings/09_Nitrogen/gallowayTOG_global_N_cycle.pdf.

Galloway, J N, F J Dentener, D G Capone, E W Boyer, R W Howarth, S P Seitzinger, G P Asner, et al. 2004. *Nitrogen Cycles : Past , Present , and Future*.

Galloway, James N., William H. Schlesinger, Hiram Levy, Anthony Michaels, and Jerald L. Schnoor. 1995. "Nitrogen Fixation: Anthropogenic Enhancement-Environmental Response." *Global Biogeochemical Cycles* 9 (2): 235–52. doi:10.1029/95GB00158.

Galloway, JN, FJ Dentener, DG Capone, EW Boyer, RW Howarth, SP Seitzinger, GP Asner, et al. 2004. "Nitrogen Cycles: Past, Present, and Future." *Biogeochemistry* 70: 153–226.

Galloway, J.N., A.R. Townsend, J.W. Erisman, M. Bekunda, Z. Cai, J.R. Freney, L.A. Martinelli, S.P. Seitzinger, and M.A. Sutton. 2008. "Transformation of the Nitrogen Cycle: Recent Trends, Questions, and Potential Solutions." *Science* 320 (5878): 889–92.

Gleeson, Tom, Leslie Smith, Nils Moosdorf, Jens Hartmann, Hans H. Dürr, Andrew H. Manning, Ludovicus P. H. van Beek, and A. M. Jellinek. 2011. "Mapping Permeability over the Surface of the Earth: MAPPING GLOBAL PERMEABILITY." *Geophysical Research Letters* 38 (2): n/a-n/a. doi:10.1029/2010GL045565.

Gleixner, Gerd, Natacha Poirier, Roland Bol, and Jérôme Balesdent. 2002. "Molecular Dynamics of Organic Matter in a Cultivated Soil." *Organic Geochemistry* 33 (3): 357–366.

Godsey, Sarah E., James W. Kirchner, and David W. Clow. 2009. "Concentration-Discharge Relationships Reflect Chemostatic Characteristics of US Catchments." *Hydrological Processes* 23 (13): 1844–64. doi:10.1002/hyp.7315.

Goolsby, D.A., W.A. Battablin, G.B. Lawrence, R.S. Artz, B.T. Aulenbach, R.P. Hooper, D.R. Keeney, and G.J. Stensland. 1999. "Flux and Sources of Nutrients in the Mississippi-Atchafalaya River Basin." Technical Report. Integrated Assessment on Hypoxia in the Gulf of Mexico. National Oceanic and Atmospheric Administration National Ocean Service Coastal Ocean Program. http://repositories.tdl.org/tamug-ir/handle/1969.3/27186?show=full.

Goyette, Jean-Olivier, Elena M. Bennett, Robert W. Howarth, and Roxane Maranger. 2016. "Changes in Anthropogenic Nitrogen and Phosphorus Inputs to the St. Lawrence Sub-Basin over 110 Years and Impacts on Riverine Export." *Global Biogeochemical Cycles*, January, 2016GB005384. doi:10.1002/2016GB005384.

GRCA. 2016. "Grand River Information Network." Accessed 2016. https://maps.grandriver.ca/index.html.

Green, Christopher T., Barbara A. Bekins, Stephen J. Kalkhoff, Robert M. Hirsch, Lixia Liao, and Kimberlee K. Barnes. 2014. "Decadal Surface Water Quality Trends under Variable Climate, Land Use, and Hydrogeochemical Setting in Iowa, USA." *Water Resources Research* 50 (3): 2425–43. doi:10.1002/2013WR014829.

Grimvall, Anders, Per Stålnacke, and Andrzej Tonderski. 2000. "Time Scales of Nutrient Losses from Land to Sea — a European Perspective." *Ecological Engineering* 14 (4): 363–71. doi:10.1016/S0925-8574(99)00061-0.

Grizzetti, B, F Bouraoui, K Granlund, S Rekolainen, and G Bidoglio. 2003. "Modelling Diffuse Emission and Retention of Nutrients in the Vantaanjoki Watershed

(Finland) Using the SWAT Model." *Ecological Modelling* 169 (1): 25–38. doi:10.1016/S0304-3800(03)00198-4.

Gruber, Nicolas, and James N. Galloway. 2008. "An Earth-System Perspective of the Global Nitrogen Cycle." *Nature* 451 (7176): 293–96. doi:10.1038/nature06592.

Guan, Tiffany T. Y., and Richard A. Holley. 2011. *Hog Manure Management, the Environment and Human Health*. Springer Science & Business Media.

Haag, Daniel, and Martin Kaupenjohann. 2000. "Biogeochemical Models in the Environmental Sciences." *HYLE–International Journal for Philosophy of Chemistry* 6 (2): 117–142.

———. 2001. "Landscape Fate of Nitrate Fluxes and Emissions in Central Europe: A Critical Review of Concepts, Data, and Models for Transport and Retention." *Agriculture, Ecosystems & Environment* 86 (1): 1–21.

Haan, C. T., D. E. Storm, T. Al-Issa, S. Prabhu, G. J. Sabbagh, and D. R. Edwards. 1998. "Effect of Parameter Distributions on Uncertainty Analysis of Hydrologic Models." *Transactions of the ASAE (USA)*. http://agris.fao.org/agris-search/search.do?recordID=US1997080351.

Haitjema, H.M. 1995. *Analytic Element Modeling of Groundwater Flow*. Academic Press. http://scholar.google.ca.proxy.lib.uwaterloo.ca/scholar?q=haitjema+travel+time+equation&hl=en&as_sdt=0%2C5&as_ylo=1995&as_yhi=1995.

Hamilton, Stephen K. 2012a. "Biogeochemical Time Lags May Delay Responses of Streams to Ecological Restoration." *Freshwater Biology* 57 (July): 43–57. doi:10.1111/j.1365-2427.2011.02685.x.

Han, Haejin, and J. David Allan. 2008. "Estimation of Nitrogen Inputs to Catchments: Comparison of Methods and Consequences for Riverine Export Prediction." *Biogeochemistry* 91 (2/3): 177–99.

Helsel, D.R., and R.M. Hirsch. 1992. *Statistical Methods in Water Resources*. Vol. 49. Elsevier.

Hipel, K. W., and A. I. McLeod. 1994. *Time Series Modelling of Water Resources and Environmental Systems*. Elsevier.

Hirsch, R., Douglas L. Moyer, and Stacey A. Archfield. 2010. "Weighted Regressions on Time, Discharge, and Season (WRTDS), with an Application to Chesapeake Bay River Inputs1." *JAWRA Journal of the American Water Resources Association* 46 (5): 857–80. doi:10.1111/j.1752-1688.2010.00482.x.

Hirsch, R.M., and L.A. De Cicco. 2014. *User Guide to Exploration and Graphics for RivEr Trends (EGRET) and dataRetrieval: R Packages for Hydrologic Data (Version 2.0, February 2015)*. Vol. 4, chap. A10. US Geological Survey Techniques and Methods. USGS.

Hofstra, N., and A. F. Bouwman. 2005. "Denitrification in Agricultural Soils: Summarizing Published Data and Estimating Global Annual Rates." *Nutrient Cycling in Agroecosystems* 72 (3): 267–78. doi:10.1007/s10705-005-3109-y.

Hong, Bongghi, Dennis P. Swaney, and Robert W. Howarth. 2011. "A Toolbox for Calculating Net Anthropogenic Nitrogen Inputs (NANI)." *Environmental Modelling & Software* 26 (5): 623–33. doi:10.1016/j.envsoft.2010.11.012.

———. 2013. "Estimating Net Anthropogenic Nitrogen Inputs to U.S. Watersheds: Comparison of Methodologies." *Environmental Science & Technology* 47 (10): 5199–5207. doi:10.1021/es303437c.

Houghton, R. A., and J. L. Hackler. 2000. "Changes in Terrestrial Carbon Storage in the United States. 1: The Roles of Agriculture and Forestry." *Global Ecology and Biogeography* 9 (2): 125–144.

Houlton, Benjamin Z., Elizabeth Boyer, Adrien Finzi, James Galloway, Allison Leach, Daniel Liptzin, Jerry Melillo, Todd S. Rosenstock, Dan Sobota, and Alan R. Townsend. 2013. "Intentional versus Unintentional Nitrogen Use in the United States: Trends, Efficiency and Implications." *Biogeochemistry* 114 (1–3): 11–23. doi:10.1007/s10533-012-9801-5.

Howarth, Robert, Francis Chan, Daniel J Conley, Josette Garnier, Scott C Doney, Roxanne Marino, and Gilles Billen. 2011. "Coupled Biogeochemical Cycles: Eutrophication and Hypoxia in Temperate Estuaries and Coastal Marine Ecosystems." *Frontiers in Ecology and the Environment* 9 (1): 18–26. doi:10.1890/100008.

Howarth, Robert, Dennis Swaney, Gilles Billen, Josette Garnier, Bongghi Hong, Christoph Humborg, Penny Johnes, Carl-Magnus Mörth, and Roxanne Marino. 2011. "Nitrogen Fluxes from the Landscape Are Controlled by Net Anthropogenic Nitrogen Inputs and by Climate." *Frontiers in Ecology and the Environment* 10 (1): 37–43. doi:10.1890/100178.

Howarth, R.W., G. Billen, D. Swaney, A. Townsend, N. Jaworski, K. Lajtha, and Z. Zhao-Liang. 1996. "Regional Nitrogen Budgets and Riverine N & P Fluxes for the Drainages to the North Atlantic Ocean: Natural and Human Influences." In *Nitrogen Cycling in the North Atlantic Ocean and Its Watersheds*, 75–139. Netherlands: Springer.

Howarth, R.W., E.W. Boyer, W.J. Pabich, and J.N. Galloway. 2002. "Nitrogen Use in the United States from 1961-2000 and Potential Future Trends." *Ambio* 31 (2): 88–96.

Howarth, R.W., D.P. Swaney, E.W. Boyer, R. Marino, N. Jaworski, and C. Goodale. 2006. "The Influence of Climate on Average Nitrogen Export from Large Watersheds in the Northeastern United States." *Biogeochemistry* 79 (1–2): 163–86. doi:10.1007/s10533-006-9010-1.

Howden, Nicholas J. K., Tim P. Burt, Fred Worrall, Simon Mathias, and Mick J. Whelan. 2011a. "Nitrate Pollution in Intensively Farmed Regions: What Are the Prospects for Sustaining High-Quality Groundwater?" *Water Resour. Res.* 47 (November): W00L02. doi:10.1029/2011WR010843.

Jaffe, D.A. 1992. "The Nitrogen Cycle." *International Geophysics* 50: 263–84.

Janssen, B. H. 1984. "A Simple Method for Calculating Decomposition and Accumulation of 'young'soil Organic Matter." *Plant and Soil* 76 (1–3): 297–304.

Janzen, H. H. 2001. "Soil Science on the Canadian Prairies-Peering into the Future from a Century Ago." *Canadian Journal of Soil Science* 81 (4): 489–503.

Janzen, H.H., K.A. Beauchemin, Y. Bruinsma, C.A. Campbell, R.L. Desjardins, B.H. Ellert, and E.G. Smith. 2003. "The Fate of Nitrogen in Agroecosystems- An Illustration Using Canadian Estimates.pdf." *Nutrient Cycling in Agroecosystems* 67: 85–102.

Jarvie, Helen P., Andrew N. Sharpley, Bryan Spears, Anthony R. Buda, Linda May, and Peter J. A. Kleinman. 2013. "Water Quality Remediation Faces Unprecedented Challenges from 'Legacy Phosphorus.'" *Environmental Science & Technology* 47 (16): 8997–98. doi:10.1021/es403160a.

Jarvie, Helen P., Andrew N. Sharpley, Paul J. A. Withers, J. Thad Scott, Brian E. Haggard, and Colin Neal. 2013. "Phosphorus Mitigation to Control River Eutrophication: Murky Waters, Inconvenient Truths, and 'Postnormal' Science." *Journal of Environment Quality* 42 (2): 295. doi:10.2134/jeq2012.0085.

Jawitz, J.W., A.D. Fure, G.G. Demmy, S. Berglund, and P.S.C. Rao. 2005. "Groundwater Contaminant Flux Reduction Resulting from Nonaqueous Phase Liquid Mass Reduction." *Water Resources Research* 41 (10).

Jenkinson, D. S. 1990. "An Introduction to the Global Nitrogen Cycle." *Soil Use and Management* 6 (2): 56–61.

Jha, Manoj K., P. W. Gassman, and J. G. Arnold. 2007. "Water Quality Modeling for the Raccoon River Watershed Using SWAT." *Transactions of the ASAE* 50 (2): 479–493.

Jindal, Priyanka. 2010. "A Study of the Groundwater Travel Time Distribution at a Rural Watershed in Iowa: A Systems Theory Approach to Groundwater Flow Analysis." http://lib.dr.iastate.edu/etd/11454/.

Jury, W.A., D. Russo, G. Streile, and H. El Abd. 1990. "Solute Transport through Layered Soil Profiles: Zero and Perfect Travel Time Correlation Models." *Water Resources Research* 26 (1): 13–20.

Kellogg, Charles Edwin. 1936. *Development and Significance of the Great Soil Groups of the United States*. U.S. Dept. of Agriculture.

Kellogg, Robert L., Charles H. Lander, David C. Moffitt, and Noel Gollehon. 2000. "Manure Nutrients Relative to the Capacity of Cropland and Pastureland to Assimilate Nutrients: Spatial and Temporal Trends for the United States." *Proceedings of the Water Environment Federation* 2000 (16): 18–157.

Kemp, Melody J., and Walter K. Dodds. 2001. "Spatial and Temporal Patterns of Nitrogen Concentrations in Pristine and Agriculturally-Influenced Prairie Streams." *Biogeochemistry* 53 (2): 125–141.

Kemp, W. M., W. R. Boynton, J. E. Adolf, D. F. Boesch, W. C. Boicourt, G. Brush, J. C. Cornwell, et al. 2005. "Eutrophication of Chesapeake Bay: Historical Trends and Ecological Interactions." *Marine Ecology Progress Series* 303 (21): 1–29.

Kemp, W. M., J. M. Testa, D. J. Conley, D. Gilbert, and J. D. Hagy. 2009. "Temporal Responses of Coastal Hypoxia to Nutrient Loading and Physical Controls." *Biogeosciences* 6 (12): 2985–3008.

Kling, C. L., Y. Panagopoulos, S. S. Rabotyagov, A. M. Valcu, P. W. Gassman, T. Campbell, M. J. White, et al. 2014. "LUMINATE: Linking Agricultural Land Use, Local Water Quality and Gulf of Mexico Hypoxia." *European Review of Agricultural Economics* 41 (3): 431–59. doi:10.1093/erae/jbu009.

Kopáček, Jiří, Josef Hejzlar, and Maximilian Posch. 2013. "Factors Controlling the Export of Nitrogen from Agricultural Land in a Large Central European Catchment during 1900–2010." *Environmental Science & Technology*, May. doi:10.1021/es400181m.

Korol, Maurice, Gina Rattray, Farm Input Markets Unit, Farm Income, and Adaptation Policy Directorate. 2000. "Canadian Fertilizer Consumption, Shipments and Trade." *Agriculture and Agri-Food Canada, Ont. In Web Http://Www. Agr. Gc. Ca/Policy/Cdnfert/Text. Html*. http://www4.agr.gc.ca/resources/prod/doc/pol/pub/canfert/pdf/canfert97_98_e.pdf.

Kowalenko, C. Grant. 2001. "Assessment of Leco CNS-2000 Analyzer for Simultaneously Measuring Total Carbon, Nitrogen, and Sulphur in Soil." *Communications in Soil Science and Plant Analysis* 32 (13–14): 2065–2078.

Kroeze, C., R. Aerts, N. van Breemen, D. van Dam, P. Hofschreuder, M. Hoosbeek, J. de Klein, K. van der Hoek, H. Kros, and H. van Oene. 2003. "Uncertainties in the Fate of Nitrogen I: An Overview of Sources of Uncertainty Illustrated with a Dutch Case Study." *Nutrient Cycling in Agroecosystems* 66 (1): 43–69.

Kronvang, Brian, Hans E. Andersen, Christen Børgesen, Tommy Dalgaard, Søren E. Larsen, Jens Bøgestrand, and Gitte Blicher-Mathiasen. 2008. "Effects of Policy Measures Implemented in Denmark on Nitrogen Pollution of the Aquatic Environment." *Environmental Science & Policy* 11 (2): 144–52. doi:10.1016/j.envsci.2007.10.007.

"Lake Erie Nutrient Reduction Plan Released." 2015. *Great Lakes Commission | Commission Des Grands Lacs*. September 29. http://glc.org/announce/2015-lake-erie-nutrient-reduction-plan-released/.

Lal, R., R. F. Follett, and J. M. Kimble. 2003. "Achieving Soil Carbon Sequestration in the United States: A Challenge to the Policy Makers." *Soil Science* 168 (12): 827–45. doi:10.1097/01.ss.0000106407.84926.6b.

Langford, Malcolm, and Inga Winkler. 2014. "Muddying the Water? Assessing Target-Based Approaches in Development Cooperation for Water and Sanitation." *Journal of Human Development and Capabilities* 15 (2–3): 247–60. doi:10.1080/19452829.2014.896321.

Leip, Adrian, Beat Achermann, Gilles Billen, Albert Bleeker, Alexander Bouwman, Wim de Vries, Ulli Dragosits, et al. 2011. "Integrating Nitrogen Fluxes at the European Scale." http://centaur.reading.ac.uk/28386/.

Leip, Adrian, Wolfgang Britz, Franz Weiss, and Wim de Vries. 2011. "Farm, Land, and Soil Nitrogen Budgets for Agriculture in Europe Calculated with CAPRI." *Environmental Pollution* 159 (11): 3243–53. doi:10.1016/j.envpol.2011.01.040.

Lewis, David Bruce, Jason P. Kaye, Corinna Gries, Ann P. Kinzig, and Charles L. Redman. 2006a. "Agrarian Legacy in Soil Nutrient Pools of Urbanizing Arid Lands." *Global Change Biology* 12 (4): 703–9. doi:10.1111/j.1365-2486.2006.01126.x.

———. 2006b. "Agrarian Legacy in Soil Nutrient Pools of Urbanizing Arid Lands." *Global Change Biology* 12 (4): 703–9. doi:10.1111/j.1365-2486.2006.01126.x.

Li, Changsheng, Neda Farahbakhshazad, Dan B. Jaynes, Dana L. Dinnes, William Salas, and Dennis McLaughlin. 2006. "Modeling Nitrate Leaching with a Biogeochemical Model Modified Based on Observations in a Row-Crop Field in Iowa." *Ecological Modelling* 196 (1–2): 116–30. doi:10.1016/j.ecolmodel.2006.02.007.

Lindsey, B.D., S.W. Phillips, C.A. Donnelly, G.K. Speiran, L.N. Plummer, J.K. Bohlke, M.J. Focazio, W.C. Burton, and E. Busenberg. 2003. "Residence Times and Nitrate Transport in Ground Water Discharging to Streams in the Chesapeake Bay Watershed." Water-Resources Investigations Report 03–4035. New Cumberland, Pennsylvania: U.S. Geological Survey.

Lindsey, B.D., and M.G. Rupert. 2012. "Methods for Evaluating Temporal Groundwater Quality Data and Results of Decadal-Scale Changes in Chloride, Dissolved Solids, and Nitrate Concentrations in Groundwater in the United States, 1988-2010."

Scientific Investigations Report 2012–5049. National Water Quality Assessment Program. US Geological Survey Reston, VA. http://pubs.usgs.gov/sir/2009/5086/.

Liu, C., M. Watanabe, and Q. Wang. 2008. "Changes in Nitrogen Budgets and Nitrogen Use Efficiency in the Agroecosystems of the Changjiang River Basin between 1980 and 2000." *Nutrient Cycling in Agroecosystems* 80 (1): 19–37.

Loomer, H.A., and S.E. Cooke. 2011. "Water Quality in the Grand River Watershed: Current Conditions & Trends (2003–2008)." Draft. 2011: Grand River Conservation Authority. http://www.grandriver.ca/water/2011_WaterQualityReport.pdf.

Lovett, Gary M., and Christine L. Goodale. 2011. "A New Conceptual Model of Nitrogen Saturation Based on Experimental Nitrogen Addition to an Oak Forest." *Ecosystems* 14 (4): 615–31. doi:10.1007/s10021-011-9432-z.

MacDonald, G. K., E. M. Bennett, P. A. Potter, and N. Ramankutty. 2011. "Agronomic Phosphorus Imbalances across the World's Croplands." *Proceedings of the National Academy of Sciences* 108 (7): 3086–91. doi:10.1073/pnas.1010808108.

MacDonald, G.K., and E.M. Bennett. 2009. "Phosphorus Accumulation in Saint Lawrence River Watershed Soils: A Century-Long Perspective." *Ecosystems* 12 (4): 621–35.

Malone, R. W., D. B. Jaynes, T. C. Kaspar, K. R. Thorp, E. Kladivko, L. Ma, D. E. James, J. Singer, X. K. Morin, and T. Searchinger. 2014. "Cover Crops in the Upper Midwestern United States: Simulated Effect on Nitrate Leaching with Artificial Drainage." *Journal of Soil and Water Conservation* 69 (4): 292–305. doi:10.2489/jswc.69.4.292.

Maloszewski, P., and A. Zuber. 1982. "Determining the Turnover Time of Groundwater Systems with the Aid of Environmental Tracers: 1. Models and Their Applicability." *Journal of Hydrology* 57 (3): 207–31.

Manzoni, Stefano, and Amilcare Porporato. 2009. "Soil Carbon and Nitrogen Mineralization: Theory and Models across Scales." *Soil Biology and Biochemistry* 41 (7): 1355–79. doi:10.1016/j.soilbio.2009.02.031.

Mayer, Bernhard, Elizabeth W. Boyer, Christine Goodale, Norbert A. Jaworski, Nico Van Breemen, Robert W. Howarth, Sybil Seitzinger, Gilles Billen, Kate Lajtha, and Knute Nadelhoffer. 2002. "Sources of Nitrate in Rivers Draining Sixteen Watersheds in the Northeastern US: Isotopic Constraints." *Biogeochemistry* 57 (1): 171–197.

McGuire, Kevin J., and Jeffrey J. McDonnell. 2006a. "A Review and Evaluation of Catchment Transit Time Modeling." *Journal of Hydrology* 330 (3–4): 543–63. doi:10.1016/j.jhydrol.2006.04.020.

———. 2006b. "A Review and Evaluation of Catchment Transit Time Modeling." *Journal of Hydrology* 330 (3–4): 543–63. doi:10.1016/j.jhydrol.2006.04.020.

McIsaac, G.F., M.B. David, G.Z. Gertner, and D.A. Goolsby. 2001. "Nitrate Flux in the Mississippi River." *Nature* 414: 166–67.

McMahon, P. B., K. F. Dennehy, B. W. Bruce, J. K. Böhlke, R. L. Michel, J. J. Gurdak, and D. B. Hurlbut. 2006a. "Storage and Transit Time of Chemicals in Thick Unsaturated Zones under Rangeland and Irrigated Cropland, High Plains, United States." *Water Resources Research* 42 (3): n/a-n/a. doi:10.1029/2005WR004417.

———. 2006b. "Storage and Transit Time of Chemicals in Thick Unsaturated Zones under Rangeland and Irrigated Cropland, High Plains, United States." *Water Resources Research* 42 (3). doi:10.1029/2005WR004417.

Meals, Donald W, Steven a Dressing, and Thomas E Davenport. n.d. "Lag Time in Water Quality Response to Best Management Practices: A Review." *Journal of Environmental Quality* 39 (1): 85–96. doi:10.2134/jeq2009.0108.

Meals, Donald W., Steven A. Dressing, and Thomas E. Davenport. 2010. "Lag Time in Water Quality Response to Best Management Practices: A Review." *Journal of Environment Quality* 39 (1): 85. doi:10.2134/jeq2009.0108.

Messer, Tiffany L., Michael R. Burchell, Garry L. Grabow, and Deanna L. Osmond. 2012. "Groundwater Nitrate Reductions within Upstream and Downstream Sections of a Riparian Buffer." *Ecological Engineering* 47 (October): 297–307. doi:10.1016/j.ecoleng.2012.06.017.

Michalak, Anna M., Eric J. Anderson, Dmitry Beletsky, Steven Boland, Nathan S. Bosch, Thomas B. Bridgeman, Justin D. Chaffin, Kyunghwa Cho, Rem Confesor, and Irem Dalo\uglu. 2013. "Record-Setting Algal Bloom in Lake Erie Caused by Agricultural and Meteorological Trends Consistent with Expected Future Conditions." *Proceedings of the National Academy of Sciences* 110 (16): 6448–6452.

Mikhailova, E.A., R.B. Bryant, I.I. Vassenev, S.J. Schwager, and C.J. Post. 2000. "Cultivation Effects on Soil Carbon and Nitrogen Contents at Depth in the Russian Chernozem." *Soil Science Society of America Journal* 64 (2): 738. doi:10.2136/sssaj2000.642738x.

Mishra, Srikanta. 2009. "Uncertainty and Sensitivity Analysis Techniques for Hydrologic Modeling." *Journal of Hydroinformatics* 11 (3–4): 282. doi:10.2166/hydro.2009.048.

Mitsch, William J., John W. Day, J. Wendell Gilliam, Peter M. Groffman, Donald L. Hey, Gyles W. Randall, and Naiming Wang. 2001. "Reducing Nitrogen Loading to the Gulf of Mexico from the Mississippi River Basin: Strategies to Counter a Persistent Ecological Problem Ecotechnology—the Use of Natural Ecosystems to Solve Environmental Problems—should Be a Part of Efforts to Shrink the Zone of Hypoxia in the Gulf of Mexico." *BioScience* 51 (5): 373–388.

Molenat, Jerome, and Chantal Gascuel-Odoux. 2002. "Modelling Flow and Nitrate Transport in Groundwater for the Prediction of Water Travel Times and of Consequences of Land Use Evolution on Water Quality." *Hydrological Processes* 16 (2): 479–92. doi:10.1002/hyp.328.

"Monitoring of Trends in Rural Water Quality in Southern Ontario - Eco Issues." 2013. Accessed August 6. http://www.ecoissues.ca/index.php/Monitoring_of_Trends_in_Rural_Water_Qualit y_in_Southern_Ontario.

Muleta, Misgana K., and John W. Nicklow. 2005. "Sensitivity and Uncertainty Analysis Coupled with Automatic Calibration for a Distributed Watershed Model." *Journal of Hydrology* 306 (1): 127–145.

Mulholland, Patrick J., Ashley M. Helton, Geoffrey C. Poole, Robert O. Hall, Stephen K. Hamilton, Bruce J. Peterson, Jennifer L. Tank, et al. 2008. "Stream Denitrification across Biomes and Its Response to Anthropogenic Nitrate Loading." *Nature* 452 (7184): 202–5. doi:10.1038/nature06686.

Mulholland, Patrick J., H. Maurice Valett, Jackson R. Webster, Steven A. Thomas, Lee W. Cooper, Stephen K. Hamilton, and Bruce J. Peterson. 2004. "Stream Denitrification and Total Nitrate Uptake Rates Measured Using a Field 15N Tracer Addition Approach." *Limnology and Oceanography* 49 (3): 809–820.

Murphy, Jennifer, Robert M. Hirsch, and Lori A. Sprague. 2013. *Nitrate in the Mississippi River and Its Tributaries, 1980-2010: An Update*. US Geological Survey. http://pubs.usgs.gov/sir/2013/5169/.

Murty, Danuse, Miko UF Kirschbaum, Ross E. Mcmurtrie, and Heather Mcgilvray. 2002. "Does Conversion of Forest to Agricultural Land Change Soil Carbon and Nitrogen? A Review of the Literature." *Global Change Biology* 8 (2): 105–123.

NCSS. 2014. "National Cooperative Soil Characterization Database." Accessed September 17. http://ncsslabdatamart.sc.egov.usda.gov/datause.aspx.

Ng, Tze Ling, J. Wayland Eheart, Ximing Cai, and Fernando Miguez. 2010. "Modeling Miscanthus in the Soil and Water Assessment Tool (SWAT) to Simulate Its Water Quality Effects As a Bioenergy Crop." *Environmental Science & Technology* 44 (18): 7138–44. doi:10.1021/es9039677.

Niu, Shuli, Aimée T. Classen, Jeffrey S. Dukes, Paul Kardol, Lingli Liu, Yiqi Luo, Lindsey Rustad, et al. 2016. "Global Patterns and Substrate-Based Mechanisms of the Terrestrial Nitrogen Cycle." *Ecology Letters*, March, n/a-n/a. doi:10.1111/ele.12591.

NOAA. 2015. "2015 Gulf of Mexico Dead Zone 'above Average.'" http://www.noaanews.noaa.gov/stories2015/080415-gulf-of-mexico-dead-zone-above-average.html.

Osterman, L.E., R.Z. Poore, P.W. Swarzenski, D.B. Senn, and S.E. DiMarco. 2009. "The 20th-Century Development and Expansion of Louisiana Shelf Hypoxia, Gulf of Mexico." *Geo-Marine Letters* 29 (6): 405–14.

Parris, Kevin. 1998. "Agricultural Nutrient Balances as Agri-Environmental Indicators: An OECD Perspective." *Environmental Pollution* 102 (1, Supplement 1): 219–25. doi:10.1016/S0269-7491(98)80036-5.

Phillips, S.W., M.J. Focazio, and L.J. Bachman. 1999. "Discharge, Nitrate Load, and Residence Time of Groundwater in the Chesapeake Bay Watershed." Fact Sheet FS-150-99. Denver, CO: U.S. Geological Survey. http://md.water.usgs.gov/publications/fs-150-99/html/.

Pijanowski, Bryan, Deepak K. Ray, Anthony D. Kendall, Jonah M. Duckles, and David W. Hyndman. 2007. "Using Backcast Land-Use Change and Groundwater Travel-Time Models to Generate Land-Use Legacy Maps for Watershed Management." *Ecology and Society* 12 (2): 25.

Porporato, A., P. D'odorico, F. Laio, and I. Rodriguez-Iturbe. 2003. "Hydrologic Controls on Soil Carbon and Nitrogen Cycles. I. Modeling Scheme." *Advances in Water Resources* 26 (1): 45–58.

Post, W.M., and J. Pastor. 1985. "Global Patterns of Soil Nitrogen Storage." *Nature* 317: 613–16.

Price, C.V., N. Nakagaki, K.J. Hitt, and R.M. Clawges. 2007. "Enhanced Historical Land-Use and Land-Cover Data Sets of the U.S. Geological Survey: Polygon Format Files." 240. USGS Digital Data Series. Reston, Va.: U.S. Geological Survey.

Prior, J. 1991. *Landforms of Iowa*. Iowa City, IA: University of Iowa Press. http://sustainableag.unl.edu/pdf/landformsofiowacari.pdf.

Puckett, L. J. 2004. "Hydrogeologic Controls on the Transport and Fate of Nitrate in Ground Water beneath Riparian Buffer Zones: Results from Thirteen Studies across the United States." *Water Science & Technology* 49 (3): 47–53.

Puckett, Larry J., Anthony J. Tesoriero, and Neil M. Dubrovsky. 2011a. "Nitrogen Contamination of Surficial Aquifers—A Growing Legacy [†]." *Environmental Science & Technology* 45 (3): 839–44. doi:10.1021/es1038358.

Quynh, Le Thi Phuong, Gilles Billen, Josette Garnier, Sylvain Théry, Cédric Fézard, and Chau Van Minh. 2005. "Nutrient (N, P) Budgets for the Red River Basin (Vietnam and China)." *Global Biogeochemical Cycles* 19 (2). doi:10.1029/2004GB002405.

Rabalais, N. N., R. J. Diaz, L. A. Levin, R. E. Turner, D. Gilbert, and J. Zhang. 2010. "Dynamics and Distribution of Natural and Human-Caused Hypoxia." *Biogeosciences* 7 (2): 585–619.

Rabalais, Nancy N., R. Eugene Turner, and Donald Scavia. 2002. "Beyond Science into Policy: Gulf of Mexico Hypoxia and the Mississippi River." *BioScience* 52 (2): 129. doi:10.1641/0006-3568(2002)052[0129:BSIPGO]2.0.CO;2.

Rabotyagov, Sergey, Todd Campbell, Manoj Jha, Philip W. Gassman, Jeffrey Arnold, Lyubov Kurkalova, Silvia Secchi, Hongli Feng, and Catherine L. Kling. 2010. "Least-Cost Control of Agricultural Nutrient Contributions to the Gulf of Mexico Hypoxic Zone." *Ecological Applications* 20 (6): 1542–1555.

Rabotyagov, Sergey S., Todd D. Campbell, Michael White, Jeffrey G. Arnold, Jay Atwood, M. Lee Norfleet, Catherine L. Kling, et al. 2014. "Cost-Effective Targeting of Conservation Investments to Reduce the Northern Gulf of Mexico Hypoxic Zone." *Proceedings of the National Academy of Sciences* 111 (52): 18530–35. doi:10.1073/pnas.1405837111.

Ramankutty, N., and J.A. Foley. 1999. "Estimating Historical Changes in Global Land Cover: Croplands from 1700 to 1992." *Global Biogeochemical Cycles* 13 (4): 997–1027.

Reckhow, K.H., P.E. Norris, R.J. Budell, D.M. Di Toro, J.N. Galloway, H. Greening, A.N. Sharpley, A. Shirmhhammadi, and P.E. Stacey. 2011. *Achieving Nutrient and Sediment Reduction Goals in the Chesapeake Bay: An Evaluation of Program Strategies and Implementation*. Washington, D.C.: National Academies Press.

Reicosky, D.C. 2003. "Tillage-Induced CO2 Emissions and Carbon Sequestration: Effect of Secondary Tillage and Compaction." In *Conservation Agriculture*, 291–300. Netherlands: Springer. http://scholar.google.ca.proxy.lib.uwaterloo.ca/scholar?hl=en&q=reicosky+2003+tillage-induced&btnG=&as_sdt=1%2C5&as_sdtp=.

Rinaldo, Andrea, Paolo Benettin, Ciaran J. Harman, Markus Hrachowitz, Kevin J. McGuire, Ype van der Velde, Enrico Bertuzzo, and Gianluca Botter. 2015. "Storage Selection Functions: A Coherent Framework for Quantifying How Catchments Store and Release Water and Solutes." *Water Resources Research* 51 (6): 4840–47. doi:10.1002/2015WR017273.

Rockström, Johan, Malin Falkenmark, Louise Karlberg, Holger Hoff, Stefanie Rost, and Dieter Gerten. 2009. "Future Water Availability for Global Food Production: The

Potential of Green Water for Increasing Resilience to Global Change." *Water Resources Research* 45 (7): W00A12. doi:10.1029/2007WR006767.

Rockström, Johan, Will Steffen, Kevin Noone, Åsa Persson, F Stuart I I I Chapin, Eric Lambin, Timothy M Lenton, et al. 2009. "Planetary Boundaries : Exploring the Safe Operating Space for Humanity." *Ecology And Society* 14 (2): 32.

Ruddy, Barbara C., David L. Lorenz, and David K. Mueller. 2006. *County-Level Estimates of Nutrient Inputs to the Land Surface of the Conterminous United States, 1982-2001*. US Department of the Interior, US Geological Survey. http://pubs.usgs.gov/sir/2006/5012/.

Sanford, W.E., and J.P. Pope. 2013. "Quantifying Groundwater's Role in Delaying Improvements to Chesapeake Bay Water Quality." *Environmental Science & Technology* 47 (23): 13330–38.

Scanlon, Bridget R., Robert C. Reedy, and Kevin F. Bronson. 2008. "Impacts of Land Use Change on Nitrogen Cycling Archived in Semiarid Unsaturated Zone Nitrate Profiles, Southern High Plains, Texas." *Environmental Science & Technology* 42 (20): 7566–72. doi:10.1021/es800792w.

Schilling, K. E., M. D. Tomer, Y.-K. Zhang, T. Weisbrod, P. Jacobson, and C. A. Cambardella. 2007. "Hydrogeologic Controls on Nitrate Transport in a Small Agricultural Catchment, Iowa." *Journal of Geophysical Research* 112 (G3). doi:10.1029/2007JG000405.

Schilling, Keith E., and Peter Jacobson. 2010. "Groundwater Conditions under a Reconstructed Prairie Chronosequence." *Agriculture, Ecosystems & Environment* 135 (1–2): 81–89. doi:10.1016/j.agee.2009.08.013.

Schilling, Keith E., Priyanka Jindal, Nandita B. Basu, and Matthew J. Helmers. 2012. "Impact of Artificial Subsurface Drainage on Groundwater Travel Times and Baseflow Discharge in an Agricultural Watershed, Iowa (USA)." *Hydrological Processes* 26 (20): 3092–3100. doi:10.1002/hyp.8337.

Schilling, Keith E., and Calvin F. Wolter. 2007. "A GIS-Based Groundwater Travel Time Model to Evaluate Stream Nitrate Concentration Reductions from Land Use Change." *Environmental Geology* 53 (2): 433–43. doi:10.1007/s00254-007-0659-0.

Schindler, David W. 2006. "Recent Advances in the Understanding and Management of Eutrophication." *Limnology and Oceanography* 51 (1part2): 356–363.

Schlesinger, W.H. 2008. "On the Fate of Anthropogenic Nitrogen." *PNAS* 106 (1): 203–8.

Schlesinger, W.H., and E. Bernhardt. 2013. *Biogeochemistry: An Analysis of Global Change*. 3rd ed. Waltham, MA: Academic Press. https://www.elsevier.com/books/biogeochemistry/schlesinger/978-0-12-385874-0.

Science Advisory Board. 2011. "Reactive Nitrogen in the United States: An Analysis of Inputs, Flows, Consequences, and Management Options." Washington, D.C.: Office of the U.S. EPA Administrator.

Sebilo, M., B. Mayer, B. Nicolardot, G. Pinay, and A. Mariotti. 2013. "Long-Term Fate of Nitrate Fertilizer in Agricultural Soils." *Proceedings of the National Academy of Sciences* 110 (45): 18185–89. doi:10.1073/pnas.1305372110.

Seitzinger, S., John A. Harrison, J. K. Böhlke, A. F. Bouwman, R. Lowrance, B. Peterson, C. Tobias, and G. Van Drecht. 2006. "Denitrification across Landscapes and Waterscapes: A Synthesis." *Ecological Applications* 16 (6): 2064–2090.

144

Sharpley, Andrew, Helen P. Jarvie, Anthony Buda, Linda May, Bryan Spears, and Peter Kleinman. 2013. "Phosphorus Legacy: Overcoming the Effects of Past Management Practices to Mitigate Future Water Quality Impairment." *Journal of Environment Quality* 42 (5): 1308. doi:10.2134/jeq2013.03.0098.

Six, J., R.T. Conant, E.A. Paul, and K. Paustian. 2002a. "Stabilization Mechanisms of Soil Organic Matter: Implications for C-Saturation of Soil." *Plant and Soil* 241: 155–76.

Smil, V. 1999a. "Nitrogen in Crop Production: An Account of Global Flows." *Global Biogeochemical Cycles* 13 (2): 647–62.

Smil, Vaclav. 1999. "Detonator of the Population Explosion." *Nature* 400 (6743): 415–415.

Smith, C.M>, M.B. David, C.A. Mitchell, M.D. Masters, K.J. Anderson-Teixeira, C.J. Bernacchi, and E.H. DeLucia. 2012. "Reduced Nitrogen Losses after Conversion of Row Crop Agriculture to Perennial Biofuel Crops." *Journal of Environment Quality* 42 (1): 219–28.

Smith, S. V., R. O. Sleezer, W. H. Renwick, and R. W. Buddemeier. 2005. "Fates of Eroded Soil Organic Carbon: Mississippi Basin Case Study." *Ecological Applications* 15 (6): 1929–40.

Soil Survey Staff. 2015. "National Value Added Look Up (Valu) Table Database for the Gridded Soil Survey Geographic (gSSURGO) Database for the United States of America and the Territories, Commonwealths, and Island Nations Served by the USDA-NRCS." United States Department of Agriculture, Natural Resources Conservation Service. https://gdg.sc.egov.usda.gov/.

Solomon, Dawit, F. Fritzsche, J. Lehmann, Mamo Tekalign, and W. Zech. 2002. "Soil Organic Matter Dynamics in the Subhumid Agroecosystems of the Ethiopian Highlands." *Soil Science Society of America Journal* 66 (3): 969–978.

Sousa, Marcelo R., Jon P. Jones, Emil O. Frind, and David L. Rudolph. 2013. "A Simple Method to Assess Unsaturated Zone Time Lag in the Travel Time from Ground Surface to Receptor." *Journal of Contaminant Hydrology* 144 (1): 138–51. doi:10.1016/j.jconhyd.2012.10.007.

Spoelstra, John, Sherry L. Schiff, Richard J. Elgood, Ray G. Semkin, and Dean S. Jeffries. 2001. "Tracing the Sources of Exported Nitrate in the Turkey Lakes Watershed Using 15 N/ 14 N and 18 O/ 16 O Isotopic Ratios." *Ecosystems* 4 (6): 536–44. doi:10.1007/s10021-001-0027-y.

Sprague, Lori A., Robert M. Hirsch, and Brent T. Aulenbach. 2011. "Nitrate in the Mississippi River and Its Tributaries, 1980 to 2008: Are We Making Progress?" *Environmental Science & Technology* 45 (17): 7209–16. doi:10.1021/es201221s.

Stallard, Robert F. 1998. "Terrestrial Sedimentation and the Carbon Cycle: Coupling Weathering and Erosion to Carbon Burial." *Global Biogeochemical Cycles* 12 (2): 231–57. doi:10.1029/98GB00741.

Stenback, Greg A., William G. Crumpton, Keith E. Schilling, and Matthew J. Helmers. 2011. "Rating Curve Estimation of Nutrient Loads in Iowa Rivers." *Journal of Hydrology* 396 (1–2): 158–69. doi:10.1016/j.jhydrol.2010.11.006.

Stowe, William. 2016. "Swimming Upstream: Des Moines Water Works Asks for Agricultural Accountability in A State That Claims to 'Feed the World.'" *ROOTSTALK | A Prairie Journal of Culture, Science and the Arts* 2 (1): 32–37.

Strock, J. S., P. M. Porter, and M. P. Russelle. 2004. "Cover Cropping to Reduce Nitrate Loss through Subsurface Drainage in the Northern US Corn Belt." *Journal of Environmental Quality* 33 (3): 1010–1016.

Swaney, Dennis P, Bongghi Hong, Chaopu Ti, Robert W Howarth, and Christoph Humborg. 2012a. "Net Anthropogenic Nitrogen Inputs to Watersheds and Riverine N Export to Coastal Waters: A Brief Overview." *Current Opinion in Environmental Sustainability* 4 (2): 203–11. doi:10.1016/j.cosust.2012.03.004.

Tesoriero, Anthony J., and Larry J. Puckett. 2011. "O $_2$ Reduction and Denitrification Rates in Shallow Aquifers." *Water Resources Research* 47 (12): n/a-n/a. doi:10.1029/2011WR010471.

Thompson, Jonathan R., Dunbar N. Carpenter, Charles V. Cogbill, and David R. Foster. 2013. "Four Centuries of Change in Northeastern United States Forests." *PLOS ONE* 8 (9): e72540. doi:10.1371/journal.pone.0072540.

Thompson, S. E., N. B. Basu, J. Lascurain, A. Aubeneau, and P. S. C. Rao. 2011. "Relative Dominance of Hydrologic versus Biogeochemical Factors on Solute Export across Impact Gradients." *Water Resources Research* 47 (10). doi:10.1029/2010WR009605.

Thompson, Sally E., C. J. Harman, R. Schumer, J. S. Wilson, N. B. Basu, P. D. Brooks, S. D. Donner, et al. 2011. "Patterns, Puzzles and People: Implementing Hydrologic Synthesis." *Hydrological Processes* 25 (20): 3256–66. doi:10.1002/hyp.8234.

Throop, H.L., S.R. Archer, H.C. Monger, and S. Waltman. 2012. "When Bulk Density Methods Matter: Implications for Estimating Soil Organic Carbon Pools in Rocky Soils." *Journal of Arid Environments* 77 (February): 66–71. doi:10.1016/j.jaridenv.2011.08.020.

Tilman, David, Kenneth G. Cassman, Pamela A. Matson, Rosamond Naylor, and Stephen Polasky. 2002. "Agricultural Sustainability and Intensive Production Practices." *Nature* 418 (6898): 671–677.

Torn, M., S.E. Trumbore, O.A. Chadwick, P.M. Vitousek, and D.M. Hendricks. 1997. "Mineral Control of Soil Organic Carbon Storage and Turnover." *Nature* 389: 170–73.

Turner, Peter A., Timothy J. Griffis, Xuhui Lee, John M. Baker, Rodney T. Venterea, and Jeffrey D. Wood. 2015. "Indirect Nitrous Oxide Emissions from Streams within the US Corn Belt Scale with Stream Order." *Proceedings of the National Academy of Sciences* 112 (32): 9839–43. doi:10.1073/pnas.1503598112.

Turner, R. Eugene, and Nancy N. Rabalais. 2003. "Linking Landscape and Water Quality in the Mississippi River Basin for 200 Years." *Bioscience* 53 (6): 563–572.

———. 2004. "Suspended Sediment, C, N, P, and Si Yields from the Mississippi River Basin." *Hydrobiologia* 511 (1–3): 79–89.

Turner, R. Eugene, Nancy N. Rabalais, and Dubravko Justic. 2008. "Gulf of Mexico Hypoxia: Alternate States and a Legacy." *Environmental Science & Technology* 42 (7): 2323–27.

USDA. 2015. "USDA Funding to Help Clean Waterways in Mississippi River Basin | USDA Newsroom." http://www.usda.gov/wps/portal/usda/usdahome?contentidonly=true&contentid=2015/04/0089.xml.

USEPA. 2008. "Mississippi River/Gulf of Mexico Watershed Nutrient Task Force Gulf Hypoxia Action Plan 2008 for Reducing, Mitigatin, and Controlling Hypoxia in Teh Northern Gulf of Mexico and Improving Water Quality in the Mississippi River Basin." United States Environmental Protection Agency.

van Breemen, N., E.W. Boyer, C.L. Goodale, N.A. Jaworski, K. Paustian, S.P. Seitzinger, B. Lajtha, D. van Dam, and R.W. Howarth. 2002. "Where Did All the Nitrogen Go? Fate of Nitrogen Inputs to Large Watersheds in the Northeastern U.S.A." *Biogeochemistry* 57–58 (1): 267–93.

van der Velde, Y., G. H. de Rooij, J. C. Rozemeijer, F. C. van Geer, and H. P. Broers. 2010. "Nitrate Response of a Lowland Catchment: On the Relation between Stream Concentration and Travel Time Distribution Dynamics" *Water Resources Research* 46 (11): n/a-n/a. doi:10.1029/2010WR009105.

van Egmond, Klaas, Ton Bresser, and Lex Bouwman. 2002a. "The European Nitrogen Case." *Ambio* 31 (2): 72–78.

Van Meter, K.J., and Basu. n.d. "Time Lags in Watershed-Scale Nutrient Transport: An Exploration of Dominant Controls." *In Preparation*.

Van Meter, K.J., and Nandita B. Basu. 2015. "Catchment Legacies and Time Lags: A Parsimonious Watershed Model to Predict the Effects of Legacy Storage on Nitrogen Export." Edited by Yiguo Hong. *PLOS ONE* 10 (5): e0125971. doi:10.1371/journal.pone.0125971.

Van Meter, K.J., N.B. Basu, J.J. Veenstra, and C.L. Burras. 2016. "The Nitrogen Legacy: Emerging Evidence of Nitrogen Accumulation in Anthropogenic Landscapes." *Environmental Research Letters* 11 (3): 35014. doi:10.1088/1748-9326/11/3/035014.

Van Meter, K.J., N.B. Van Cappellen, and N.B. Basu. in prep. "Two Centuries of Nitrogen Dynamics: Legacy Sources and Sinks in the Mississippi and Susquehanna River Basins." *In Preparation*.

van Puijenbroek, P. J. T. M., P. Cleij, and H. Visser. 2014. "Aggregated Indices for Trends in Eutrophication of Different Types of Fresh Water in the Netherlands." *Ecological Indicators* 36 (January): 456–62. doi:10.1016/j.ecolind.2013.08.022.

Van Remortel, R.D., and D.A. Shields. 1993. "Comparison of Clod and Core Methods for Determination of Soil Bulk Density." *Communications in Soil Science & Plant Analysis* 24 (17–18): 2517–28.

Veenstra, J.J. 2010. *Fifty Years of Agricultural Soil Change in Iowa*. Ames, IA: Iowa State University. http://gradworks.umi.com.proxy.lib.uiowa.edu/34/17/3417963.html.

Veenstra, J.J., and C.L. Burras. 2015. "Soil Profile Transformation after 50 Years of Agricultural Land Use." *Soil Science Society of America Journal* 79 (4): 1154. doi:10.2136/sssaj2015.01.0027.

Vidon, Philippe, Craig Allan, Douglas Burns, Tim P. Duval, Noel Gurwick, Shreeram Inamdar, Richard Lowrance, Judy Okay, Durelle Scott, and Steve Sebestyen. 2010. "Hot Spots and Hot Moments in Riparian Zones: Potential for Improved Water Quality Management1." *JAWRA Journal of the American Water Resources Association* 46 (2): 278–98. doi:10.1111/j.1752-1688.2010.00420.x.

Vitousek, P.M., J.D. Aber, R.W. Howarth, G.E. Likens, P.A. Matson, D.W. Schindler, W.H. Schlesinger, and D.G. Tilman. 1997. "Human Alteration of the Global

Nitrogen Cycle: Sources and Consequences." *Ecological Applications* 7 (3): 737–50.

Walvoord, M.A., F.M. Philips, D.A. Stonestrom, R.D. Evans, P.C. Hartsough, B.D. Newman, and R.G. Striegl. 2003. "A Reservoir of Nitrate beneath Desert Soil." *Science* 302 (5647): 1021–24.

Wang, Hongjie, Minhan Dai, Jinwen Liu, Shuh-Ji Kao, Chao Zhang, Wei-Jun Cai, Guizhi Wang, Wei Qian, Meixun Zhao, and Zhenyu Sun. 2016. "Eutrophication-Driven Hypoxia in the East China Sea off the Changjiang Estuary." *Environmental Science & Technology* 50 (5): 2255–63. doi:10.1021/acs.est.5b06211.

Wellen, C., G.B. Arhonditsis, T. Labencki, and D. Boyd. 2012. "A Bayesian Methodological Framework for Accommodating Interannual Variability of Nutrient Loading with the SPARROW Model." *Water Resources Research* 48 (10).

West, Tristram O., and Wilfred M. Post. 2002. "Soil Organic Carbon Sequestration Rates by Tillage and Crop Rotation." *Soil Science Society of America Journal* 66 (6): 1930. doi:10.2136/sssaj2002.1930.

Whitmore, A.P., N.J. Bradbury, and P.A. Johnson. 1992. "Potential Contribution of Ploughed Grassland to Nitrate Leaching." *Agriculture, Ecosystems & Environment* 39 (3): 221–33.

Withers, Paul, Colin Neal, Helen Jarvie, and Donnacha Doody. 2014. "Agriculture and Eutrophication: Where Do We Go from Here?" *Sustainability* 6 (9): 5853–75. doi:10.3390/su6095853.

Worrall, F., T. P. Burt, N. J. K. Howden, and M. J. Whelan. 2009. "Fluvial Flux of Nitrogen from Great Britain 1974–2005 in the Context of the Terrestrial Nitrogen Budget of Great Britain." *Global Biogeochem. Cycles* 23 (3): GB3017. doi:10.1029/2008GB003351.

Worrall, F., N. J. K. Howden, and T. P. Burt. 2015. "Evidence for Nitrogen Accumulation: The Total Nitrogen Budget of the Terrestrial Biosphere of a Lowland Agricultural Catchment." *Biogeochemistry*, February. doi:10.1007/s10533-015-0074-7.

Wu, Yiping, and Shuguang Liu. 2012. "Impacts of Biofuels Production Alternatives on Water Quantity and Quality in the Iowa River Basin." *Biomass and Bioenergy* 36 (January): 182–91. doi:10.1016/j.biombioe.2011.10.030.

Xu, H., H. W. Paerl, B. Qin, G. Zhu, N. S. Hall, and Y. Wu. 2015. "Determining Critical Nutrient Thresholds Needed to Control Harmful Cyanobacterial Blooms in Eutrophic Lake Taihu, China." *Environmental Science & Technology* 49 (2): 1051–59. doi:10.1021/es503744q.

Yadav, S., and D.B. Wall. 1998. "Benefit-Cost Analysis of Best Management Practices Implemented to Control Nitrate Contamination of Groundwater." *Water Resources Research* 34 (3): 497–504.

Yan, Xiaoyuan, Chaopu Ti, Peter Vitousek, Deli Chen, Adrian Leip, Zucong Cai, and Zhaoliang Zhu. 2014. "Fertilizer Nitrogen Recovery Efficiencies in Crop Production Systems of China with and without Consideration of the Residual Effect of Nitrogen." *Environmental Research Letters* 9 (9): 95002. doi:10.1088/1748-9326/9/9/095002.

Young, R.A., C.A. Onstad, D.D. Bosch, and W.P. Anderson. 1989. "AGNPS: A Nonpoint-Source Pollution Model for Evaluating Agricultural Watersheds." *Journal of Soil and Water Conservation* 44 (2): 168–73.

Zaehle, S. 2013. "Terrestrial Nitrogen-Carbon Cycle Interactions at the Global Scale." *Philosophical Transactions of the Royal Society B: Biological Sciences* 368 (1621): 20130125–20130125. doi:10.1098/rstb.2013.0125.

Zhang, X. 2016. "Spatio-Temporal Patterns in Net Anthropogenic Nitrogen and Phosphorus Inputs across the Grand River Watershed." Waterloo, ON: University of Waterloo.

Zhang, Y.-K., and K.E. Schilling. 2006. "Increasing Streamflow and Baseflow in Mississippi River since the 1940s: Effect of Land Use Change." *Journal of Hydrology* 324 (1–4): 412–22. doi:10.1016/j.jhydrol.2005.09.033.

Zimmerman, M., and L. Dooley. 2014. "Water Quality Assessment of the Lower West Branch-Susquehanna River: Focuse on Sewage Treatment." *Journal of the Pennsylvania Academy of Science* 88 (1): 40–46.

Appendix 1 - Chapter 2 Supplementary Material

A1.1 Synthesis of Mass Balance Studies

Supplementary Table A1.1 Net nitrogen retention per hectare of total basin area. Although the occurrence of N retention is universal, the retention magnitudes vary with location and are to some extent a function of the percent of basin area in cropland, with higher percent of cropland area leading to greater retention. Net retention is defined here as the difference between net N inputs and riverine output and may include denitrification, sediment burial, or long-term storage in subsurface reservoirs (Gilles Billen et al. 2009a). Net N inputs (also referred to as the N surplus (Leip, Britz, et al. 2011)) are defined as the difference between anthropogenic N inputs (main components are atmospheric N deposition, fertilizer N application and agricultural fixation as well as animal and human consumption) and outputs (main components are crop and animal production).

Study Region	Area (km2)	% Cropland	Net Retention (kg ha^{-1} y^{-1})	Time Period
Mississippi River Basin, U.S.(Hong, Swaney, and Howarth 2013)	3,208,700	27%	17	1987-1997
Upper Mississippi Basin, U.S.(Mark B. David, Drinkwater, and McIsaac 2010b)	214,344	30%	16.8	1997-2006
Northeastern U.S. Watersheds (Boyer et al. 2002)	248,326	19%	19	early 1990s
Canada (Janzen et al. 2003)	9,985,000	3%	1.1	1996
Thames Basin, UK (Howden et al. 2011a)	10,000	47%	100	1940-2008
Seine, NW Europe (Gilles Billen et al. 2009a)	76,370	53%	40	2000
Somme, NW Europe (Gilles Billen et al. 2009a)	76,370	53%	40	2000
Scheldt, NW Europe (Gilles Billen et al. 2009a)	19,860	39%	89	2000

Netherlands (Kroeze et al. 2003)	41,543	26%	229	1995
Europe (van Egmond, Bresser, and Bouwman 2002b)	5,939,044	21%	23.2	2001
Changjiang River Basin, China (Liu, Watanabe, and Wang 2008)	1.81×10^6	13%	40	2000
Red River Basin, Vietnam & China (Quynh et al. 2005)	153,207	37%	16.3	2004
Jiulong River Watershed, China (N. Chen et al. 2008)	14,700	18%	40.8	2008
Piracicaba Basin (Filoso et al. 2003)	10,927	31%	22.6	1995-1997

A1.2 Soil Resampling Studies

A1.2.1 Sample Analysis.

Total soil N (TN) was measured by the dry combustion method using a Leco elemental analyzer (St. Joseph, MI, USA). Current TN values were compared with the historically reported NCSS values, which were determined by the Kjeldahl method. As the older Kjeldahl method and newer dry combustion techniques have been confirmed to provide comparable results, the historically reported N concentrations were used without correction (Kowalenko 2001). All further details of this study are provided in Veenstra (Veenstra 2010). TN concentrations for the samples were measured by the dry combustion method and compared with historical soil sampling information for the sites published by the National Cooperative Soil Survey (NCSS 2014).

A1.2.2 Statistical Analysis.

Bulk density and TN concentration data obtained from both historical and current samples was tested for normality based on application of the Shapiro-Wilk test (Helsel and Hirsch 1992). The Wilcoxon signed-rank test (comparison of paired samples) (Helsel and Hirsch 1992), was used to determine whether differences between historical and current TN values for the resampling studies were statistically significant at the 5% significance level (Helsel and Hirsch 1992). Because bulk density values were not available for all of the historical samples, the non-paired Wilcoxon rank sum test was used to determine whether differences between historical and current BD values were statistically significant at a 5% significance level. Mass-per-area estimates were calculated based on equation 2, and error on the mass-per-area values was estimated by propagating the standard errors of both the bulk density and the TN concentration values.

A1.2.3 Bulk Density Measurements.

Although analytical results for soil TN and OC content are typically reported as mass-per-mass values, it is useful to express changes in soil TN and OC on a mass-per-area basis (kg ha^{-1}) in order to place them within the context of management practices and ongoing inputs and outputs to the soil system. However, to make such estimates

of mass-per-area changes in soil nutrients, soil bulk density values must be utilized. As soil bulk density values can also change over time in response to changing management practices, mass-per-area calculations can be subject to significant uncertainty (Ellert and Bettany 1995; Throop et al. 2012). For example, if soil bulk density has increased and soil is sampled to a fixed depth, apparent increases in soil N or C may be overestimated due to the greater mass of soil being sampled (Murty et al. 2002). Therefore, in order to properly carry out the unit conversion from mass-per-mass to mass-per-area values, it must first be determined whether any significant changes in bulk density have occurred. If changes in bulk density have occurred, it is recommended that an equivalent soil mass (ESM) method be used for the mass-per-area calculation to avoid over- or underestimating changes in N and C stocks (Ellert and Bettany 1995).

In the Iowa study, while historical bulk densities were obtained using the clod method, current bulk densities were determined using the soil core method. It has been noted that bulk density (BD) values obtained by the soil core method are consistently lower than those obtained by the "clod method" (Throop et al. 2012), which was used for all historical NCSS samples, according to the following relationship (Van Remortel and Shields 1993):

$$\text{Clod BD} = (1.011 \pm 0.042 \text{ x Core BD}) + 0.068 \pm 0.048$$

$$(A1.1)$$

Therefore, for accurate comparison with historically reported BD values, current soil core bulk densities were corrected based on supplemental **Equation A1.1**. All reported values for bulk density were standardized to depth layers of 25 cm (0-25 cm, 25-50 cm, 50-75 cm, 75-100 cm).

For the Iowa and Illinois resampling studies, our results indicated no significant changes in bulk density for any of the four layers from 0-100 cm ($p > 0.4$, Wilcoxon rank sum test) (supplementary **Tables A1.2 and A1.3)**. Regression analysis for the NCSS data also showed no significant changes in soil bulk density values ($p > 0.2$). The lack of any statistically significant trend in bulk density over our study period is reasonable considering that the most significant changes in bulk density typically arise from changes in land use, most notably in the initial years after

153

conversion of forested land or grasslands to cultivated areas, and the majority of cropland in the MRB had already been placed under cultivation by the early 20th century (Murty et al. 2002; R. E. Turner and Rabalais 2003). Due to this lack of a significant temporal trend in the bulk density data, we used mean bulk density values at each depth to estimate the accumulation in mass-per-area (kg ha-1) from the reported mass-per-mass values as follows(Ellert and Bettany 1995):

$$M_{element} = conc * \rho_b * T * 10 \qquad (A1.2)$$

where, $M_{element}$ = element mass per unit area (kg ha^{-1}), $conc$ = element concentration (g Mg-1), ρ_b = bulk density (g/cm^3), and T = thickness of the soil layer (m). The standard error of the corrected bulk density values was propagated using equation 2 to estimate the standard error associated with the mass-per-area values.

Supplementary Table A1.2. Bulk densities (BD) estimated for the Iowa study. Current bulk densities estimated using the soil core method were corrected using Equation 2 to estimate BD by clod method. The latter was compared with historical BD values, and it was determined that there was no statistically significant differences between the historical and current values (p<0.01).

0-25 cm	Historical BD (g/cm3) (clod method)	Current BD (g/cm3) (soil core method)	Current BD (g/cm3) (predicted clod BD)	Difference (g/cm3)	p-value
0-25 cm	1.47 ± 0.02	1.41 ± 0.01	1.49 ± 0.08	0.02 ± 0.08	0.60
25-50 cm	1.50 ± 0.02	1.43 ± 0.01	1.51 ± 0.08	0.01 ± 0.08	0.74
50-75 cm	1.58 ± 0.02	1.48 ± 0.02	1.56 ± 0.08	-0.02 ± 0.08	0.46
75-100 cm	1.67 ± 0.02	1.56 ± 0.02	1.64 ± 0.08	-0.03 ± 0.09	0.75

Supplementary Table A1.3. Historical and current values for TN, OC, and BD from the Illinois Study (David et al. 2009).

	Depth (cm)	Historical g/Mg-soil	Current	n	Difference g/Mg-soil	p-value
Total Nitrogen	0-20	2,730 ± 180	2,580 ± 120	6	-150 ± 216	0.516
	20-50	1,090 ± 130	1,390 ± 160	6	300 ± 206	0.14
	50-100	300 ± 30	490 ± 40	6	200 ± 50	0.016
Organic Carbon	0-20	34,880 ± 1890	29,910 ± 1,900	6	-4970 ± 2,680	0.109
	20-50	12,620 ± 2,610	15,630 ± 2,230	6	3,020 ± 3,433	0.219
	50-100	3,370 ± 510	5,170 ± 170	6	1,800 ± 538	0.031
	0-20	1.25 ± 0.03	1.34 ± 0.03	6	0.09 ± 0.04	0.172
Bulk Density	20-50	1.38 ± 0.06	1.52 ± 0.03	6	0.14 ± 0.06	0.063
	50-100	1.47 ± 0.04	1.46 ± 0.03	6	-0.01 ± 0.05	0.406

A1.3 Trend Analysis for MRB Soil Data

A multiple linear regression model (MLR) was used to test for negative or positive trends over time in TN for samples obtained across the MRB between 1980 and 2010. A total of 2069 samples were available at the 0 – 25 cm depth, 1759 samples for the 25 – 50 cm depth, 1505 samples for 50 – 75 cm, and 1320 samples with complete data from 0 - 100 cm. **Supplementary Table A1.4** provides a summary of the number of samples available at each depth range across the study period (1980-2010). Regression analysis was used to test variables related to location within the MRB (latitude and longitude), soil texture (clay, silt and sand content) and climate (annual precipitation, mean annual temperature) and to identify those having a significant relationship with TN values and having maximum explanatory power, as determined by the p-values. The normality of the model residuals was tested using the Shapiro-Wilk test. The statistical significance of the MLR coefficient values was established to a 95% confidence interval.

Correlations between a variety of exogenous variables and soil TN were explored at 25-cm intervals from 0-100 cm (**Supplementary Table A1.5)** to identify and control for factors that could impact levels of TN in the sampled soils and thus obscure or distort any observed rate of change (Helsel and Hirsch 1992). The correlations thus identified were used in a MLR model that allowed for the better detection of increasing or decreasing trends in the parameters of interest.

Percent clay, silt and sand values were all found to correlate significantly with TN ($p<0.0001$) (**Supplementary Table A1.5**). However, clay alone was selected for inclusion in the MLR model due to its stronger relationship with TN and to avoid issues of collinearity. Both latitude and longitude (decimal degrees) were found to be positively correlated with TN ($p<0.0001$) in the surface layer (0-25 cm), though the strength of the correlations decreased in the deeper layers, particularly for the relationship between longitude and TN (**Supplementary Table A1.5**). These findings are suggestive of higher levels of TN in northern and eastern portions of the MRB, which is consistent with previous work showing higher levels of soil organic matter in these regions, thus suggesting the appropriateness of including both of these variables in the MLR model (Post and Pastor 1985). Although our findings regarding

155

latitude and longitude are suggestive of the impact of regional differences in climate on TN levels, we found little correlation between temporal trends in either mean annual temperature or total yearly precipitation and the soil TN and OC, particularly from 0-25 cm (**Supplementary Table A1.5**). Accordingly, neither temperature nor precipitation variables were included in the MLR model. Based on the identified relationships, a regression model was developed of the form

$$y = \beta_0 + \beta_1 T + \beta_2 LAT + \beta_3 LONG + \beta_0 CLAY + \varepsilon \qquad (A1.3),$$

where y represents the predicted TN content (g/Mg-soil), T is time (y), $\beta_0, \beta_1, \beta_2, \beta_3, \beta_4$ are regression coefficients, and LAT, LONG and CLAY are the model variables representing latitude and longitude (decimal degrees) and the percent soil clay content (% value), respectively. The obtained coefficient values for the MLR model are given in **Supplementary Table A1.6**.

Although soil organic matter content is known to vary spatially as a function of variations in climate, vegetation and soil characteristics, which could potentially confound the results of such an analysis, spatial variability in soil organic matter has been found to be minimal in agricultural areas as compared to forested or other undisturbed sites (Conant, Smith, and Paustian 2003). Accordingly, our analysis was carried out under the assumption that the long history of intensive agriculture (>50 years) in the MRB, with the large-scale cultivation of a limited number of field crops, would limit some of the inherent spatial variability found in SOM in less disturbed sites. In addition, we attempted to address potential problems stemming from landscape heterogeneity by means of the following: (1) a large sample size (>2000 samples across the MRB; (2) use of a multiple linear regression approach to control for soil type and regional differences in climate; and (3) a sufficiently long time frame (30 years) to allow for magnitudes of change over time to become detectable above the noise created by spatial heterogeneity.

As described in the text, trend analysis was carried out at each depth range (0-25, 25-50, 50-75, 75-100) with all of the available samples for that range, and also over the entire 100-cm depth using the subset of 1320 samples. A table is provided in the text (**table 2**) with the results for the full sample set at each depth. We also provide here (**Supplementary Table A1.7)** a summary of results for the 1320-

sample subset. Note that for the smaller subset presented here, the N accumulation is less weighted toward the upper half meter (13.2 g Mg^{-1}, 0-25 cm and 7.3 g Mg^{-1}, 25-50 cm for the full dataset vs. 10.3 g Mg^{-1}, 0-25 cm and 1.9 g Mg^{-1}, 25-50 cm for the 1320-sample subset). We speculate that this difference in accumulation rates is likely due to differences in soil characteristics between areas where deeper sampling has been carried out and those where there has been only shallow sampling. NCSS sampling guidelines specify that sampling should be done to the parent material or to a maximum depth of 2 m (Burt 2009). Accordingly, areas with shallower sampling depths are also likely areas with a shallower soil layers. In such areas, the downward growth of roots can be limited due to increased bulk densities and shallow bedrock (Canadell et al. 1996), thus leading to root matter and soil organic matter in general being more concentrated in the upper layers. In such areas, N accumulation would therefore be more likely to occur in the upper layers, whereas in areas with deeper soil layers, roots matter would also extend deeper, and accumulation would be less limited to the upper layers. Due to this likely difference in accumulation dynamics between areas with shallow vs deep soil layers, we have used the more conservative estimate of accumulation for the 0-100 cm layer suggested by the analysis of the 1320-sample subset.

Supplementary Table A1.4. The table provides a summary of samples available at each depth range across the study period (1980-2010).

	Number of Samples			
Years	0-25 cm	25-50 cm	50-75 cm	0-100 cm
1980-1984	185	143	77	45
1985-1989	247	154	85	59
1990-1994	440	358	282	250
1995-1999	319	307	294	234
2000-2004	493	452	435	415
2005-2010	385	345	332	317
Total	2069	1759	1505	1320

Supplementary Table A1.5. Correlation analysis to evaluate explanatory variables for inclusion in multiple linear regression model.

Soil Parameter	Explanatory Variables	0-25 p-value	25-50 p-value	50-75 p-value	75-100 p-value
Total Nitrogen	Spatial				
	Latitude	<0.0001	<0.0001	0.001	0.643
	Longitude	<0.0001	0.089	0.014	0.519
	Soil Texture				
	Clay Content	<0.0001	<0.0001	<0.0001	<0.0001
	Silt Content	<0.0001	<0.0001	<0.0001	<0.0001
	Sand Content	<0.0001	<0.0001	<0.0001	<0.0001
	Climate				
	Precipitation	0.046	<0.001	0.008	0.003
	Temperature	0.104	0.041	0.037	0.274

Supplementary Table A1.6. Coefficients for multiple linear regression analysis of 2069 NCSS samples over the period 1980-2010

Soil Parameter	Depth (cm)	n	β_0 (INTERCEPT)	β_1 (TIME)	β_2 (LAT)	β_3 (LONG)	β_4 (CLAY)	R^2	p-value
	0-25	2069	-26,584	13.2	95.2	28.0	28.1	0.345	<0.0001
	25-50	1759	-15,350	7.2	41.3	2.4	16.1	0.237	<0.0001
Total Nitrogen	50-75	1505	-8,290	3.8	19.3	-2.5	13.1	0.231	<0.0001
	75-100	1320	-182	1.6	12.2	2.0	10.7	0.202	<0.0001
	0-100	1320	-7,378	3.4	48.9	9.7	16.9	0.307	<0.0001

Supplementary Table A1.7. Accumulation rates for TN in soil samples across the Mississippi Basin (1980-2010) based on MLR analysis of the NCSS dataset. Samples included herein are those for which complete data was able from 0-100 cm. Accumulation rates are given on both a mass-per-mass (g Mg^{-1} y^{-1}) and mass-per-area basis (kg ha^{-1} y^{-1}), and in depth increments of 25 cm.

Soil Parameter	Depth (cm)	Number (n)	Bulk Density (g cm^{-3})	Rate of Change (g Mg^{-1} y^{-1})	Rate of Change (kg ha^{-1} y^{-1})	p-value
	0-25	1320	1.55	10 ± 3.0	40 ± 11.6	<0.001
	25-50	1320	1.61	1.9 ± 2.0	7.6 ± 7.3	0.354
Total Nitrogen	50-75	1320	1.64	0.8 ± 1.6	3.4 ± 6.6	0.614
	75-100	1320	1.65	1.6 ± 1.4	6.6 ± 5.8	0.250
	0-100	1320	1.61	3.4 ± 1.6	55 ± 25.80	0.003

A1.4 Conceptual Model

In the pre-cultivation period (Phase I), we assume low net N inputs of 5 kg ha^{-1} y^{-1}, a typical value for biological nitrogen fixation in a grassland ecosystem (Bouwman 2005). In the initial steady-state condition, the total initial mass of SON is estimated to be 4,500 kg ha^{-1} (Burke et al. 2002). At steady state, the size of the active pool (M_{act_0}) is equal to $\frac{a}{k}$, leading to a mass of 31 kg ha^{-1} in the active pool and 4469 kg ha^{-1} in the protected pool (M_{prot}) (**Figure 2.4**). The mineralization rate constant ($k = 0.16$ y^{-1}) was empirically derived based on observed declines in groundwater nitrate concentrations in a chronosequence study carried out in central Iowa (Van Meter and Basu 2015). Similar rate constant values have been obtained based on documented declines in SON content after the plowing of permanent grassland (Whitmore, Bradbury, and Johnson 1992).

The start of cultivation (Phase II, $t = 50$) makes possible a release of SON by breaking up aggregate structures in the soil, thus removing the primary physical protection mechanism offered by the grassland soil (Six et al. 2002a). More specifically, cultivation allows for the conversion of a proportion of the protected pool to active status, such that it can be mineralized over time. Burke et al. (2002) estimate a mean loss of SON of approximately 30% following cultivation in cropland soils of the North American grassland region. Accordingly, we assume that with the start of cultivation (start of Phase II) M_{prot} is reduced from 4469 kg ha^{-1} to 3128 kg ha^{-1}. In addition, net N inputs to the system are assumed to decrease during this period (a= -3.8 kg ha^{-1} y^{-1}) as lands are subjected to intensive cropping practices, but with little input of fertilizer (Burke et al. 2002).

After the first 20 years of cultivation ($t = 70$ y), we assume crop productivity to be diminished due to the two decades of low-input, intensive agriculture (Phase III). With outputs reduced, the system re-enters a period of positive but low net inputs ($a=5$ kg ha^{-1} y^{-1}). The next major change ($t=110$ y) comes mid-20th century, as commercial fertilizers become available and there is increased adoption of N-fixing crops such as soybeans (Mark B. David, Drinkwater, and McIsaac 2010b), causing the system to transition from a low-input to a high-input state (Phase IV). Throughout Phase IV, we assume a linear increase in net N inputs, from 5 kg ha^{-1} y^{-1} in 1950 to

41.5 kg ha^{-1} y^{-1} in 2000. The evolution of the soil N pools in response to this changing input regime is discussed in Section 2.5.2.

Appendix 2 - Chapter 4 Supplementary Material

A2.1   Nitrogen Surplus Calculations

A2.1.1 Biological Nitrogen Fixation

Biological nitrogen fixation (BNF) by soybeans and other N-fixing crops was calculated based on state-level crop production data obtained through the U.S. Agricultural Census (http://www.agcensus.usda.gov/) and U.S. Agricultural Survey (USDA-NASS). The total N fixed by N-fixing crops (BNF_{crop}, kg-N/ha), excluding alfalfa, was calculated, using a yield-based approach, as the product of N in harvested product, the percentage of this N attributable to N fixation (Han and Allan, 2008), and a factor of 1.5, to account for both above- and below-ground inputs (Hong et al. 2013). N attributable to N fixation was assumed to be 74% for soybeans and 50% for other pulses (Hong et al. 2013, Han and Allan, 2008). For alfalfa, N fixation (BNF_{alf}, kg-N/ha) was calculated as the product of the area planted in alfalfa and area-based fixation rates (Hong et al. 2011), divided by the total cropland per administrative area (county/state). BNF for pasture areas (BNF_{past}) and non-leguminous crops was considered to be 5 kg ha^{-1} y^{-1}, and for wetland rice 25 kg ha-1 y-1 (Bouwman et al. 2005; V. Smil 1999b). Net BNF for non-agricultural land (BNF_{nat}) was assumed to be 25% of 3 kg ha^{-1} y^{-1} (Cleveland et al. 1999; Schlesinger and Bernhardt 2013).

A2.1.2 Nitrogen Fertilizer

Fertilizer application rates are based on estimates of county-level N fertilizer application for the conterminous U.S. (Ruddy, Lorenz, and Mueller 2006), aggregated to the watershed scale. Application rates of fertilizer N to pasture ($FERT_{past}$) are based on the 1996 FAO estimate of mean N fertilizer application to pasture land (FAO 1996; Francis 2000), with the values being scaled over time as a percentage of the total N fertilizer application. Application to cropland ($FERT_{crop}$) is calculated as the difference between total N fertilizer application and application of pasture land.

A2.1.3 Manure

Manure N inputs to the land surface were calculated based on the method of Ruddy et al. (2006), with modifications and additional parameterization as described below. State-level manure N inputs from each livestock class were calculated as the product of the livestock population (state-level livestock data collected by the U.S. Agricultural Survey) and the N nutrient content of the manure (**Supplemental Table 1**). The manure N produced per livestock unit was assumed to increase over time for both beef and dairy cattle based on changes between pre-1945 and current production practices (Smil et al. 1999), with values changing as indicated in the table. Values were assumed to scale linearly upwards from 1945-1985, and then remain constant after that point. For each state, livestock was divided into two class: (1) animals raised in confined feeding operations, and (2) unconfined animals, according to Kellogg et al. (R. L. Kellogg et al. 2000). Manure produced in confinement was assumed to be stored and subsequently spread either to cropland (MAN_{crop}) or pastureland (MAN_{past}), or directed to manure lagoons (Bouwman et al. 2005). The percent of manure N going to holding lagoons was calculated based on a maximum recommended land application rate of 200 kg-N/ha-y (REF), with quantities above this threshold going to lagoons and subsequently to surface water. Thirty-six percent of all manure was assumed to be lost to NH_3 volatilization (Smil et al. 1999). Fifty percent of all stored and available animal manure was assumed to be applied to cropland, with the remainder being distributed to pastureland (Bouwman et al. 2005). Atmospheric N deposition (*DEP*) was calculated across the study watershed based on county-level deposition estimates by Ruddy et al. (2006), data from the National Atmospheric Deposition Program/National Trends Network (NADP/NTN; data available at *http://nadp.sws.uiuc.edu/*), and long-term modeled estimates by Dentener et al (2006).

Supplementary Table A2.1. Per-head nitrogen (N) waste for the major livestock classes.

Livestock Group	N Waste (kg/head)	References
Beef Cattle		
pre-1945	30	Hong et al. (2011)
current	58.51	Smil et al. (1999)
Dairy Cattle		
pre-1945	45	Hong et al. (2011)
current	121	Smil et al. (1999)
Hogs	5.84	Hong et al. (2011)
Chickens		
Broilers	0.07	Hong et al. (2011)
Non-Broilers	0.55	Hong et al. (2011)
Turkeys	0.39	Hong et al. (2011)
Sheep	5	Hong et al. (2011)

A2.1.4 Atmospheric Deposition

For the period 1982-2001, atmospheric deposition data for both oxidized (NO_x) and reduced (NH_3,NH_4^+) forms of N was obtained from Ruddy et al. (2006). For the years 2002-2015, values were obtained from the National Atmospheric Deposition Program/National Trends Network (NADP/NTN; data available at *http://nadp.sws.uiuc.edu/*). For the years previous to 1982, we used data obtained from Dentener et al. (2006), with interpolated values being used between the 1860 and 1982 data points.

A2.1.5 Crop and Pasture N Output

The crop output term (*CROP*, kg/ha) is based on the removal of N from cropped areas in harvested crop (Bouwman et al. 2005). Specific values were calculated by multiplying the harvested quantities of major crops, using yield values reported by the Agricultural Survey (USDA-NASS), by the percent N in harvested crops, using literature values (Hong et al. 2011, Bouwman et al. 2005). Pasture N output (GRASS; kg/ha) was calculated as follows, as adapted from Bouwman et al. (2005):

$$GRASS = 0.6 * (FERT_{past} + MAN_{past})$$

163

Supplementary Table A2.2. Parameter Range Values for Monte Carlo Calibration Process (Susquehanna)

Parameter	Description	Range Min	Max
k_p	soil mineralization rate constant, passive pool (y^{-1})	6.8×10^{-5}	1.7×10^{-3}
k_a	soil mineralization rate constant, active pool (y^{-1})	0.09	0.17
n	soil porosity	0.33	0.60
s	soil water content	0.35	0.65
λ_s	soil denitrification rate constant (y^{-1})	0.25	0.75
h_c	protection coefficient, cultivated land	0.14	0.26
h_{nc}	protection coefficient, non-cultivated land	0.28	0.52
μ	mean groundwater travel time (y)	3	27
γ	denitrification rate constant, groundwater (y^{-1})	0.01	0.30
λ_{pop}	denitrification rate constant, human waste (y^{-1})	0.56	1

Supplementary Table A2.3. Parameter Sensitivity Results for Soil Organic N and Catchment N Load (Mississippi). Absolute values of the standardized regression coefficients (SRCs) provide a measure of the relative importance of each parameter on the outcome of interest, and the signs indicate whether a parameter has a positive or negative correlation with that outcome (Muleta and Nicklow 2005). Modeled SON levels are primarily impacted by soil mineralization rate and protection coefficient parameters, while stream N loading is more sensitive to denitrification rate constants and groundwater travel times.

Parameter	MEDIAN SOIL ORGANIC N, 1950-2014			STREAM N LOADING, 1980-2014		
	Step Number	SRC	p-value	Step Number	SRC	p-value
k_p	1	0.999	<0.000	-	-	0.271
k_n	4	-0.005	<0.000	8	0.026	<0.000
n	-	-	0.648	6	-0.102	<0.000
s	-	-	0.662	5	-0.109	<0.000
λ_s	-	-	0.598	1	-0.631	<0.000
h_c	3	0.017	<0.000	7	-0.083	<0.000
h_{nc}	2	-0.037	<0.000	9	-0.015	0.031
μ	-	-	0.696	3	-0.467	<0.000
γ	-	-	0.662	2	-0.560	<0.000
λ_{pop}	-	-	0.333	6	-0.128	<0.000

Supplementary Table A2.4. Parameter Sensitivity Results for Soil Organic N and Catchment N Load (Susquehanna). Absolute values of the standardized regression coefficients (SRCs) provide a measure of the relative importance of each parameter on the outcome of interest, and the signs indicate whether a parameter has a positive or negative correlation with that outcome (Muleta and Nicklow 2005). Modeled SON levels are primarily impacted by soil mineralization rate and protection coefficient parameters, while stream N loading is more sensitive to denitrification rate constants and groundwater travel times.

Parameter	MEDIAN SOIL ORGANIC N, 1950-2014			STREAM N LOADING, 1980-2014		
	Step Number	SRC	p-value	Step Number	SRC	p-value
k_p	1	0.986	<0.000	-	-	0.520
k_n	4	-0.010	0.002	-	-	0.716
n	-	-	0.268	-	-	0.483
s	-	-	0.296	-	-	0.398
λ_s	-	-	0.106	1	-0.508	<0.000
h_c	3	0.008	<0.000	-	-	0.665
h_{nc}	2	0.110	<0.000	-	-	0.067
μ	-	-	0.336	2	-0.453	<0.000
γ	-	-	0.658	3	-0.627	<0.000
λ_{pop}	-	-	0.770	4	-0.244	<0.000

Supplementary Table A2.5. Summary of Calibration Results for the MRB and SRB

Parameter	MRB Calibrated Value (median)	SRB Calibrated Value (median)
k_p	1.4×10^{-4}	9.2×10^{-4}
k_a	0.11	0.13
n	0.47	0.46
s	0.50	0.51
λ_s	0.54	0.57
h_c	0.37	0.41
h_{nc}	0.48	0.60
μ	16.0	15.6
γ	0.11	0.27
λ_{pop}	0.83	0.83

Appendix 3 - Chapter 5 Supplementary Material

A3.1. Observed vs Predicted Concentration Values for the Speed River at Wellington Road
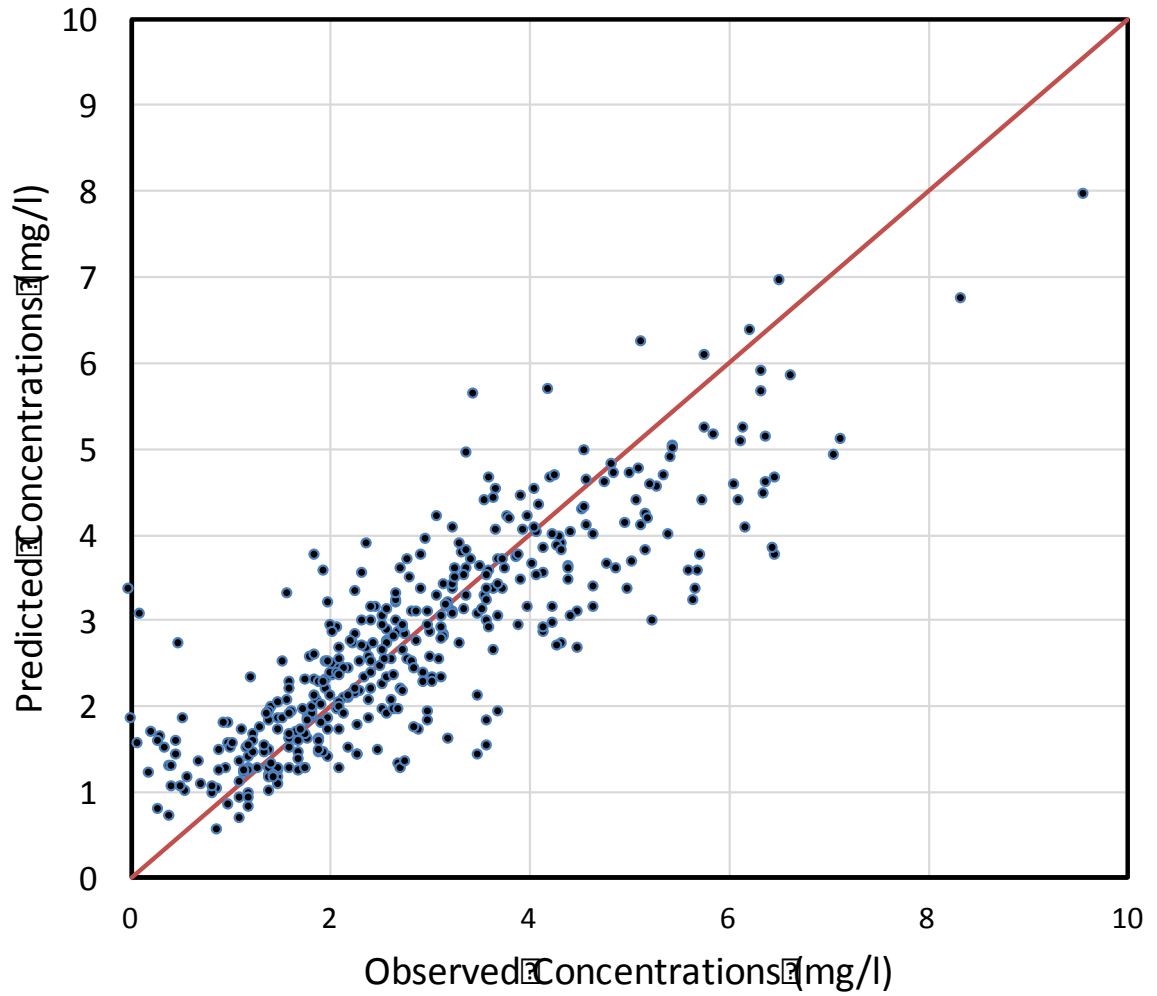
Supplementary Figure A3.2. Observed vs Predicted Concentration Values for the Speed River at Wellington Road
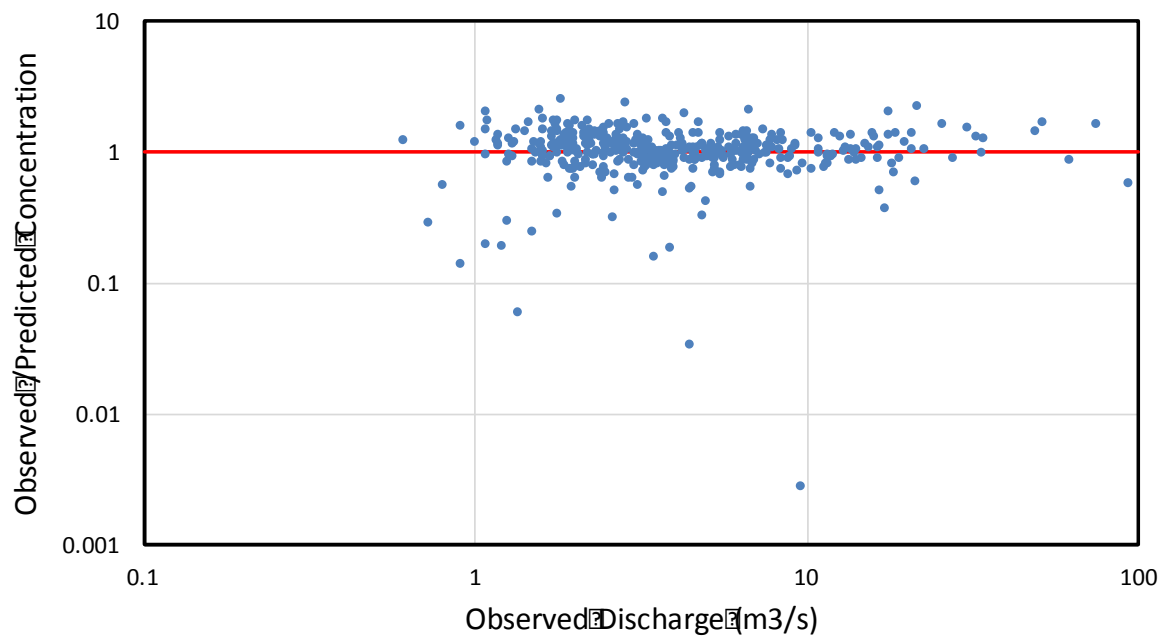
Supplementary Table A3.1 Error statistics for modeled concentration data for the 16 study watersheds.

Station ID	Mean Error	Mean Absolute Error	RMS Error	Nash Sutcliffe Efficiency	Percent Bias	Number of Data Points
400902	-0.07	0.77	1.26	0.52	-0.02	484
401002	-0.05	0.55	0.80	0.59	-0.02	532
401602	-0.13	1.41	2.02	0.46	-0.03	484
402402	-0.02	0.54	0.85	0.56	-0.01	346
402702	-0.01	0.54	0.83	0.54	0.00	292
403202	0.14	1.23	1.77	0.43	0.04	428
403602	-0.12	0.61	0.84	0.71	-0.04	408
403702	-0.01	0.26	0.46	0.45	-0.01	473
405102	-0.01	1.27	1.75	0.59	0.00	375
406702	0.01	0.23	0.40	0.59	0.01	364
407702	-0.04	0.78	1.06	0.52	-0.02	344
409202	-0.02	0.54	0.80	0.57	-0.01	340
409302	-0.05	0.47	0.70	0.43	-0.03	357
410202	0.01	0.25	0.38	0.51	0.01	353
410302	0.05	0.55	0.79	0.46	0.03	302
410602	-0.03	0.77	1.21	0.30	-0.01	360